Proposition and Application of a Simple Third-moment Reliability Index

2017

WANG Jiao

TABLE OF CONTENTS

CHAPTER 1

Introduction

1.1 Background

Civil infrastructure facilities, including buildings, bridges, transportation networks and public utilities must designed to satisfy the service requirement and withstand environmental events such as earthquake, wind and snow. In engineering design, an important consideration is how to handle the unavoidable uncertainties of the environmental events and ensure structural safety. Several decades ago, many standards have recognized this problem. For example, the design wind speed and ground snow loads were recorded and determined from the probability distributions for the annual extreme fasted mile wind speed and the annual extreme ground snow load. For ordinary structures, the design value for these parameters is that value which has a probability of being exceed of 0.02 in any year (the 50-year mean recurrence interval value). Similarly, the acceptance criteria for concrete strength in ACI Standard 318-14 [1] are designed to insure that the probability of obtaining concrete with a strength less than f_c' is less than 10 percent.

In the presence of uncertainty, absolute reliability is an unattainable goal. However, in current codes and guidelines, the load and resistance factors (LRF) are used to handle the effects of these uncertainties and the target reliability (in terms of the required safety index) is used to ensure structural safety [2-3]. Over the past 40 years, many researchers have been working on the improvement of the method of structural reliability and the load and resistance factors design (LRFD) [4-6]. Compared with the first-generation probability-based limit states design (PBLSD) methods (the first and second order reliability methods), the third moment method offers advantages in both simplicity and accuracy. However, it leaves much to be improved in the 3M method.

In structural engineering, with a given service lifetime, reliability index is an indicator of safety level. Conversely, with a given critical reliability index (or critical failure probability), the service lifetime is an indicator of durability. To upkeep the safety and

increase the service life of civil infrastructure facilities, a large amount of labor and money should be invested in maintenance or reconstruction [7-8]. Therefore it is also important to evaluate structural service lifetime with appropriate method. Considering the environmental uncertainties, probabilistic method with high-efficiency and high-accuracy is required.

1.1.1 Third-moment reliability index

As shown in Fig. 1-1a, in civil engineering, $R - S = 0$ is the original criterion of survival and failure of structures, where R and S are the interior resistance and the exterior deterioration load effect, respectively.

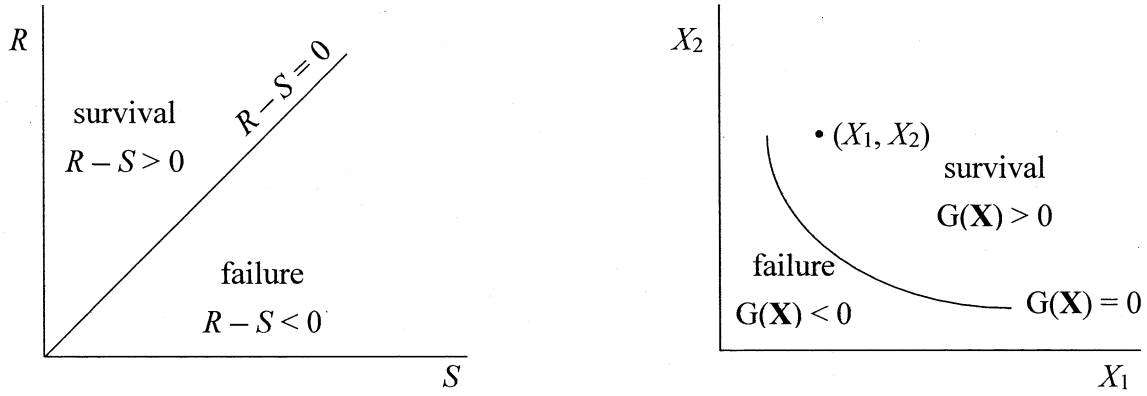

(a) Linear two-variable problem (b) Nolinear two-variable problem

Fig. 1-1 Reliability calculation

When evaluating structural reliability, the most important step is to calculate the failure probability (i.e., the reliability index) of a structure; this is given as

$$P_f = \text{Prob}[Z = G(\mathbf{X}) \le 0] = \int_{G(\mathbf{X}) \le 0} f(\mathbf{x}) d\mathbf{x} \tag{1-1}$$

where $\mathbf{X}$ is a vector of random variables representing uncertain structural quantities and P_f is the failure probability. $f(\mathbf{x})$ is the probability density function (PDF) of the limit state function $G(\mathbf{X})$. The domain of integration, $G(\mathbf{X}) \le 0$, denotes the failure set, as shown in Fig. 1-1b (Nolinear two-variable problem is taken as an example). As shown in Fig. 1-2, the shaded area to the left of zero is equal to the failure probability.

Difficulty in computing failure probability has led to the development of various approximation methods, among which the first-order reliability method (FORM) [9] is now used worldwide in engineering codes. However, in the case of multiple design points [10], FORM is inconvenient. Because of insufficient accuracy when applying FORM to

nonlinear performance functions, the second-order reliability method (SORM) [11] has been proposed to improve FORM. Although SORM is more accurate than FORM, it also requires the calculation of the design point and the curvature of failure of the limit state at the design point. However, when the PDFs of the basic random variables are unknown, neither FORM nor SORM are applicable. For such cases, sampling simulation methods [12-14] are known to be sufficiently accurate; however, when the performance function is complicated or high reliability is required, such methods are time-consuming.

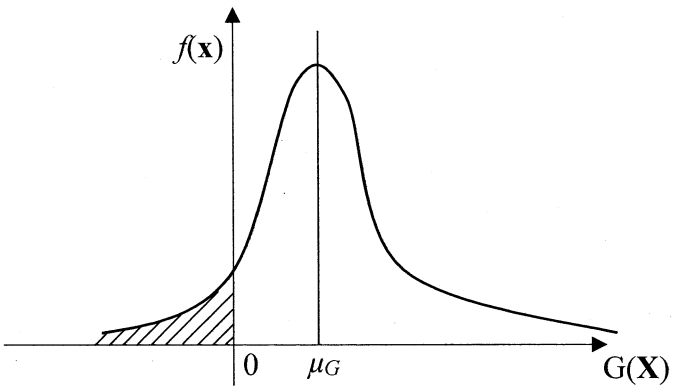

Figure 1-2 Illustration of the concept of failure probability

3M methods have been proved to require neither iteration nor computation of derivatives and have no shortcomings associated with the design point [15]. However, existing 3M methods do have some limitations: in some cases, due to the method's mathematical formula, existing 3M methods either cannot be used to calculate the failure probability or result in large errors. By focusing on the problems in the mathematical formulae of existing 3M methods, namely, the inclusion of the square root, the unknown value of the denominator, and the logarithmic term in the approximation formula, the proposition of a simple 3M method with relatively high accuracy and no limitations is significant.

1.1.2 Load and resistance factors

Design codes have incorporated probabilistically-based load and resistance factor formats based on first and second order reliability methods [2-3]. However, there are inevitable shortcomings of the first and second order reliability methods. Then some simplification methods were proposed [15-17]. According to the Mori method, all random variables are assumed to have known PDFs and are transferred into lognormal random variables.

However, the PDFs of some random variables do not obey lognormal distribution and are often difficult to obtain. In Zhao's research [15], the iteration computation of the target mean resistance is simplified to one time. But the applicable range is restricted for the inevitable mathematical limitations. Therefore, it is necessary to propose an easier method to completely avoid the iteration, at the same time, accurate enough, without or with less limitation in applicable range.

1.1.3 Application of third-moment reliability in structural durability

Chloride-induced corrosion can shorten the service life of concrete structures. For countries like Japan, with a coastline of about 30,000 km, the chloride corrosion is particularly serious. Reliable predictions of life cycle performance of concrete structures are critical to the optimization of their life cycle design and maintenance to minimize their life cycle costs. As shown in Fig. 1-3, the time of corrosion-induced failure can be expressed with respect to corrosion level. Engineers have always recognized the presence of uncertainty in the influence factors and probabilistic methods has been applied to solve the problem, typically, Monte-Carlo (MC) simulation [18-19]. One of the reasons that MC simulation is widely used in probabilistic analysis of structural durability is that it is a simple simulation technique. It is possible to calculate the failure probability with only a little background in probability and statistics [20]. And it is accurate when the number of samples is large. However, the requirement of the distribution of random variables is inevitable. In the case of the performance function is complex or the reliability is very large, MC simulation is time-consuming. Therefore, in recent years the moment method is proved capable and applied to durability design [21-22]. The result of 3M method is identical with MC simulation but very few researchers chose it to do the probabilistic analysis [23]. One of the reasons is the existing 3M method is imperfect. Whether it is efficient and applicable to structural durability design is required further verification.

Although significant efforts have made by scientific committees and have led to specific publications [24-25], in which probabilistic durability design is recommended, European regulation concerning durability of concrete structures [24] do not yet mention any threshold reliability level regarding the corroded RC structures. Moreover, the choice of a threshold reliability level is not a straightforward task. According to usual probabilistic approach [24-26] the reliability level is expressed in terms of the reliability index β. Some values have been proposed for the target reliability index, for instance β_T = 1.3 in [27], with the assumption that corrosion is likely to start as soon as the steel is depassivated. For concretes of precast components, a lower value, β_T = 1, has been

suggested recently in [27]. For different reliability requirement, the influence mode of the environment and structure character on the durability design is yet to be studied. The proposition of an efficient and accurate 3M method to solve this problem is significant.

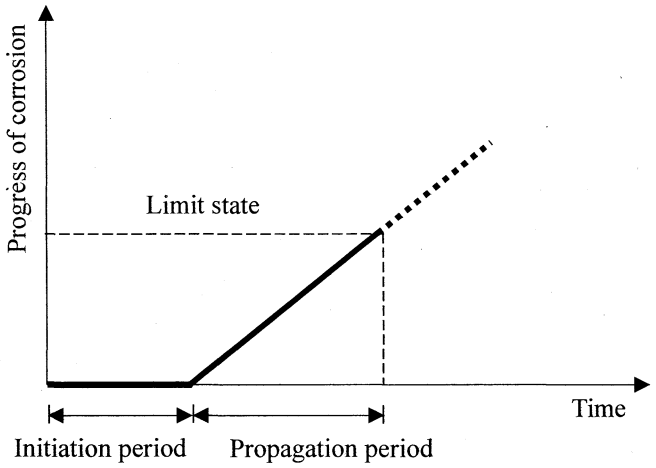

Fig. 1-3 Determination of service life with respect to corrosion of RC structure

1.2 Objective

This study is aim to solve three main problems.

Firstly, the shortcomings of the existing 3M methods will be verified. A simple and accurate 3M method will be proposed without any mathematical limitations in equations. The proposed 3M method, with wider applicable range, can be applied to analyze the case that is out of the applicable range of the existing methods. Both the reliabilities of simple structure and system will be analyzed with the existing methods and the proposed method. Moreover, with the new method, the structural reliability design is safe and material-saving.

Secondly, the proposed 3M method will be used in the calculation of load and resistance factors. Simultaneously, the two step recursive optimization in the computation process of the target mean resistance will be further simplified to no iteration. And the computation accuracy of the new method will be higher than the existing methods in most cases.

Thirdly, it will be proved that the proposed 3M method is applicable to the structural durability design. The RC structures in chloride-rich environment will be taken to be analyzed. A full set of methods will be proposed, including the sensitive analysis of environment influence factor, the corrosion and cover cracking prediction and reliability evaluation of structures.

1.3 Organization

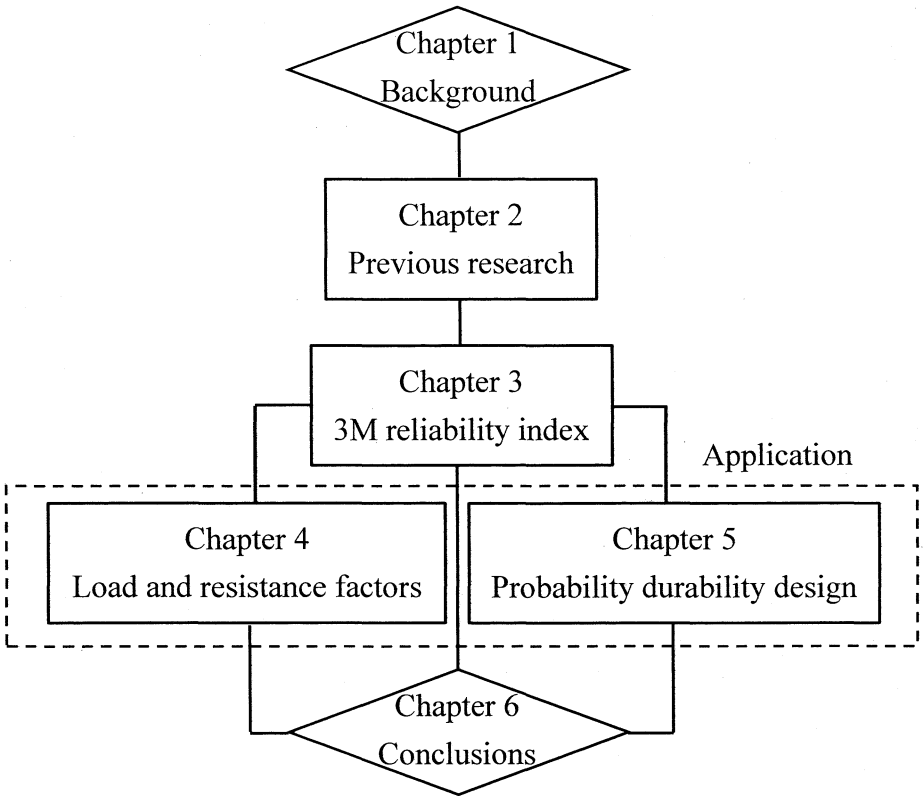

The background and pervious research were introduced in Chapter 1 and 2, respectively.

The thesis consisted of two parts: (1) proposition of a simple third-moment method (Chapter 3), (2) application of the new method (Chapter 4 and 5). Then the application was divided into two parts: the application in the calculation of load and resistance factor (Chapter 4) and the application in probabilistic durability design (Chapter 5). In Chapter 4, the analysis focused on the structures under loads (e.g. dead load, live load, wind load, snow load *et al.*), while in Chapter 5, the analysis focused on the corroded structures in chloride-rich environment. In Chapter 4, the reliability assessment was given based on a design service life. More than the application of 3M method, simplification of the calculation process of load and resistance factors was given in Chapter 4. Similarly, the corrosion evaluation method of RC structures was also improved. The reliability analysis in Chapter 5 was translated into probabilistic durability design, which means based on a given critical reliability, the service life of structure was predicted. In fact, the analysis in Chapter 5 was an inverse operation of the analysis in Chapter 4.

In the last Chapter, the significant innovations in Chapter 3 to 5 was summarized and

the shortcoming in this thesis was pointed out.

REFERENCES

[1] ACI 318-14. Building Code Requirements for Reinforced Concrete. *American Concrete Institute*, 2014.

[2] ASCE Standard 7-10. Minimum design loads for buildings and other structures. 2010.

[3] AIJ. Recommendations for limit state design of buildings. 2002.

[4] Ang A. H-S. Reliability-based design criteria for infrastructure systems – a new look. *Sustainable Development of Critical Infrastructure CDRM 8*, ASCE, 2014: 1-16.

[5] Ellingwood B.R. LRFD: implementing structural reliability in professional practice. *Engrg. Struct.*, 2000, 22(2):106-115.

[6] Zhao Y.G. *et al.* A simple third-moment method for structural reliability. *Journal of Asian Architecture and Building Engineering*, 2006, 5 (1): 129-136.

[7] Agrawal A.K. *et al.* Advances in corrosion monitoring systems for highway bridges. *Structure Congress*, 2005: 1-5.

[8] Cheung M.M.S. *et al.* Life-cycle cost analysis and management of reinforced /prestressed concrete structures. *Life-Cycle Cost and Performance of Civil Infrastructure Systems*, 2007: 19-37.

[9] Shinozuka M. Basic analysis of structural safety. *J Struct Engrg, ASCE*, 1983, 109 (3): 721-40.

[10] Barranco-Cicilia F. *et al.* Structural reliability analysis of limit state functions with multiple design points using evolutionary strategies. *Ingeniería Investigacióny Tecnología*, 2009, 10(2): 87-97.

[11] Der K.A. *et al.* Second-order reliability approximations. *J Engrg Mech ASCE*, 1987, 113(8): 1208-1225.

[12] Nie J. *et al.* Finite element-based structural reliability assessment using efficient directional simulation. *J. Eng. Mech.*, 2005, 131: 259-267.

[13] Hurtado J.E. Filtered importance sampling with support vector margin: a powerful method for structural reliability analysis. *Struct. Saf.*, 2007, 29: 2-15.

[14] Lu Z.Z. *et al.* Reliability sensitivity method by line sampling. *Struct. Saf.*, 2008, 30: 517-532.

[15] Zhao Y.G. *et al.* Estimation of load and resistance factors using third-moment method based on the 3P-lognormal distribution. *Frontiers of Architecture and Civil Engineering in China*, 2011, 5: 315.

[16] Mori Y. Practical method for load and resistance factors for use in limit state design

(in Japanese), *J. of Struct. Constr. Eng., AIJ*, 2002, 559: 39-46.

[17] Ugata T. Reliability analysis considering skewness of distribution-Simple evaluation of load and resistance factors (in Japanese), *J. of Struct. Constr. Eng., AIJ*, 2000, 529: 43-50.

[18] Li Q. *et al.* Model-based durability design of concrete structures in Hong Kong-Zhuhai-Macau sea link project. *Strut. Saf.*, 2015, 53: 1-12.

[19] Duprat F. *et al.* Accelerated carbonation tests for the probabilistic prediction of the durability of concrete structures. Constr. Build. Mater., 2014, 66: 597-605.

[20] Haldar A. *et al.* Probability, Reliability and Statistical Methods in Engineering Design. 2000.

[21] Duracrete. Probabilistic performance based durability design of concrete structures. *Brite euram project BE95-1347*, 2000.

[22] Faroz S.A. *et al.* Reliability of a corroded RC beam based on Bayesian updating of the corrosion model. *Eng. Struct.* 2016, 126: 457-468.

[23] Mun S. Inversion analysis to determine design parameters for reliability assessment in pavement structures. *Can. J. Eng.*, 2014, 41: 845-855.

[24] Eurocode 2. EN 1992-1-1, Design of Concrete Structures. *General rules and rules for buildings*, Paris, AFNOR. 2007.

[25] International Federation of Structural Concrete. FIB bulletin 34, model code for service life design. Lausanne: IFSC-fib, 2006.

[26] Joint Committee of Structural Safety. Probabilistic model code, 2001.

[27] Mai-Nhu J. *et al.* Probabilistic approach for durable design of concrete cover: application to carbonation. *Eurj. Environ. Civ. Eng*, 2012, 16: 264-72.

List of publications

Referred papers

[1] Zhang X., **Wang J.**, Zhao Y., Tang L., and Xing F. Time-dependent probability assessment for chloride induced corrosion of RC structures using the third-moment method. *Construction and Building Materials*, 2015, 76: 232-244.

[2] **Wang J.**, Saito T. and Zhao Y. Third-moment method of determining load and resistance factors without iteration. *J. Struct. Engrg. AIJ*, 2016, 62B: 291-297.

[3] **Wang J.**, Lu Z., Zhang X., Saito T. and Zhao Y. A simple third-moment reliability index. JAABE. (accepted)

International conference paper

[4] **Wang J.**, Zhang X. and Zhao Y. Probabilistic lifetime analysis of reinforced concrete structures in chloride-rich environments. *4th International Symposium on Reliability Engineering and Risk Management.* May 20-24, 2014, Taipei: 177-180.

[5] **Wang J.**, Zhao Y. and Zhang X. A simple third-moment method for the calculation of the reliability index. *The 17th Working Conference of the IFIP Working Group 7.5 on Reliability and Optimization of Structural Systems (IFIP 2014).* Jul. 3-7, 2014, Huangshan, China.

[6] **Wang J.**, Zhao Y. and Saito T. Simplification of the iteration procedure of determining load and resistance factors. *International Symposium on Reliability of Engineering Systems (SRES 2015).* Oct. 15-17, 2015, Hangzhou, China.

[7] **Wang J.**, Zhao Y. and Saito T. Sensitivity Study on Marine RC Structures Using the Third-Moment Method. *International Symposium on Reliability of Engineering Systems (SRES 2015).* Oct. 21-24, 2015, Taipei, China.

[8] **Wang J.**, Lu Z. and Zhao Y. A simple third-moment reliability index. *5th International Symposium on Reliability Engineering and Risk Management (ISRERM 2016)*, August 17 - 20, Seoul, Korea.

Domestic conference paper

[9] **Wang J.**, Saito T. and Zhao Y. Probabilistic lifetime prediction of reinforced concrete structures in marine environments. *Summaries of technical papers of Annual Meeting, AIJ*, 2014, 113-114.

[10] **Wang J.**, Zhao Y. and Saito T. Determination of load and resistance factors without iteration, part 1: proposition of method. *Summaries of technical papers of Annual Meeting, AIJ*, 2015, 77-78.

[11] Zhao Y., **Wang J.** and Saito T. Determination of load and resistance factors without iteration, part 2: investigation of the proposed method. *Summaries of technical papers of Annual Meeting, AIJ*, 2015, 79-80.

CHAPTER 2

Previous research

2.1 Introduction

There are a lot of methods of reliability index, as introduced in Chapter 1. In Section 2.2, the details of four typical methods, namely, FORM, 3M-1, 3M-2 and MC simulation were introduced and the shortcomings of them were further analyzed. Because of the proposed method is an improved method of the existing 3M methods, 3M-1 and 3M-2, they were emphatically introduced in this section.

In Section 2.3, three methods for the calculation of load and resistance factors, namely, ASCE method, Mori's method and Zhao's method, were introduced. The details of the calculation process and the comparison of them were given. And the advantages and limitations of the existing 3M methods were emphatically analyzed.

In Section 2.4, the application of 3M method in durability analysis of RC structures was introduced. Especially the sensitive analysis of the influence factors, such as the mean value, the coefficient of variation of them was proposed. The process of modeling the corrosion initiation and cover cracking and predicting the service life of RC structures was introduced in details. The comparison of 3M method and other methods in durability analysis was presented. Moreover, the shortcomings of the existing corrosion models of RC structures was pointed out.

2.2 Existing methods of reliability index

2.2.1 First-order reliability method (FORM)

As introduced in Chapter 1, the limit state function could be linear or nonlinear due to the relationship and distributions of random variables. If the joint probability density function (PDF) of the random variables decays rapidly as one moves away from the minimum distance point, then the first-order estimate of reliability is quite accurate. If the decay of

the joint PDF is slow and the limit state is highly nonlinear, then one has to use a higher-order approximation for the reliability computation. Consider the two limit states shown in Fig. 2-1, one linear and one nonlinear. Both limit states have the same distance point, but the failure domains are different for the two cases. The FORM method will give the same reliability estimate for both cases. But it is apparent that the failure probability of the nonlinear limit state should be less than that of the linear limit state, due to the difference in the failure domains. The curvature of the nonlinear limit state is ignored in the FORM method, which uses only a first-order approximation at the minimum distance point. Thus the curvature of the limit state around the minimum distance point determines the accuracy of the first-order approximation in FORM.

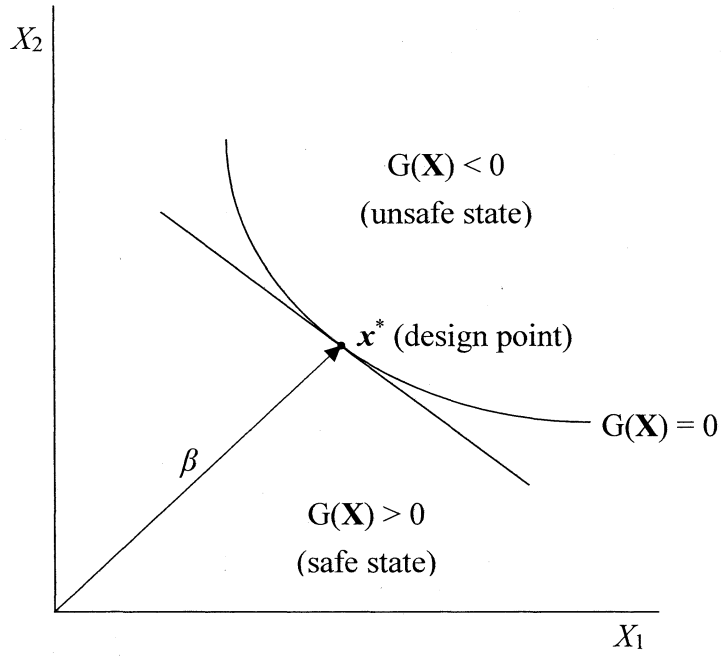

Fig. 2-1 Linear and nonlinear limit state

The Taylor series expansion of a general nonlinear function $G(X_1, X_2, \ldots, X_n)$ at the value $(x_1^*, x_2^*, \ldots, x_n^*)$ is [1]

$$G(X_1, X_2, \ldots, X_n) = G(x_1^*, x_2^*, \ldots, x_n^*) + \sum_{i=1}^{n} (x_i - x_i^*) \frac{\partial g}{\partial X_i} + \frac{1}{2} \sum_{i=1}^{n} \sum_{j=1}^{n} (x_i - x_i^*)(x_j - x_j^*) \frac{\partial^2 g}{\partial X_i \, \partial X_j} + \ldots \tag{2-1}$$

where the derivatives are evaluated at the design point of the X_i's.

The variables $(X_1, X_2, \ldots, X_n)$ are used in Eq. (2-1) in a generic sense. One should use

the appropriate set of variables and notation depending on the space being considered. In the case of reliability analysis, the first-order or second-order approximation to $G(\mathbf{X})$ is being constructed in the space of standard normal variables, at the minimum distance point. However, this design point is not a priori known hence should be determined by iterative method. The details of iteration was not discussed in this thesis.

2.2.2 Third-moment method (3M method)

2.2.2.1 Principle of 3M method

Without loss of generality, the limit state function Z can be standardized by

$$Z_s = \frac{Z - \mu_G}{\sigma_G} \tag{2-2}$$

where μ_G and σ_G are the mean and standard deviation of $G(\mathbf{X})$, respectively.

According to the definition of the probability, the failure probability can be expressed as

$$\begin{aligned} P_f &= \mathrm{P}[G(\mathrm{X}) \le 0] = \mathrm{P}[Z_s \sigma_G + \mu_G \le 0] \\ &= \mathrm{P}\left[Z_s \le -\frac{\mu_G}{\sigma_G} \right] = \mathrm{P}[Z_s \le -\beta_{2M}] \end{aligned} \tag{2-3}$$

where

$$\beta_{2M} = \frac{\mu_G}{\sigma_G} \tag{2-4}$$

is the second-moment (2M) reliability index.

Suppose the standardized variable Z_s can be expressed as a function of its third moment α_{3G};

$$Z_u = S(u, \alpha_{3G}) \tag{2-5}$$

where u is the standard normal variable, and α_{3G} is the skewness of $G(\mathbf{X})$ [2].

Substituting Eq. (2-5) into Eq. (2-3), the failure probability can be expressed as

$$P_f = \mathrm{P}[z_u = S(u, \alpha_{3G}) \le -\beta_{2M}] \tag{2-6}$$

if the inverse function of S is

$$u = S^{-1}(Z_u) \tag{2-7}$$

According to Eqs. (2-6) and (2-7), it is not difficult to obtain

$$P_f = P\left[u \le S^{-1}\left(-\beta_{2M}\right)\right] = \Phi\left[S^{-1}\left(-\beta_{2M}\right)\right] \tag{2-8}$$

Therefore, the reliability index is expressed as

$$\beta_{3M} = -\Phi^{-1}(P_f) = -S^{-1}(-\beta_{2M}) \tag{2-9}$$

For the first three moments of $G(\mathbf{X})$ used in Eq. (2-9), the reliability index calculated by Eq. (2-9) is called the 3M reliability index — thus the name, the 3M reliability method. From Eq. (2-9), if the inverse function of $S(u)$ is obtainable, the 3M reliability index can be given.

2.2.2.2 3M method based on 3P lognormal distribution

With the first three moments of the performance function $z = G(\mathbf{X})$, assuming that Z_u obeys three-parameter (3P) lognormal distribution [3], the relationship between Z_u and u is given as

$$Z_u = S(u) = u_b\left(1 - \frac{1}{\sqrt{A}}\exp\left[Sign(\alpha_{3G})\sqrt{\ln(A)}u\right]\right) \tag{2-10}$$

where

$$A = 1 + \frac{1}{u_b^2} \tag{2-11a}$$

$$u_b = (a+b)^{\frac{1}{3}} + (a-b)^{\frac{1}{3}} - \frac{1}{\alpha_{3G}} \tag{2-11b}$$

$$a = -\frac{1}{\alpha_{3G}}\left(\frac{1}{\alpha_{3G}^2} + \frac{1}{2}\right), b = \frac{1}{2\alpha_{3G}^2}\sqrt{\alpha_{3G}^2 + 4} \tag{2-11c}$$

where $Sign(x)$ is −1, 0, or 1 while x is negative, zero, or positive, respectively.

The relationship between u_b and α_{3G} is given as

$$\alpha_{3G} = -\left(3 + \frac{1}{u_b^2}\right)\frac{1}{u_b} \tag{2-12}$$

For small α_{3G}, i.e., $\alpha_{3G} \leqslant 1$, it has been derived that [4]

$$Z_u = \frac{3}{\alpha_{3G}}\left\{1 - \exp\left[\frac{\alpha_{3G}}{3}\left(u - \frac{\alpha_{3G}}{6}\right)\right]\right\} \tag{2-13}$$

$$u = \frac{\alpha_{3G}}{6} + \frac{3}{\alpha_{3G}} \ln\left(1 - \frac{1}{3}\alpha_{3G} Z_u\right) \tag{2-14}$$

According to Eqs. (2-9) and (2-14), the 3M reliability index is obtained as

$$\beta_{3M-1} = -\frac{\alpha_{3G}}{6} - \frac{3}{\alpha_{3G}} \ln\left(1 - \frac{1}{3}\alpha_{3G}\beta_{2M}\right) \tag{2-15}$$

2.2.2.3 3M method based on 3P square normal distribution

In another formula of the 3M reliability index, Z_u is assumed to obey 3P square normal distribution [5], the u-Z_u transformation is expressed as

$$Z_u = S(u) = a_1 + a_2 u + a_3 u^2 \tag{2-16}$$

where

$$a_3 = -a_1 = \pm\sqrt{2}\cos\left[\frac{\pi + |\theta|}{3}\right] \tag{2-17}$$

$$a_2 = \sqrt{1 - 2a_3^2} \tag{2-18}$$

$$\theta = \tan^{-1}\left(\frac{\sqrt{8 - \alpha_{3G}^2}}{\alpha_{3G}}\right) \tag{2-19}$$

For $-1 < \alpha_{3G} < 1$, a_3 can be simplified as [6]

$$a_3 = \alpha_{3G}/6 \tag{2-20}$$

where the simplification error is less than 2%.

Then, it can be derived that

$$Z_u = \frac{1}{6}\alpha_{3G}\left(1 - u^2\right) - u \tag{2-21}$$

$$u = \frac{\sqrt{9 + \alpha_{3G}^2 - 6\alpha_{3G} Z_u} - 3}{\alpha_{3G}} \tag{2-22}$$

Using the relationship in Eq. (2-9), the 3M reliability index is obtained as [7]

$$\beta_{3M-2} = \frac{3 - \sqrt{9 + \alpha_{3G}^2 - 6\alpha_{3G}\beta_{2M}}}{\alpha_{3G}} \tag{2-23}$$

2.2.2.4 Limitations of existing 3M methods

It has been shown that the applicable range of $\beta_{3M\text{-}1}$ and $\beta_{3M\text{-}2}$ is expressed as

$$\frac{-120r}{\beta_{2M}} \le \alpha_{3G} \le \frac{40r}{\beta_{2M}} \tag{2-24}$$

where r is the allowable relative difference.

However, there are other limitations for the calculation of the reliability index for $\beta_{3M\text{-}1}$ and $\beta_{3M\text{-}2}$.

First, for the antilogarithm of Eq. (2-15), the limitation is

$$\begin{aligned} 1-\frac{1}{3}\alpha_{3G}\beta_{2M} &> 0 \\ \alpha_{3G}\beta_{2M} &< 3 \end{aligned} \tag{2-25}$$

where $\alpha_{3G} \neq 0$.

Furthermore, for the square root of the numerator and the variable of the denominator in Eq. (2-23), the following qualification should be observed:

$$\begin{aligned} 9+\alpha_{3G}^2-6\alpha_{3G}\beta_{2M} &\ge 0 \\ 6\alpha_{3G}\beta_{2M} &\le 9+\alpha_{3G}^2 \\ \beta_{2M} &\le \frac{9+\alpha_{3G}^2}{6\alpha_{3G}} \end{aligned} \tag{2-26}$$

where $\alpha_{3G} \neq 0$ also. Fig.2-2 shows that the difference between the two reliability indices increases as $|\alpha_{3G}|$ increases; the further α_{3G} is from 0, the greater the error. In fact, in the case of negative α_{3G}, the exact value calculated by Monte-Carlo (MC) simulation is in the middle of the two reliability indices calculated by $\beta_{3M\text{-}1}$ and $\beta_{3M\text{-}2}$. Furthermore, in the case of a positive α_{3G}, the result of MC simulation is below the values of $\beta_{3M\text{-}1}$ and $\beta_{3M\text{-}2}$. Because the MC simulation can only be used for analysis of practical examples, different 3M reliability indices will be compared with MC simulation results in Chapter 3.

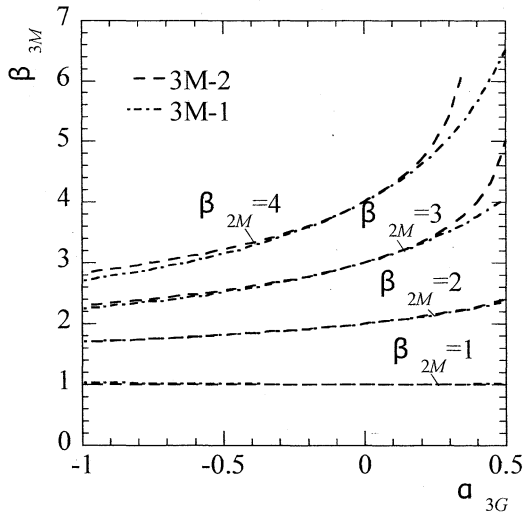

Fig. 2-2 β_{3M} with respect to α_{3G}

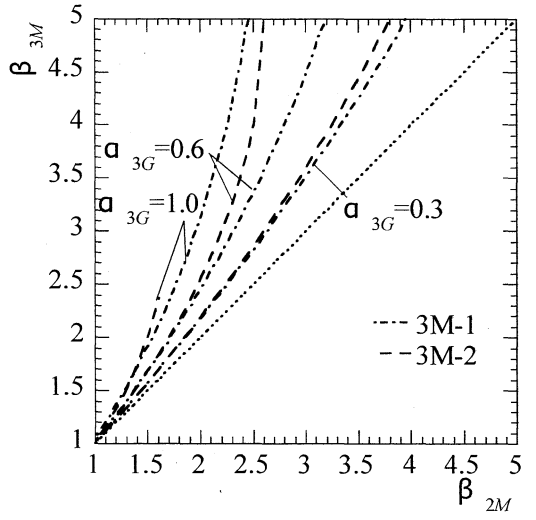

Fig. 2-3 β_{3M} with respect to β_{2M} ($\alpha_{3G} > 0$)

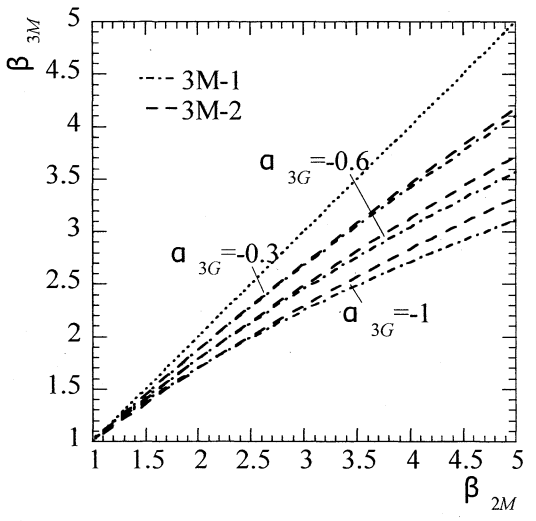

Fig. 2-4 β_{3M} with respect to β_{2M} ($\alpha_{3G} < 0$)

As shown in Figs. 2-3 and 2-4, the smaller the β_{2M}, the smaller the difference between the two reliability indices and the more reliable the approximate value, where the dotted line is the 2M method. Figs. 2-3 and 2-4 show that the difference between the two reliability indices is greater when α_{3G} is positive compared with the case when α_{3G} is negative. In other words, the 3M method is more applicable when α_{3G} is negative.

According to the formulae mentioned above, one can see that:

(1) If Eq. (2-15) cannot meet the limitation of Eqs. (2-24) and (2-25), the 3M reliability index cannot be defined.

(2) If Eq. (2-23) cannot meet the limitation of Eqs. (2-24) and (2-26), the 3M reliability index cannot be defined.

(3) If the value of β_{2M} or $|\alpha_{3G}|$ is large, their calculation error will be great.

2.2.3 Monte-Carlo simulation

Monte-Carlo (MC) simulation is a special technique that we can use to generate some result numerically without doing any physical testing. We can use results of previous tests (or other information) to establish the probability distributions of the important parameters in our problem. Then we use this distribution information to generate samples of numerical data. Take $G(\mathbf{X}) = R - S$ as an example, where R and S are normal distribution and lognormal distribution. The basic procedure is as follows [8]:

1. Randomly generate a value of R using its probability distribution information: the mean value, the coefficient of variation and distribution type.
2. Randomly generate a value of S using its probability information.
3. Calculate $G(\mathbf{X}) = R - S$.
4. Store the calculated value of $G(\mathbf{X})$.
5. Repeat steps 1-4 until a sufficient number of $G(\mathbf{X})$ values have been generated.
6. Estimate the failure probability as

$$P_f = \frac{\text{number of times that } G(\mathrm{X}) < 0}{\text{totalnumber of simulated } G(\mathrm{X}) \text{ values}} \tag{2-27}$$

The error (in percent) of a MC solution with a given sample size N can be evaluated as

$$r(\text{in}\%) = 200\sqrt{\frac{1-\overline{P}}{N\overline{P}}} \tag{2-28}$$

where $\overline{P}$ is an unbiased estimate of the probability p_f.

To insure the accuracy of reliability calculation using MC simulation, the sample size should be large enough and an appropriate software such as MATLAB and MATHEMATICA should be applied.

2.3 Existing methods of load and resistance

2.3.1 Principle of load and resistance factors

Based on the LRFD format, the performance function in structural design can be expressed as

$$\phi R_n \geq \sum \gamma_i Q_{ni} \tag{2-29}$$

where ϕ is the resistance factor, γ_i is the partial load factor to be applied to load S_i, R_n is the nominal value of the resistance, Q_{ni} is the nominal value of load Q_i.

In reliability-based design, the load and resistance factors ϕ and γ_i should be determined with a specified reliability, called the target reliability. Therefore, Eq. (2-29) should be probabilistically to the following equations.

$$G(\mathrm{X}) = R - \sum Q_i \tag{2-30}$$

where R and Q_i are random variables representing uncertainty in the resistance and load effects, respectively.

For a given target reliability β_T or target probability of failure P_{fT}, Eq. (2-30) can be expressed in terms of probability:

$$\beta \geq \beta_T, P_f \leq P_{fT} \tag{2-31}$$

where β and P_f are the reliability and the probability of failure, respectively.

If R and Q_i are mutually independent normal random variables, the second-moment (2M) method is correct and the design formula is expressed as

$$\beta_{2M} \geq \beta_T \tag{2-32}$$

where

$$\beta_{2M} = \frac{\mu_Z}{\sigma_Z} \tag{2-33a}$$

$$\mu_Z = \mu_R - \sum \mu_{Q_i}, \quad \sigma_Z = \sqrt{\sigma_R^2 + \sum \sigma_{Q_i}^2} \tag{2-33b}$$

where β_{2M} is the 2M reliability index; μ_Z and σ_Z are the mean value and standard deviation of the performance function $G(\mathbf{X})$, respectively; μ_R and σ_R are the mean value and standard deviation of R, respectively; and μ_{Qi} and σ_{Qi} are the mean value and standard deviation of Q_i, respectively.

Substituting Eq. (2-33) in Eq. (2-32), the load and resistance factors can be expressed as

$$\mu_R(1 - \alpha_R V_R \beta_T) \geq \sum \mu_{S_i}(1 + \alpha_{Q_i} V_{Q_i} \beta_T) \tag{2-34}$$

Comparing Eq. (2-34) with Eq. (2-29), the load and resistance factors can be expressed as

$$\phi = (1 - \alpha_R V_R \beta_T) \frac{\mu_R}{R_n} \tag{2-35a}$$

$$\gamma_i = (1 + \alpha_{Q_i} V_{Q_i} \beta_T) \frac{\mu_{Q_i}}{Q_{ni}} \tag{2-35b}$$

where V_R and V_{Qi} are the coefficient of variation for R and Q_i, respectively; and α_R and α_{Qi} are the sensitivity coefficients of R and Q_i, respectively, where

$$\alpha_R = \frac{\sigma_R}{\sigma_Z}, \quad \alpha_{Q_i} = \frac{\sigma_{Q_i}}{\sigma_Z} \tag{2-36}$$

As introduced above, the 2M method is based on the assumption of all the variables obey normal distribution and are independent of each other. In the case of R and Q_i are other random variables, the 2M reliability in Eq. (2-33) is incorrect. Therefore other methods were proposed, typically, the FORM [9]. The load and resistance factors can be obtained as

$$\phi = \frac{R^*}{R_n}, \gamma_i = \frac{Q_i^*}{Q_{ni}} \tag{2-37}$$

where R^* and Q_i^* are the values of the variables R and Q_i, respectively, at the design point of the FORM. Because R^* and Q_i^* are usually obtained using derivative-based iterations, explicit expressions of R^* and Q_i^* are not available. Some simplifications have been proposed to avoid iterative computations.

2.3.2 Mori method

As an approximate method, all of the variables are considered obeying lognormal distribution and are independent of each other. The load and resistance factors can be expressed as [10]

$$\gamma_i = \frac{1}{\sqrt{1 + V_{Q_i}^2}} \exp(\alpha_{Q_i} \zeta_{Q_i} \beta_T) \frac{\mu_{Q_i}}{Q_{ni}} \tag{2-38a}$$

$$\varphi = \frac{1}{\sqrt{1 + V_R^2}} \exp(-\alpha_R \zeta_R \beta_T) \frac{\mu_R}{R_n} \tag{2-38b}$$

where V_{Qi} and V_R are the coefficient of variation of the loads and resistance, ζ_{Qi} and ζ_R are the standard deviation of ln$R$ and ln$Q$.

$$\zeta^2 = \ln(1 + V^2)$$

The sensitivity coefficients of R and Q_i, α_R and α_{Qi} are calculated by

$$\alpha_R = \alpha_R^* \cdot u \tag{2-39a}$$

$$\alpha_{Q_i} = \alpha^*_{Q_i} \cdot u \tag{2-39b}$$

where

$$\alpha^*_R = \frac{\sigma_{\ln R}}{\sqrt{\sigma_{\ln R}{}^2 + \sum (c_j \cdot \sigma_{\ln Q_j})^2}} \tag{2-40}$$

$$\alpha^*_{Q_i} = \frac{c_i \cdot \sigma_{\ln Q_i}}{\sqrt{\sigma_{\ln R}{}^2 + \sum (c_j \cdot \sigma_{\ln Q_j})^2}} \tag{2-41}$$

$$u = \frac{1.05}{1 - \left(1 - \sqrt{(\alpha^*_R)^2 + (\max\{\alpha^*_{Q_i}\})^2}\right) \cdot \Phi\left(\frac{\max\{V_{Q_i}\} - 0.6}{0.4}\right)} \tag{2-42}$$

$$c_i = \frac{\exp\left(\lambda^*_{Q_i} + \frac{1}{2}\sigma_{\ln Q_i}{}^2\right)\frac{Q_{ni}}{G_n}\frac{\mu_{Q_i}}{Q_{ni}}}{\sum_j \exp\left(\lambda^*_{Q_j} + \frac{1}{2}\sigma_{\ln Q_j}{}^2\right)\frac{Q_{nj}}{G_n}\frac{\mu_{Q_j}}{Q_{nj}}} \tag{2-43}$$

where

$\lambda^*_{Q_i}$ — the mean value of $\ln(S_{ni}/\mu_{Si})$;

G_n — the nominal value of dead load;

μ_{Si}/S_{ni} — the rate of the mean value and the nominal value of load;

Φ — standard normal distribution function.

2.3.3 The existing 3M method

In Zhao's 3M method based on 3P-lognormal distribution (3M-1) [11], the two step recursive optimization is used to avoid the iteration computation:

$$\mu_{RT} = \sum \mu_{Q_i} + \beta_{2T}\sigma_Z \tag{2-44}$$

$$\mu_{R_0} = \sum \mu_{Q_i} + \sqrt{\beta_T^{3.5} \sum \sigma^2_{Q_i}} \tag{2-45}$$

where

μ_{RT} — the target mean resistance;

μ_{R0} — the original target mean resistance;

σ_Z — the standard deviation of $G(\mathbf{X})$;

β_{2T} — the target 2M reliability, which is obtained by the 3M method

$$\beta_{3M} = -\frac{\alpha_{3Z}}{6} - \frac{3}{\alpha_{3Z}} \ln\left(1 - \frac{1}{3}\alpha_{3Z}\beta_{2M}\right) \tag{2-46}$$

The inverse function of Eq. (2-46) is expressed as

$$\beta_{2T} = \frac{3}{\alpha_{3Z}}\left\{1 - \exp\left[\frac{\alpha_{3Z}}{3}\left(-\beta_{3T} - \frac{\alpha_{3Z}}{6}\right)\right]\right\} \tag{2-47}$$

where

$$\alpha_{3Z} = \frac{1}{\sigma_Z^3}\left(\alpha_{3R}\sigma_R^3 - \sum \alpha_{3S_i}\sigma_{Q_i}^3\right) \tag{2-48}$$

The steps for determining the load and resistance factors using this method are as follows:

1. Calculate μ_{R0} using Eq. (2-45).
2. Calculate σ_Z, α_{3Z} and β_{2T} using Eq. (2-33b), Eq. (2-48) and Eq. (2-47), respectively.
3. Calculate μ_{RT} with Eq. (2-44).
4. Repeat step 2 with μ_{RT}. Then with the values of σ_Z, α_{3Z} and β_{2T}, calculate α_R and α_{Qi} with Eq. (2-36).
5. Determine the load and resistance factors with Eq. (2-35).

The shortcoming of the calculation process is that one time iteration calculation of σ_Z, α_{3Z} and β_{2T} is inevitable. And Eq. (2-47) is complicated. When Equation (2-46) is used for the calculation of 3M reliability, there is a mathematical limitation in as

$$\alpha_{3Z} < \frac{3}{\beta_{2M}} \tag{2-49}$$

2.3.4 ASCE method

According to ASCE 7-10, the "principle action-companion action" format is proposed, in which one load is taken at its maximum value while other loads are taken at their point-in-time values. Based on the comprehensive reliability analysis performed to support their development, it was found that these load factors are well approximated by [12]

$$\gamma_Q = (\mu_Q / Q_n)(1 + \alpha_Q \beta V_Q) \tag{2-50}$$

in which α_Q is a sensitivity coefficient that is approximately equal to 0.8 when Q is a principal action and 0.4 when Q is a companion action. This approximation is valid for a broad range of common probability distributions used to model structural loads. The load factor is an increasing function of the bias in the estimation of the nominal load, the

variability in the load, and the target reliability index, as common sense would dictate.

As an example, the load factors in the following combination are based on achieving a β of approximately 3.0 for a ductile limit state with moderate consequences (e.g., formation of first plastic hinge in a steel beam).

$$1.2D+1.6L+0.5(L_r \text{ or } S \text{ or } R) \tag{2-51}$$

where D is dead load, L is live load, L_r is roof live load, S is snow load and R is rain load.

For live load acting as a principal action, $\mu_Q/Q_n = 1.0$ and $V_Q = 0.25$; for live load acting as a companion action, $\mu_Q/Q_n \approx 0.3$ and $V_Q \approx 0.6$. Substituting these statistics into Eq. (2-51), γ_Q = 1.0[1+0.8(3)(0.25)] =1.6 (principal action) and γ_Q = 0.3[1+0.4(3)(0.6)] =0.52 (companion action). If an engineer wished to design for a limit state probability that is less than the standard case by a factor of approximately 10, β would increase to approximately 3.7, and the principal live load factor would increase to approximately 1.74.

Similarly, resistance factors that are consistent with the aforementioned load factors are well approximated for most materials by

$$\phi = (\mu_R/R_n)\exp[-\alpha_R \beta V_R] \tag{2-52}$$

in which α_R is a sensitivity coefficient equal approximately to 0.7. For the limit state of yielding in an ASTM A992 steel tension member with specified yield strength of 50 ksi (345MPa), μ_R/R_n = 1.06 (under a static rate of load) and V_R = 0.09. Eq. (2-52) then yields ϕ = 1.06 exp[–(0.7)(3.0)(0.09)] = 0.88. The resistance factor for yielding in Section D of the AISC Specification (2010) [13] is 0.9. If a different performance objective were to require that the target limit state probability be decreased by a factor of 10, then ϕ would decrease to 0.84, a reduction of about 7%. Engineers wishing to compute alternative resistance factors for engineered wood products and other structural components where duration-of-load effects might be significant are advised to review the reference materials provided by their professional associations before using Eq. (2-52).

There are two key issues that must be addressed to utilize Eq. (2-50) and Eq. (2-52): selection of reliability index, β, and determination of the load and resistance statistics.

2.4 Probabilistic durability analysis of chloride-corroded RC structure

2.4.1 Overview of mechanisms of chloride ingress into concrete structures

In general, chloride penetration through concrete can be empirically described by Fick's second law:

$$C(x,t)=C_s\left[1-erf\left(\frac{x}{2\sqrt{D\cdot t}}\right)\right] \tag{2-53}$$

where

$C(x,t)$ — the chloride content at a distance x (m) from the concrete surface at time (%/m^3);

C_s — surface chloride content (%/m^3);

D — diffusion coefficient for chloride (m^2/s);

t — time (s);

erf — Gaussian error function.

By replacing the parameter to the cover thickness (c) of the concrete structure, the initiation time for corrosion is obtained from the following formula:

$$C_{cr}=C_s\left[1-erf\left(\frac{c}{2\sqrt{D\cdot t_0}}\right)\right] \tag{2-54}$$

where

C_{cr} — the critical chloride content (%/m^3);

c — the concrete cover (m);

t_0 — the initiation time of corrosion (s).

This formula can be simplified by using a parabola function and re-written in the following form for initiation time of corrosion t_0 [14]:

$$t_0=\frac{1}{12D}\left(\frac{c}{1-(C_{cr}/C_0)^{1/2}}\right)^2 \tag{2-55}$$

As an inherent and inevitable phenomenon in the formation of concrete mixture, early-age micro cracking will obviously influence the chloride penetration into concrete and consequently the time to corrosion initiation. Previous study [15] has already found that the patterns of chloride penetration in cracked concrete are obviously different with that in sound condition. The diffusion coefficient D here can be divided into two parts (namely, D_{cr} and D_0, as shown in Fig. 2-5 and is expressed as:

$$D=\frac{D_{cr}A_{cr}+D_0A}{A_{cr}+A} \tag{2-56}$$

where D_{cr} is the value of chloride diffusion coefficient inside the early-age micro cracking, D_0 is the corresponding value for sound area, A_{cr} is the area of micro cracking (m^2), A is the exposed surface area of the concrete element (m^2).

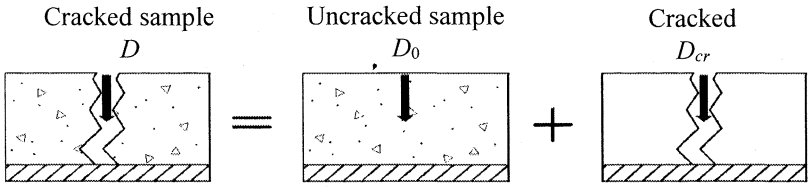

Fig. 2-5 Partition hypothesis of chloride diffusion through cracked concrete

It has been indicated that the value of chloride diffusion coefficient inside a crack of concrete cover (namely D_{cr}, m^2/s) is independent of material effects, even if tortuosity and roughness are different. Djerbi et al. suggested the following relationship between the crack width w_0 in concrete cover and its diffusion coefficient D_{cr} inside the crack:

$$\begin{cases} D_{cr} = 2\times10^{-11}w_0 - 4\times10^{-10}, 30\mu m \le w_0 \le 80\mu m \\ D_{cr} \approx 14\times10^{-10}, w_0 \ge 80\mu m \end{cases} \tag{2-57}$$

Besides penetration in the micro cracked area of concrete cover, the chloride will also diffuse in its sound area, as follows:

$$D_0 = \lambda_h \lambda_T \lambda_t D_{28} \tag{2-58}$$

where

λ_h — the correction coefficient for environmental relative humidity h (%);

λ_T — the corresponding coefficient for temperature T (K);

λ_t — the same coefficient for exposure time t_1 (day);

D_{28} — the chloride diffusion coefficient for a specimen under standard curing (28 days):

$$D_{28} = 10^{(-12.06+2.4w/c)} \tag{2-59}$$

where w/c is the water-to-cement ratio. Also the parameters λ_h, λ_t, and λ_T can be respectively expressed as:

$$\lambda_h = \left[1 + \frac{(1-h)^4}{(1-h_c)^4}\right]^{-1} \tag{2-60}$$

$$\lambda_t = \left(\frac{t_{28}}{t_1}\right)^m \tag{2-61}$$

$$\lambda_T = \exp\left[\frac{U}{R}\left(\frac{1}{T_{28}} - \frac{1}{T}\right)\right] \tag{2-62}$$

in which

h_c — the threshold relative humidity (h_c=75%);

t_{28} — the time of standard curing (28 days);

m — the age factor related to w/c by m=3(0.55 − w/c);

U — the activation energy equal to 35000 J/mol;

R — the gas constant;

T_{28} — the temperature for standard curing on day 28 (293 K).

2.4.2 Corrosion probability prediction of RC structures

Depending on the variable of interest, the corresponding performance function can be formulated, generally, as the difference between a term that is equivalent to a "resistance" and a term that is equivalent to a "load or load effect". For example, the term "resistance" here is the threshold chloride concentration C_{th}. Similarly, the term "load effect" is the chloride concentration at the steel at given time t, $C_{c,t}$. Therefore, the limit state function for corrosion initiation can be formulated as follows [16]:

$$g(C_s, c, D, C_{cr}) = C_{cr} - C_{c,t}(C_s, c, D, t) \tag{2-63}$$

Hence:

$g(C_s, c, D, C_{cr})$ = 0 = "limit state".

$g(C_s, c, D, C_{cr})$ > 0 = "desired state", or "un-corroded state".

$g(C_s, c, D, C_{cr})$ < 0 = "corrosion state", or "failure state".

The limit state equation $g(C_s, c, D, C_{cr})$ = 0 can be represented geometrically by an n-dimensional surface, which is referred to as a "failure surface" or in the case "corrosion initiation surface". Using Fick's second law of diffusion of Eq. (2-53), the limit state function for the corrosion time can be formulated as a function of four variables, as follows,

$$g(C_s, c, D, C_{cr}) = C_{cr} - C_s\left(1 - erf\frac{c}{2\sqrt{D \cdot t}}\right) \tag{2-64}$$

The probability of corrosion at time t corresponds to the integral of the probability density function $f_X(\boldsymbol{x})$ on the corrosion domain, as follows:

$$P_f = \int_{g(C_s, c, D, C_{cr}, t)<0} f_X(C_s, c, D, C_{cr})\mathrm{d}x \tag{2-65}$$

In Saassouh's paper, FORM and SORM methods are used to analyze the probability of corrosion of RC structures, while MC simulation is applied as a contrastive method. From the results of the examples, both FORM and SORM are in great agreement with MC simulation. However, in the case of the coefficient of variation of random variables is large, the errors of FORM and SORM are large. As we know, the random variables in chloride-rich environment are changeable, such as the chloride concentration on the

concrete surface. The coefficient of variation of these random variables can be quite large. Therefore, a method, with higher accuracy and efficiency, convenient for application, is considered to be significant.

2.5 Conclusions

In this Chapter, several typical previous research are introduced in details.

(1) In Section 2.2, the widely used FORM, 2M, two methods of 3M and MC simulation were introduced.

(2) In Section 2.3, the application of moment method in calculation of load and resistance factors is introduced. Three typical applications in AIJ design guideline (Mori's and Zhao's method) of Japan and ASCE 7-10 of America were introduced.

(3) In Section 2.4, the application of moment method in prediction of corrosion probability of RC structures in chloride-rich environment was introduced. A brief introduction of mechanisms of chloride ingress into concrete structures was given. Then establishment of the probabilistic model of the corrosion process was introduced.

Based on these previous research, new methods and several improvements will be proposed in Chapter 3-5.

REFERENCES

[1] Haldar A. *et al.* Probability, Reliability and Statistical Methods in Engineering Design. 2000.

[2] Zhao Y.G. *et al.* Cubic normal distribution and its significance in structural reliability. *Struct. Eng. Mech.*, 2008, 28 (3): 263-280.

[3] Tichy M. First-order third-moment reliability method. *Struct. Saf.*, 1994, 16: 189-200.

[4] Zhao Y.G. *et al.* An investigation on the third- and fourth-moment methods for structural reliability. *J. Struct. Constr. AIJ*, 2000a, 530: 21-28.

[5] Zhao Y.G. *et al.* Third-moment standardization for structural reliability analysis. *J. Struct. Engrg. ASCE*, 2000b, 126 (6): 724-732.

[6] Zhao Y.G. *et al.* An investigation on third-moment reliability indices for structural reliability analysis. *J. Struct. Constr. AIJ*, 2001, 548: 21-26.

[7] Zhao Y.G. *et al.* A simple third-moment method for structural reliability. *Journal of Asian Architecture and Building Engineering*, 2006, 5 (1): 129-136.

[8] Andrzej S. *et al.* Reliability of Strucutures. Second edition, 2012.

[9] Ang A.H.S. *et al.* Probability concepts in engineering planning and design. Vol 2: Decision, Risk, and Reliability. 1984, New York.

[10] Mori Y. Practical method for load and resistance factors for use in limit state design. *J. Struct. Constr. Eng.*, AIJ, 2002, 599: 39-46.

[11] Zhao Y.G. *et al.* Estimation of load and resistance factors using the third-moment method based on the 3P-lognormal distribution. *Frontiers of Architecture and Civil Engineering in China*, 2011, 5(3): 315-322.

[12] ASCE Standard 7-10. Minimum Design Loads for Buildings and Other Structures. 2010.

[13] AISC/ANSI 360-10. Specification for Structural Steel Buildings. 2010.

[14] Sarja A. et al. Durability design of concrete structures. *Report of the Technical Committee 130-CSL, RILEM.*

[15] Djerbi A. et al. Influence of traversing crack on chloride diffusion into concrete. *Cem. Concr. Res.*, 2008, 38(6): 877-83.

[16] Saassouh B. et al. Probabilistic modeling of chloride-induced corrosion in concrete structures using first- and second-order reliability methods. *Cem. Concr. Compos.*, 2012, 34: 1082-1093.

CHAPTER 3

Proposition of a new 3M reliability index

3.1 Introduction

In this chapter, two new third-moment reliability indices were proposed. According to the accuracy comparison of two proposed reliability indices, one of them was selected as the new index. In Section 3.2, firstly, the proposition of the reliability index was introduced. Then the advantages and disadvantages were analyzed, respectively. The applicable range and the comparison with existing 3M methods were also given. In Section 3.3, various examples were used to verify the applicability of the proposed method. In the analysis of these examples, the results of the second-moment (2M), 3M-1, 3M-2 methods and the proposed 3M-3 method were compared with the result of MC simulation, respectively.

3.2 Proposed 3M method

3.2.1 Proposed formulas

In order to overcome the limitations and insufficient accuracy of current 3M reliability indices, the variation roles of the 3M reliability indices with respect to the 2M reliability index and the third moment of the performance function are thoroughly investigated.

As introduced in Section 2.2, in the case of $\alpha_{3G} < 0$, the accurate reliability index is in the middle of results calculated by 3M-1 and 3M-2. Fitting the average value of $\beta_{3M\text{-}1}$ and $\beta_{3M\text{-}2}$, two new 3M reliability indices in the form of exponential function, using a trial and error method, can be proposed.

And in the case of $\alpha_{3G} \rightarrow 0$, with aid of a first-order Taylor expansion of e^x, it has already been shown that both $\beta_{3M\text{-}1}$ and $\beta_{3M\text{-}2}$ have the same limit when $\alpha_{3G} \rightarrow 0$ [1], expressed as

$$\beta_{2M} + \frac{1}{6}\alpha_{3G}\left(\beta_{2M}^2 - 1\right) \tag{3-1}$$

In order to obtain the same equation, the following two formulas are proposed:

$$\beta_{3M-3}=\frac{1}{3}\beta_{2M}\left[2+e^{\frac{1}{2}\alpha_{3G}\left(\beta_{2M}-\frac{1}{\beta_{2M}}\right)}\right] \tag{3-2a}$$

$$\beta_{3M-4}=\frac{5}{12}\beta_{2M}\left[\frac{7}{5}+e^{\frac{2}{5}\alpha_{3G}\left(\beta_{2M}-\frac{1}{\beta_{2M}}\right)}\right] \tag{3-2b}$$

where both $\beta_{3M\text{-}3}$ and $\beta_{3M\text{-}4}$ are fitting equations for the average value of $\beta_{3M\text{-}1}$ and $\beta_{3M\text{-}2}$.

In the case of $\alpha_{3G}\rightarrow 0$, $\beta_{3M\text{-}3}$ and $\beta_{3M\text{-}4}$ have the same limit as $\beta_{3M\text{-}1}$ and $\beta_{3M\text{-}2}$, expressed as

$$\begin{aligned}\beta_{3M-3}&=\frac{1}{3}\beta_{2M}\left[2+e^{\frac{1}{2}\alpha_{3G}\left(\beta_{2M}-\frac{1}{\beta_{2M}}\right)}\right]\\&=\frac{\beta_{2M}}{3}\left[2+1+\frac{1}{2}\alpha_{3G}\left(\beta_{2M}-\frac{1}{\beta_{2M}}\right)\right]\\&=\beta_{2M}+\frac{1}{6}\alpha_{3G}\left(\beta_{2M}^2-1\right)\end{aligned} \tag{3-3a}$$

$$\begin{aligned}\beta_{3M-4}&=\frac{5}{12}\beta_{2M}\left[\frac{7}{5}+e^{\frac{2}{5}\alpha_{3G}\left(\beta_{2M}-\frac{1}{\beta_{2M}}\right)}\right]\\&=\frac{5}{12}\beta_{2M}\left[\frac{7}{5}+1+\frac{2}{5}\alpha_{3G}\left(\beta_{2M}-\frac{1}{\beta_{2M}}\right)\right]\\&=\beta_{2M}+\frac{1}{6}\alpha_{3G}\left(\beta_{2M}^2-1\right)\end{aligned} \tag{3-3b}$$

Compared with $\beta_{3M\text{-}1}$, both two formulas do not include any logarithmic term. Compared with $\beta_{3M\text{-}2}$, they do not include any square root. With the calculation error in an acceptable range, both of them are theoretically applicable for calculating the 3M reliability index in all cases except $\beta_{2M}\rightarrow 0$.

In the case of $\beta_{2M}\rightarrow 0$, both $\lim\beta_{3M\text{-}3}$ and $\lim\beta_{3M\text{-}3}$ are expressed as

$$\lim_{\beta_{2M}\rightarrow 0^+}\beta_{3M}=\begin{cases}0\,,\ \alpha_{3G}\geq 0\\+\infty\,,\ \alpha_{3G}<0\end{cases} \tag{3-4a}$$

$$\lim_{\beta_{2M}\rightarrow 0^-}\beta_{3M}=\begin{cases}0\,,\ \alpha_{3G}\leq 0\\-\infty\,,\ \alpha_{3G}>0\end{cases} \tag{3-4b}$$

That is to say, both of two proposed 3M methods are not applicable to the case ofβ_{2M} $\rightarrow$0. However, in engineering practice the reliability index is usually much larger than 0.

3.2.2 Accuracy of the proposed formula

Compared with $\beta_{3M\text{-}1}$ and $\beta_{3M\text{-}2}$, the accuracy of $\beta_{3M\text{-}3}$ and $\beta_{3M\text{-}4}$ is analyzed. As shown in Fig. 3-1a and 3-1b, the comparison of $\beta_{3M\text{-}3}$ and $\beta_{3M\text{-}4}$ is given for β_{2M} = 1, 2, 3, 4. In the case of $\alpha_{3G} < 0$, the reliability calculated by $\beta_{3M\text{-}3}$ is in the middle of the results calculated by $\beta_{3M\text{-}1}$ and $\beta_{3M\text{-}2}$, while the reliability calculated by $\beta_{3M\text{-}4}$ is slightly lower than the results calculated by $\beta_{3M\text{-}1}$ and $\beta_{3M\text{-}2}$. That is, the proposed method $\beta_{3M\text{-}3}$ is more accurate than $\beta_{3M\text{-}4}$. In the case of $\alpha_{3G} > 0$, both the reliabilities calculated by $\beta_{3M\text{-}3}$ and $\beta_{3M\text{-}4}$ are lower than the results of $\beta_{3M\text{-}1}$ and $\beta_{3M\text{-}2}$. As introduced in Section 2.2, in the case of $\alpha_{3G} > 0$, the accurate reliability calculated by MC simulation is lower than the results calculated by $\beta_{3M\text{-}1}$ and $\beta_{3M\text{-}2}$, both of $\beta_{3M\text{-}3}$ and $\beta_{3M\text{-}4}$ are more accurate than $\beta_{3M\text{-}1}$ and $\beta_{3M\text{-}2}$, which will be analyzed in the following section. Considering the formula of $\beta_{3M\text{-}3}$ is simpler and more accurate than $\beta_{3M\text{-}4}$, $\beta_{3M\text{-}3}$ is finally regarded as the proposed method.

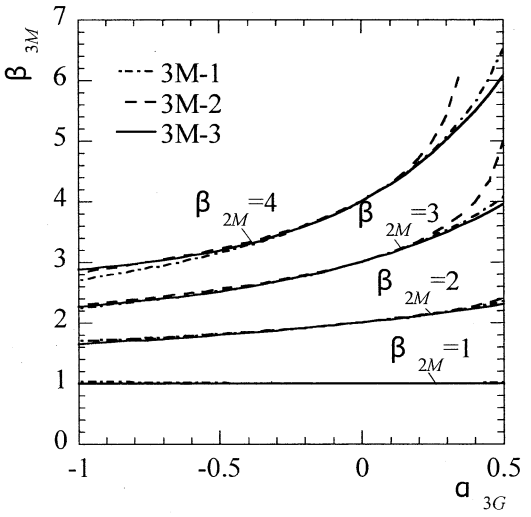

Fig. 3-1a $\beta_{3M\text{-}3}$ with respect to α_{3G}

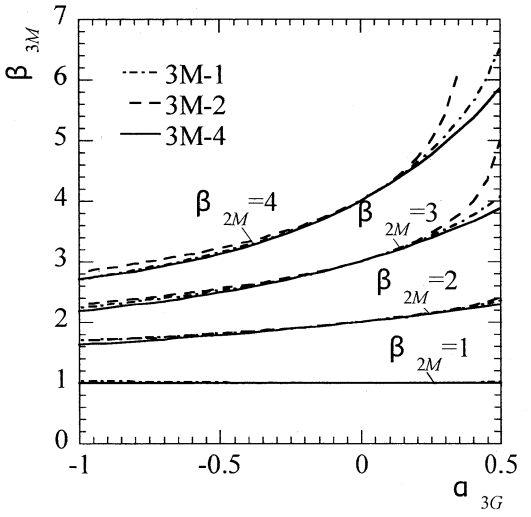

Fig. 3-1b $\beta_{3M\text{-}4}$ with respect to α_{3G}

The changes of $\beta_{3M\text{-}1}$, $\beta_{3M\text{-}2}$, and $\beta_{3M\text{-}3}$ with respect to β_{2M} are depicted in Figs. 3-2 and 3-3 for α_{3G} = 0.3, 0.6, 1.0 and −0.3, −0.6, −1.0. One can see that the differences among the three 3M reliability indices are smaller when α_{3G} is negative than when it is positive. Because $\beta_{3M\text{-}1}$ and $\beta_{3M\text{-}2}$ are not accurate when α_{3G} is large (i.e., positive), it is too early to evaluate the accuracy of $\beta_{3M\text{-}3}$ based only on comparison with $\beta_{3M\text{-}1}$ and $\beta_{3M\text{-}2}$.

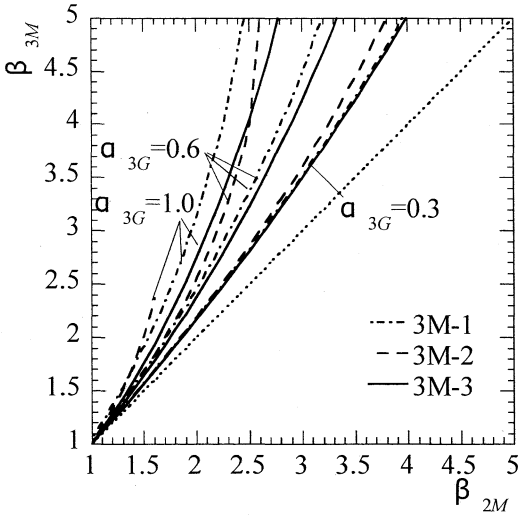

Fig. 3-2 $\beta_{3M\text{-}3}$ with respect to β_{2M} ($\alpha_{3G} > 0$)

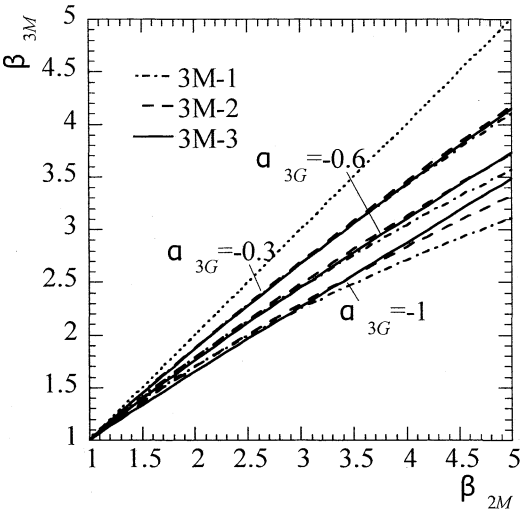

Fig. 3-3 $\beta_{3M\text{-}3}$ with respect to β_{2M} ($\alpha_{3G} < 0$)

In Tables 3-1 and 3-2, the relative difference is given as $r = 2|\beta_{av} - \beta_{3M\text{-}3}|/(\beta_{av} + \beta_{3M\text{-}3})$, where β_{av} is the average value of $\beta_{3M\text{-}1}$ and $\beta_{3M\text{-}2}$. It is shown that for the cases of $2 \leq \beta_{2M} \leq 4$ and $-1.0 \leq \alpha_{3G} \leq 0.3$, the relative difference remains at less than 5%. But $2 \leq \beta_{2M} \leq 4$ and $-1.0 \leq \alpha_{3G} \leq 0.3$ are not the applicable range of the proposed method. For the case of $\alpha_{3G} > 0.3$ or $\beta_{2M} > 4$, the relative difference is insignificant, because both $\beta_{3M\text{-}1}$ and $\beta_{3M\text{-}2}$ are inaccurate at this range. In other words, it is possible that the applicable range of the proposed method is wider than the existing methods, 3*M*-1 and 3*M*-2. Further comparison of the existing 3M methods and the MC simulation is given in Section 3.3.

Table 3-1 The relative difference between $\beta_{3M\text{-}1}$, $\beta_{3M\text{-}2}$, and $\beta_{3M\text{-}3}$ ($\alpha_{3G} > 0$)

β_{2M}	2.0			3.0			4.0			5.0		
$\alpha_{3G} > 0$	0.43	0.6	0.73	0.31	0.41	0.48	0.23	0.31	0.35	0.19	0.24	0.29
Relative difference	2%	5%	10%	2%	5%	10%	2%	5%	10%	2%	5%	10%

Table 3-2 The relative difference between $\beta_{3M\text{-}1}$, $\beta_{3M\text{-}2}$, and $\beta_{3M\text{-}3}$ ($\alpha_{3G} < 0$)

β_{2M}	2.0			3.0			4.0			5.0		
$\alpha_{3G} < 0$	−0.8	−1.72	−4.18	−1.6	−2.21	−15.74	−0.81	−1.13	−1.56	−0.57	−0.79	−1.09
Relative difference	2%	5%	10%	2%	5%	10%	2%	5%	10%	2%	5%	10%

3.2.3 The corresponding relationship between Z_u and u

According to Section 2.2.2.1 (Eq. (2-6)-(2-9)), the corresponding Z_u of Eq. (3-2a) can be expressed as

$$u = -\frac{1}{3} Z_u \left[2 + e^{\frac{1}{2}\alpha_{3G}\left(Z_u - \frac{1}{Z_u}\right)} \right] \tag{3-5}$$

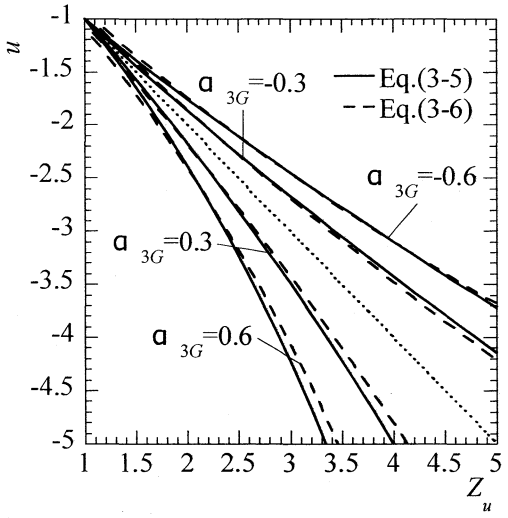

Fig. 3-4 Comparison of Eqs. (3-5) and (3-6)

Z_u can be expressed as the inverse function of Eq. (3-5). Because the inverse function of Eq. (3-2a) is nonexistent, the approximate function can be obtained and Z_u can be expressed as

$$Z_u = \frac{3.8}{\alpha_{3G}} \left[1 - e^{\frac{\alpha_{3G} u}{3.8}} \right] \tag{3-6}$$

In the case of α_{3G} equals −1 to 0.5 and Z_u equals −4.0 to −1.0, the errors of Eq. (3-6) compared with (3-5) are certified to be less than 7%, as shown in Fig. 3-4.

3.3 Application of the proposed reliability index

3.3.1 Influence of distribution type

3.3.1.1 Introduction of common distribution types

(1) The Normal distribution

The best known and most widely used probability distribution is undoubtedly Normal distribution. Its PDF for a continuous random variable X, is given by

$$f_X(x)=\frac{1}{\sigma\sqrt{2\pi}}\exp\left[-\frac{1}{2}\left(\frac{x-\mu}{\sigma}\right)^2\right] \qquad -\infty<x<\infty \tag{3-7}$$

where μ and σ are the mean and standard deviation of X.

(2) The Lognormal distribution

The random variable X is a Lognormal random variable if $Y = \ln(X)$ is normally distributed. The Lognormal distribution is also a popular probability distribution, its PDF is

$$f_X(x)=\frac{1}{\sqrt{2\pi}(\zeta x)}\exp\left[-\frac{1}{2}\left(\frac{\ln x-\lambda}{\zeta}\right)^2\right] \qquad x\geq 0 \tag{3-8}$$

where $\lambda = E(\ln X)$ and $\zeta=\sqrt{Var(\ln X)}$, are the parameters of the distribution, which means that these parameters are, respectively, also the mean and standard deviation of $\ln X$.

(3) The Gamma distribution

The PDF of a gamma random variable is useful for modeling sustained live load in buildings. In general, the Gamma distribution for a random variable X has the following PDF,

$$\begin{aligned} f_X(x)&=\frac{v(vx)^{k-1}}{\Gamma(k)}e^{-vx} \qquad x\geq 0 \\ &=0 \qquad\qquad\qquad x<0 \end{aligned} \tag{3-9}$$

where v and k are the parameters of the distribution, and $\Gamma(k)$ is the gamma function

$$\Gamma(k)=\int_0^\infty x^{k-1}e^{-x}dx \qquad \text{where } k\geq 1.0 \tag{3-10}$$

(4) Extreme Type 1 - the Gumbel distribution

Extreme value distributions, as the name implies, are useful to characterize the probabilistic nature of the extreme values (largest or smallest values) of some phenomenon over time, such as the wind speed. The PDF of the Gumbel distribution is

$$f_{Y_n}(y)=\alpha_n e^{-\alpha_n(y-u_n)}\exp\left[-e^{-\alpha_n(y-u_n)}\right] \tag{3-11}$$

in which

u_n — the most probable value of Y_n

α_n — an inverse measure of the dispersion of value of Y_n

(5) Extreme Type 2 - the Frechet distribution

The Frechet distribution sometimes gives the best approximation of the distribution of the maximum seismic load applied to a structure. The PDF is

$$f_X(x)=\frac{k}{u}\left(\frac{u}{x}\right)^{k+1}e^{-(u/x)^k} \tag{3-12}$$

where u and k are the distribution parameters.

(6) Extreme Type 3 - the Weibull distribution

The PDF is

$$f_X(x)=\begin{cases}\dfrac{k}{\lambda}\left(\dfrac{x}{\lambda}\right)^{k-1}e^{-(x/\lambda)^k} & x\geq 0\\ 0 & x<0\end{cases} \tag{3-13}$$

3.3.1.2 Influence analysis of distribution type

The simple $R-S$ reliability model is considered.

$$G(\mathrm{X})=R-S \tag{3-16}$$

where R and S are the interior resistance and the exterior deterioration load effect, respectively.

The statistical parameters of random variables are listed in Table 3-3, where $\mu_R = 50 \sim 100$ and $\mu_S = 30$ are the means of R and S, $v_R = 0.2$ and $v_S = 0.4$ are the coefficient of variation of R and S, respectively. The exact results are obtained using MC simulation for 10^6 samplings and the 2M results are given. The following six cases are investigated under the assumption that R and S obey different probability distributions (see Table 3-3).

For cases 1 - 6, as shown in Fig. 3-5, one can see that as the value of μ_R increases, the results of each 3M method moves further from the exact MC simulation. It is obvious that the 2M method is not accurate enough, while the proposed 3M method is in close agreement with the MC simulation in all cases. And it can be seen that the proposed 3M method has, either higher or at least the same accuracy as the existing methods.

Table 3-3 The probability distribution information of R and S in different cases

Case number	R	S
1	Normal	Lognormal
2	Normal	Gamma
3	Normal	Gumbel
4	Lognormal	Normal
5	Lognormal	Weibull
6	Weibull	Normal

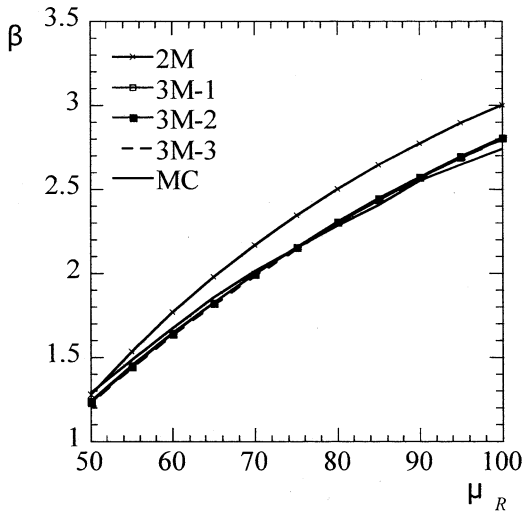

(a) Case 1

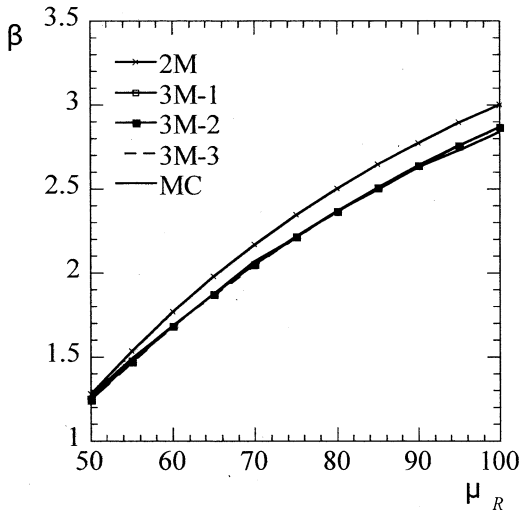

(b) Case 2

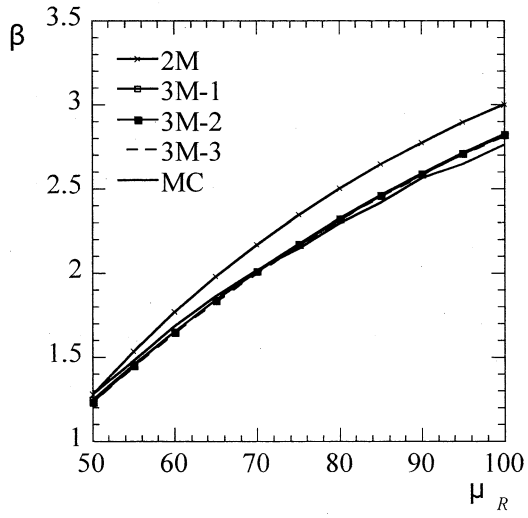

(c) Case 3

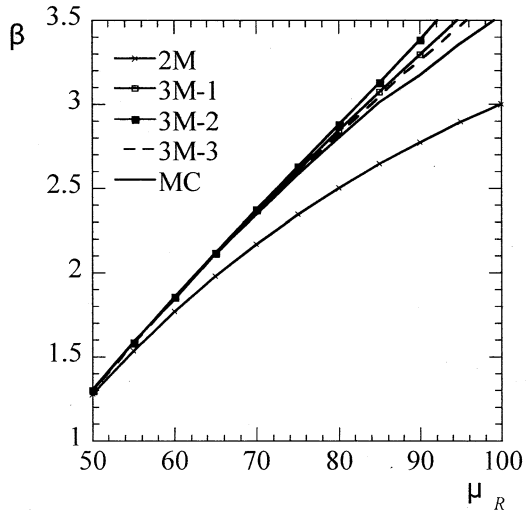

(d) Case 4

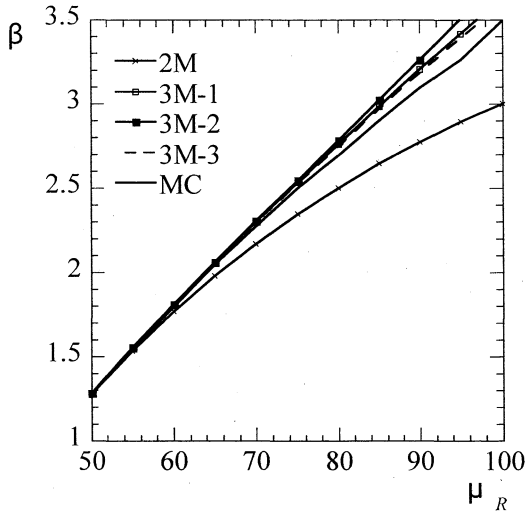

(e) Case 5

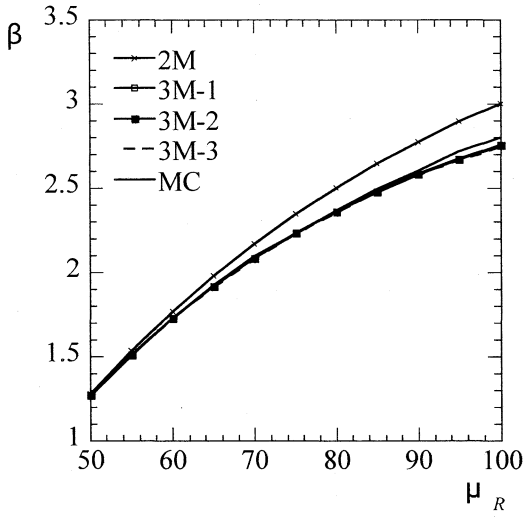

(f) Case 6

Fig.3-5 Relationship between the mean value of R and the reliability index

3.3.1.3 Error analysis of different methods

In order to verify the accuracy of different methods, the details of error is given in Fig. 3-6. The error is calculated by

$$r = \frac{|\beta_i - \beta_{MC}|}{\beta_{MC}} \times 100\% \tag{3-17}$$

where MC simulation is regarded as a comparing method.

From Figs. 3-6 (a) to (f) one can see, the error of 2M method is much greater than other 3M methods. In most cases, the error of 2M method is greater than 5%, while the error of 3M-3 is less than 5% in all cases. Since there is error in MC simulation, as introduced in Chapter 2, it is reasonable to regard error under 5% as accurate enough. In case 4 and case 5, the error of 3M-2 is also greater than 5% when α_{3G} varies, while the error of 3M-1 is also slightly larger than 3M-3. It's worth noting that in case 4 and case 5, when α_{3G} is positive the errors of three 3M methods are larger than that of α_{3G} is negative. And in the case of α_{3G} tends to 0, the errors of three 3M methods decrease, while the error of 2M increases as α_{3G} increases.

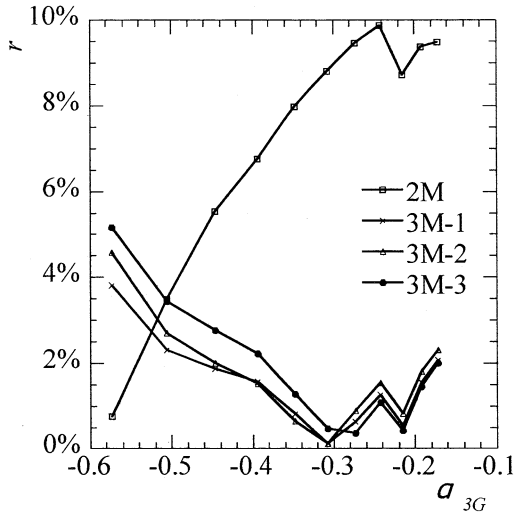

(a) Case 1

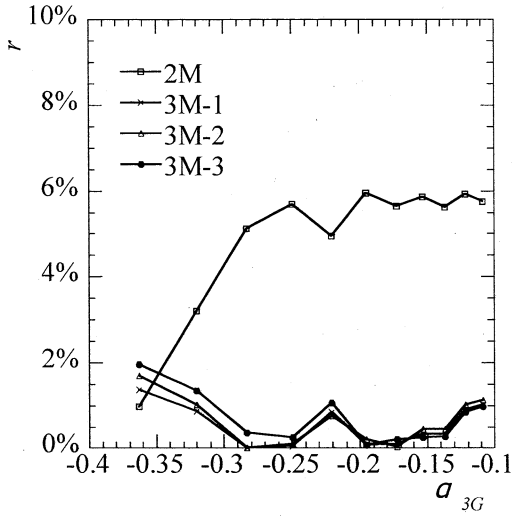

(b) Case 2

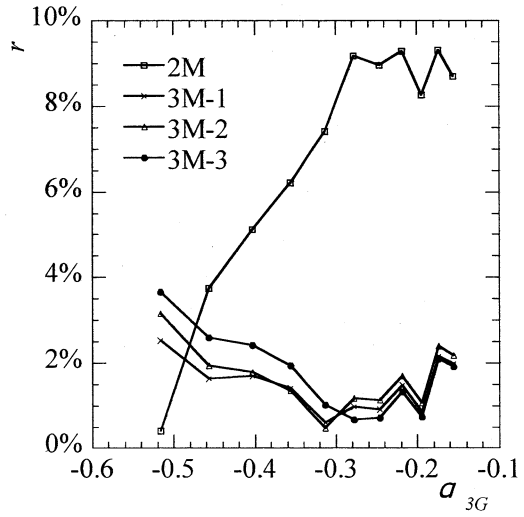

(c) Case 3

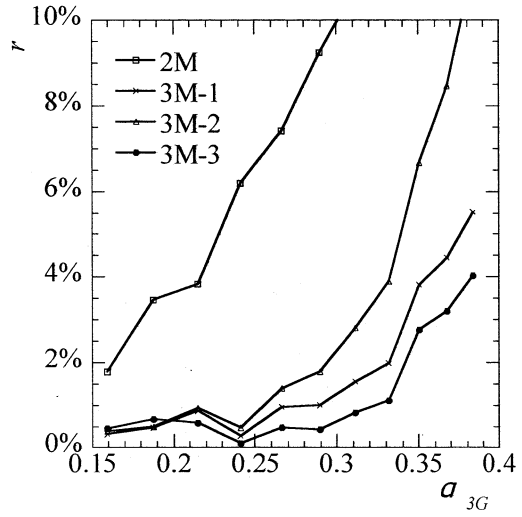

(d) Case 4

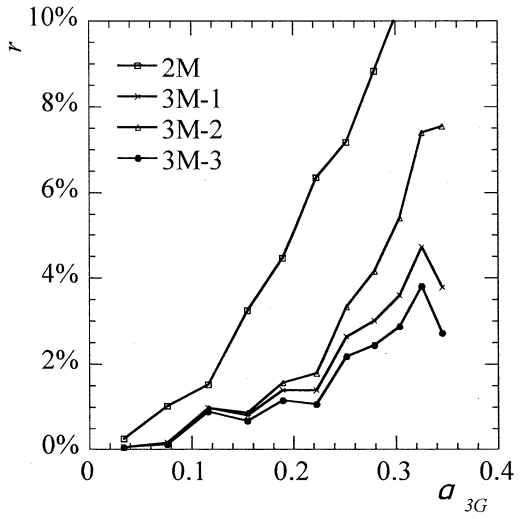

(e) Case 5

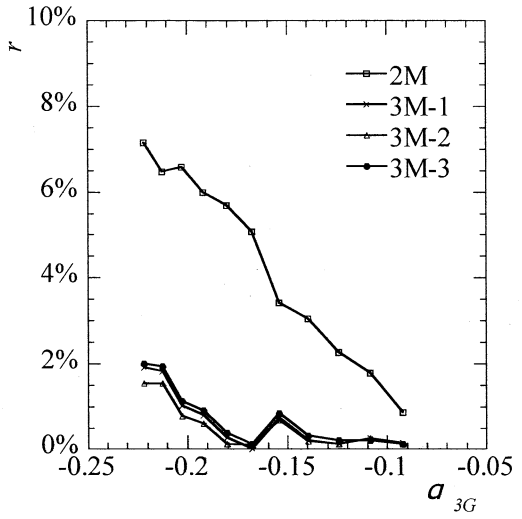

(f) Case 6

Fig.3-6 Error respect to α_{3G}

3.3.2 Influence of the number of load

Since in practical engineering design, the number of load may be much more than one. The following performance function is used to analyze the influence of the number of load on the accuracy of the proposed 3M method, where n = 2, 4, 6, 8, are considered.

$$G(\mathbf{X}) = R - \sum_{i=1}^{n} S_i \tag{3-18}$$

The distribution type of R and S_i are normal distribution and lognormal distribution, respectively, where the mean values of all loads are μ_{Si} = 30, v_R = 0.2 and v_{Si} = 0.4 are the coefficient of variation of R and S_i, respectively. The exact results are obtained using MC simulation for 10^6 samplings and the 2M results are given.

As shown in Fig. 3-7, the number of load has almost no influence on the reliability. Compared with MC simulation, the errors of all methods are lower than 5%. For the α_{3G} in all cases varies from -0.3 to 0, the results of all methods are consist with the result of MC simulation.

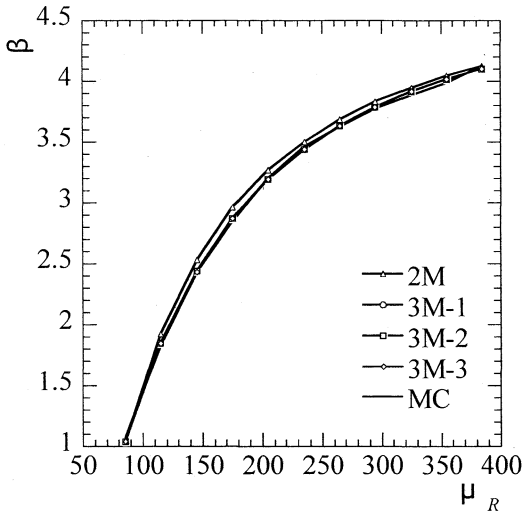

(a) 2 loads

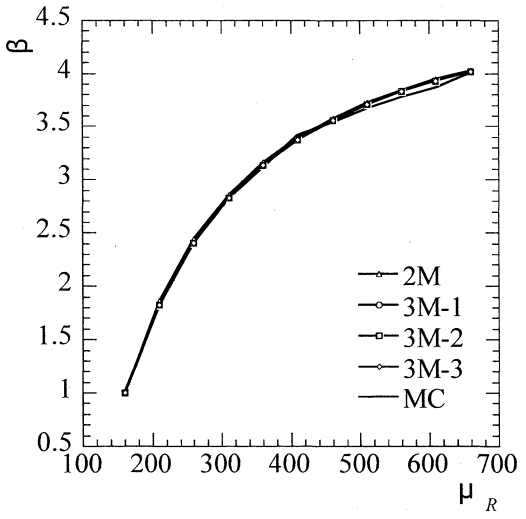

(b) 4 loads

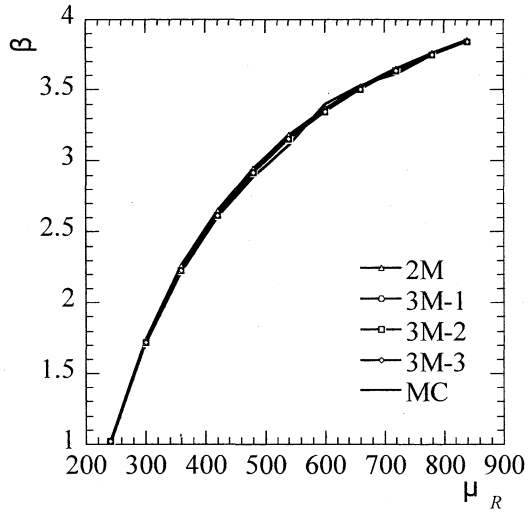

(c) 6 loads

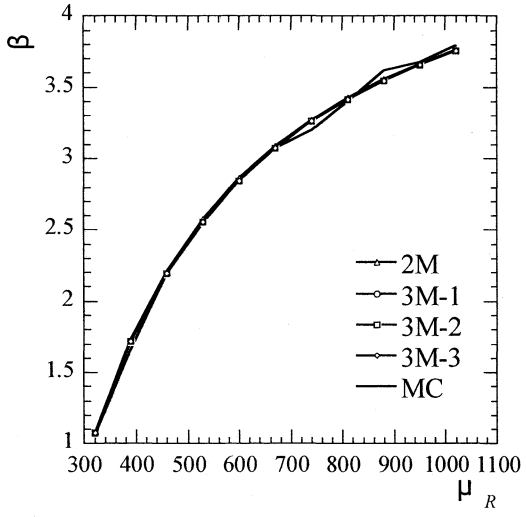

(d) 8 loads

Fig.3-7 Influence analysis of load number

3.3.3 Application in simple structure

Example 1

The analytical I-beam design problem, as shown in Fig. 3-8, introduced by [2] is considered.

The limit state function is given in terms of bending stress. The expression for the limit state can be defined as

$$G(\mathbf{X}) = \sigma_{\max} - S \tag{3-19}$$

where

$$\sigma_{\max} = \frac{Pa(L-a)d}{2LI} \tag{3-20a}$$

$$I = \frac{b_f d^3 - (b_f - t_w)(d - 2t_f)^3}{12} \tag{3-20b}$$

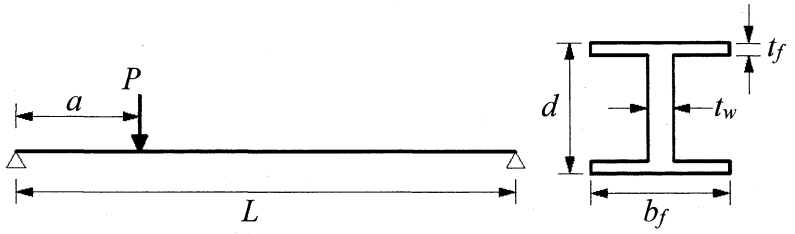

Fig.3-8 The cross section and load on the I-beam

The details of all the random variables are given in Table 3-4.

In this example, the first three moments of $G(\mathbf{X})$ can be obtained as $\mu_G = 455704$, $\sigma_G = 249347$, and $\alpha_{3G} = 1.098$. Reliability indices calculated by different methods are summarized in Table 5. The 2M is not applicable for an error of 24.04%, and the 3M-2 is out of its applicable range. Furthermore, for an error of 19.77%, the 3M-1 is considered inapplicable, as well. The 3M-3 is the only applicable method with an error as low as 5.11%.

Table 3-4 Parameters of random variables for Example 1

RVs	μ	v	Distribution
P	14000	0.4	Lognormal
L	120	0.2	Lognormal
a	72	0.08	Normal
S	170000	0.03	Normal
d	2.3	0.02	Normal
b_f	2.3	0.02	Normal
t_w	0.16	0.03	Normal
t_f	0.16	0.03	Normal

Table 3-5 Comparison of reliability indices for Example 1

Method	β	Error
2M	1.828	24.04%
3M-1	2.837	19.77%
3M-2	Out of range	—
3M-3	2.449	5.11%
MC	2.327	—

Example 2

A cantilever beam made of isotropic material, as shown in Fig. 3-9, is subjected to a distributed transverse load [3].

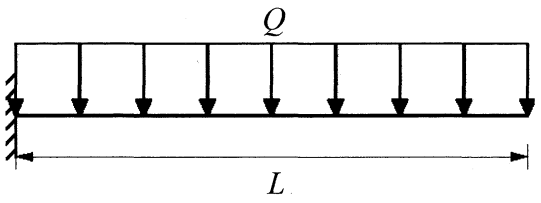

Fig. 3-9 Cantilever beam

The performance function is the tip displacement, which is expressed as

$$G(\mathbf{X}) = \delta_{cr} - \delta = \delta_{cr} - \frac{QL^4}{8EI} \tag{3-21}$$

where $\boldsymbol{X} = \{\delta_{cr}, Q, L, E, I\}$, δ_{cr} = 10 mm is the critical tip displacement (which is 1/500 of the length of the beam), Q is the constant distributed transverse load acting on the beam (μ_Q = 5 N/mm, v_Q = 0.3), L is the length of the beam (μ_L = 5000 mm, v_L = 0.04), E is the Young's modulus of the beam material (μ_E = 73000 N/mm^2, v_E = 0.01), and I is the moment of the cross-section ($\mu_I = 1.067\times10^9$ mm^4, $v_I = 0.001$). All of the random variables obey normal distribution.

In this example, the first three moments of $G(\mathbf{X})$ can be obtained as μ_G = 4.94, σ_G = 1.74, and $\alpha_{3G} = -0.388$. As shown in Table 3-6, the result of 2M is far from MC simulation, while the errors of all three 3M methods are in acceptable range. Because the result of 3M-3 has the lowest error, it is considered as the most accurate method.

Table 3-6 Comparison of reliability indices for Example 2

Method	β	Error
2M	2.838	13.93%
3M-1	2.482	0.54%
3M-2	2.499	1.22%
3M-3	2.476	0.30%
MC	2.469	—

Example 3

To demonstrate the application of 3M-1 to a more complicated problem involving several random variables, the moment capacity of a singly reinforced rectangular prismatic concrete beam is considered here. The moment capacity or resistance M_R of such a beam can be calculated using the following expression [4]:

$$M_R = A_s f_y d\left(1-\eta\frac{A_s}{bd}\frac{f_y}{f_c'}\right) \tag{3-22}$$

where

A_s — the area of the tension reinforcing bars;

f_y — the yield stress of the reinforcing bars;

d — the distance from the extreme compression fiber to the centroid of the tension reinforcing bars;

η — the concrete stress block parameter;

f_c' — the compressive strength of concrete;

b — the width of the compression face of the member.

It is extensively reported in the literature that all these variables are random. Their mean values and coefficients of variation are tabulated in Table 9. Assume further that the beam is subjected to a moment M, which is also a random variable. Its mean value and coefficient of variation are shown in Table 3-7.

The limit state function for the problem can be expressed as

$$G(\mathbf{X}) = A_s f_y d\left(1-\eta\frac{A_s}{bd}\frac{f_y}{f_c'}\right) - M \tag{3-23}$$

The probability distributions of the random variables in Eq. (3-23) are shown in Table 3-8. The results summarized in Table 3-9 clearly indicate that the distributions of random variables play a very important role in safety index or failure probability estimation.

Compared with MC simulation, the errors of 2M, 3M-1, 3M-2 and 3M-3 are given. It is obvious in all cases, the error of 3M-1 is the smallest in all methods.

Table 3-7 Design parameters of a reinforced concrete beam

RVs	Mean	Coefficient of variation
A_s (mm^2)	1006.45	0.036
f_y (MPa)	328.89	0.15
f_c' (MPa)	24.13	0.21
b (mm)	203.2	0.045
d (mm)	335.28	0.086
η	0.59	0.05
M (kN·m)	36.86	0.17

Table 3-8 Distributions of random variables in a reinforced concrete beam

RVs	Case 1	Case 2	Case 3	Case 4
A_s	Normal	Normal	Lognormal	Lognormal
f_y	Normal	Normal	Lognormal	Lognormal
f_c'	Normal	Normal	Lognormal	Lognormal
b	Normal	Normal	Lognormal	Lognormal
d	Normal	Normal	Lognormal	Lognormal
η	Normal	Normal	Lognormal	Lognormal
M	Normal	Lognormal	Normal	Lognormal

Table 3-9 Reliability indices calculated by different methods for Example 3

	Case 1		Case 2		Case 3		Case 4	
Method	β	Error	β	Error	β	Error	β	Error
2M	3.39	6.35%	3.39	5.04%	3.43	21.69%	3.43	14.68%
3M-1	3.78	4.42%	3.73	4.48%	4.59	4.79%	4.49	11.69%
3M-2	3.82	5.52%	3.75	5.04%	5.32	21.46%	5.00	24.38%
3M-3	3.77	4.14%	3.72	4.20%	4.45	1.60%	4.38	8.96%
MC	3.62	—	3.57	—	4.38	—	4.02	—

Example 4

As shown in Fig. 3-10, the horizontal displacement of a one-bay elastoplastic frame can be expressed as

$$\Delta = \frac{(D + L_S + S)HL^3}{12EI} \tag{3-24}$$

where D, L_S and S are the dead load, the live load and the snow load, respectively; E, I, H and L are the elasticity modulus, the area moment of inertia, the height and the length of the frame, respectively.

The limit state function is expressed as

$$G(\mathbf{X}) = \Delta_A - \Delta = \Delta_A - \frac{(D + L_S + S)HL^3}{12EI} \tag{3-25}$$

where Δ_A is the critical displacement of point A.

The details of random variables are shown in Table 3-10

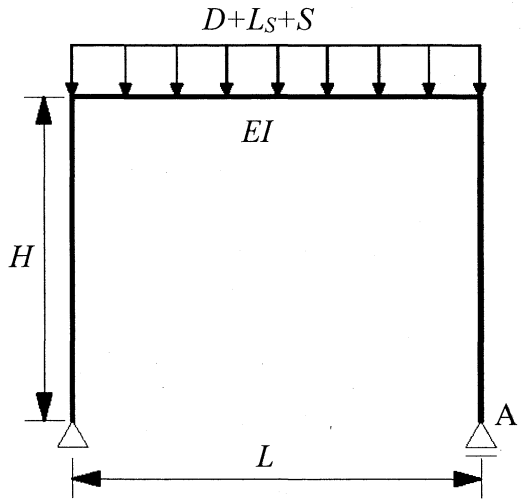

Fig. 3-10 One-story one-bay frames of Example 4

Table 3-10 Parameters of random variables for Example 4

RVs	Mean	Coefficient of variation	Distribution type
Δ	3 cm	0.1	Normal
E	2×10^{11} N/m^2	0.2	Normal
I	6.06×10^{-4} m^4	0.4	Lognormal
H	3 m	0.5	Gumbel
L	6 m	0.05	Lognormal
D	2×10^4 N/m	0.05	Lognormal
L_S	2×10^3 N/m	0.1	Lognormal
S	3×10^3 N/m	0.05	Lognormal

The α_{3G} in this example is -0.21. The calculated reliability indices and error are listed

in the Table 3-11. According to the results, the three 3M methods are accurate enough, while the 2M method is not applicable.

Table 3-11 Comparison of reliability indices for Example 4

Method	β	Error
2M	4.39	13.73%
3M-1	3.87	0.26%
3M-2	3.90	1.04%
3M-3	3.87	0.26%
MC	3.86	—

3.3.4 Application in system reliability

Example 1

This example is a one-bay elastoplastic frame, as shown in Fig. 3-11 [5],

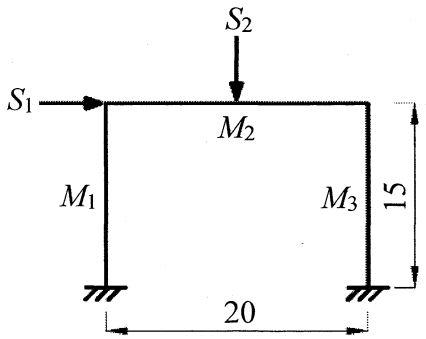

Fig. 3-11 One-story one-bay frames of Example 1

where M_1, M_2, and M_3 are the member strengths and S_1 and S_2 are the loads. The mean values of the random variables are $\mu_{M1} = \mu_{M2} = 500$ ft kip, $\mu_{M3} = 667$ ft kip, $\mu_{S1} = 50$ kip, and $\mu_{S2} = 100$ kip; the standard deviations are $\sigma_{M1} = \sigma_{M2} = 75$ ft kip, $\sigma_{M3} = 100$ft kip, $\sigma_{S1} = 15$ kip, and $\sigma_{S2} = 10$ kip.

The performance functions that correspond to the six most likely failure modes obtained from stochastic limit analysis are listed as follows:

$$g_1 = M_1 + 3M_2 + 2M_3 - 15S_1 - 10S_2 \tag{3-26a}$$

$$g_2 = 2M_1 + 2M_2 - 15S_1 \tag{3-26b}$$

$$g_3 = M_1 + M_2 + 4M_3 - 15S_1 - 10S_2 \tag{3-26c}$$

$$g_4 = 2M_1 + M_2 + M_3 - 15S_1 \quad \text{(3-26d)}$$

$$g_5 = M_1 + M_2 + 2M_3 - 15S_1 \quad \text{(3-26e)}$$

$$g_6 = M_1 + 2M_2 + M_3 - 15S_1 \quad \text{(3-26f)}$$

The performance function of the series system can be expressed as the minimum of the performance functions that corresponds to all potential failure modes, which is

$$G(\mathbf{X}) = \min\{g_1, g_2, g_3, g_4, g_5, g_6\} \quad \text{(3-27)}$$

Using the method found in [5], the first three moments of $G(\mathbf{X})$ can be obtained as μ_G = 1244.85, σ_G = 307.523, and α_{3G} = −0.307. With different methods, the reliability indices are β_{2M} = 4.048, $\beta_{3M\text{-}1}$ =3.438, $\beta_{3M\text{-}2}$ =3.480, and $\beta_{3M\text{-}3}$ =3.452. Three 3M methods are in good agreement.

Different types of distribution of the random variables were also assumed. Assuming all the member strengths and loads are Weibull random variables, the results of the different 3M methods and the MC simulation (10^6 samplings) are summarized in column 2 of Table 3-12. Results for Gamma, Gumbel, and Normal distributed random variables are also summarized in columns 3 to 5, respectively, in Table 3-12.

Table 3-12 Comparison of reliability indices for Example 1 with different types of PDFs

Method	Weibull	Gamma	Gumbel	Normal
2M	3.872 (13.51%)	4.040 (13.73%)	4.123 (27.1%)	3.980 (4.5%)
3M-1	3.572 (5.46%)	3.689 (4.90%)	3.556 (12.46%)	4.024 (5.59%)
3M-2	3.584 (5.80%)	3.713 (5.31%)	3.592 (13.46%)	4.024 (5.59%)
3M-3	3.573 (5.49%)	3.670 (4.14%)	3.566 (12.74%)	4.024 (5.59%)
MC	3.382	3.521	3.139	3.805

Note: Percentage of error in the reliability index relative to that of the MC simulation is in parenthesis.

From Table 3-12, one can observe that each of the three 3M methods is in close agreement with MC simulation, except for Gumbel distribution. In all cases, the proposed method is either more accurate than or as accurate as other methods.

Example 2

This example is a frame structure with two stories and two bays, as shown in Fig. 3-12. The mean values of the probabilistic member strength are $\mu_{M1} = \mu_{M2} = \mu_{M3} = \mu_{M6} = \mu_{M7}$ =70 ft kip, μ_{M5} = 120 ft kip, and μ_{M8} = 90 ft kip. The mean values of the probabilistic loads are μ_{S1} = 5 kip and $\mu_{S2} = \mu_{S4} = \mu_{S5}$ = 10 kip. The standard deviations of the member strength and loads are 0.15 and 0.25, respectively; the distributions of the member strength and loads are normal distribution and lognormal distribution, respectively.

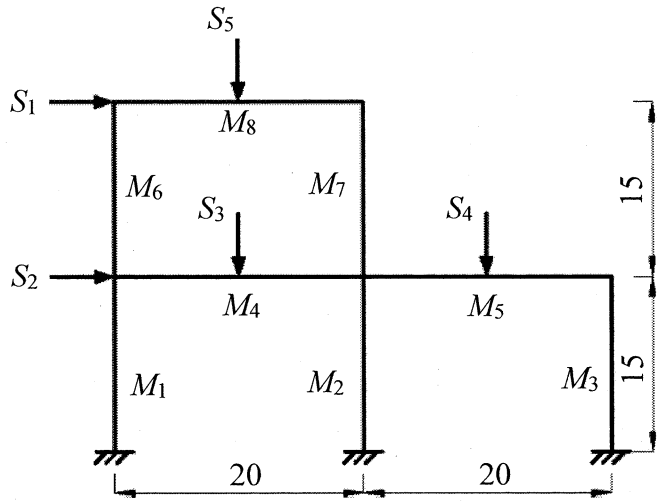

Fig. 3-12 The two-story two-bay frames of Example 2

The failure modes and corresponding performance functions are listed as follows:

$$g_1 = 2M_1 + 2M_2 + 2M_3 - 15S_1 - 15S_2 \quad (3\text{-}28a)$$

$$g_2 = M_6 + M_7 + 2M_8 - 10S_5 \quad (3\text{-}28b)$$

$$g_3 = M_3 + 3M_5 - 10S_4 \quad (3\text{-}28c)$$

$$g_4 = M_7 + 3M_8 - 10S_5 \quad (3\text{-}28d)$$

$$g_5 = 2M_1 + 2M_2 + M_3 + M_5 - 15S_1 - 15S_2 \quad (3\text{-}28e)$$

$$g_6 = M_6 + 3M_7 + 2M_8 - 15S_1 \quad (3\text{-}28f)$$

Table 3-13 Comparison of reliability indices for Example 2

Method	β	Error
2M	2.940	17.25%
3M-1	2.506	1.33%
3M-2	2.529	2.24%
3M-3	2.501	1.13%
MC	2.473	—

The performance function of the series system is the same as Eq. (3-27) in Example 1.

Using the method found in [5], the first three moments of $G(\mathbf{X})$ can be obtained as μ_G = 170.75, σ_G = 58.08, and α_{3G} = −0.457. With different methods, the results are listed in Table 3-13, which shows that the 2M result is far from MC simulation, while the error of 3M-1 and the proposed 3M-3 are accurate enough, with errors of less than 2%.

3.3.5 Application in other fields

Example 1

The proposed method is applicable in not only civil engineering but also other field. The performance function of a shaft in a speed reducer can be defined as

$$G(\mathbf{X}) = S - \frac{32}{\pi D^3}\sqrt{\frac{F^2L^2}{16} + T^2} \tag{3-29}$$

where $\boldsymbol{X} = \{S, D, F, L, T\}$;

S (MPa) — the material strength;

D (mm) — the diameter of the shaft;

F (N) — the external force, T (Nm) is the external torque;

L (mm) — the length of the shaft.

The performance function represents the difference between the strength and the maximum stress. The details of the random variables are given in Table 3-14.

Table 3-14 Parameters of random variables for Example 1

RVs	μ	v	Distribution
S	70	0.2	Lognormal
D	60	0.18	Normal
F	1500	0.5	Lognormal
L	400	0.2	Normal
T	250	0.2	Normal

Table 3-15 Comparison of reliability indices for Example 1

Method	β	Error
2M	3.529	27.82%
3M-1	2.171	20.52%
3M-2	2.248	17.08%
3M-3	2.407	10.26%
MC	2.667	—

The mean value, standard deviation, and skewness of $G(\mathbf{X})$ are obtained as $\mu_G = 61.05$, $\sigma_G = 17.30$, and $\alpha_{3G} = -1.898$, respectively. Because $|\alpha_{3G}|$ is large in this example, none of the methods are accurate; however, the 3M-3 provides the highest accuracy, as shown in Table 3-15. Its error of 10.26% is much lower than the error of 20.52% for 3M-1 and 17.08% for 3M-2.

3.4 Conclusions

Based on existing methods for calculating the 3M reliability index, this paper proposes a new 3M method in which the following improvements are considered valuable:

(1) The proposed method, with less mathematical limitation, is simpler for calculation of 3M reliability index than other existing 3M methods.

(2) Compared with other methods, the proposed method is accurate enough and its applicable range is much wider — especially in the case of negative α_{3G}. It is, therefore, considered applicable for cases out of the applicable range of existing methods.

Appendix

In the case of $\beta_{2M} \to 0^+$, if $A = e^{\frac{1}{2}\alpha_{3G}}$,

$$\begin{aligned}
\lim_{\beta_{2M}\to 0^+} \beta_{3M} &= \lim_{\beta_{2M}\to 0^+} \frac{1}{3}\beta_{2M}\left[2 + A^{\left(\beta_{2M} - \frac{1}{\beta_{2M}}\right)}\right] \\
&= \lim_{\beta_{2M}\to 0^+} \frac{1}{3}\beta_{2M}\left[2 + A^{\beta_{2M}} \cdot A^{-\frac{1}{\beta_{2M}}}\right] \\
&= \lim_{\beta_{2M}\to 0^+} \frac{1}{3}\beta_{2M}\left[2 + 1 \cdot \left(\frac{1}{A}\right)^{\frac{1}{\beta_{2M}}}\right]
\end{aligned} \tag{A-1}$$

In the case of $A \geq 1$ (i.e. $\alpha_{3G} \geq 0$),

$$\lim_{\beta_{2M}\to 0^+} \beta_{3M} = \lim_{\beta_{2M}\to 0^+} \frac{1}{3} \cdot 0[2 + 1 \cdot 0] = 0 \tag{A-2}$$

In the case of $A < 1$ (i.e. $\alpha_{3G} < 0$), if $x = 1/\beta_{2M}$

$$\lim_{\beta_{2M}\to 0^+}\beta_{3M}=\lim_{x\to+\infty}\frac{2+\left(\frac{1}{A}\right)^x}{3x}$$
$$=\lim_{B\to+\infty}\frac{\left(\frac{1}{A}\right)^x\cdot\ln\left(\frac{1}{A}\right)}{3}=+\infty \tag{A-3}$$

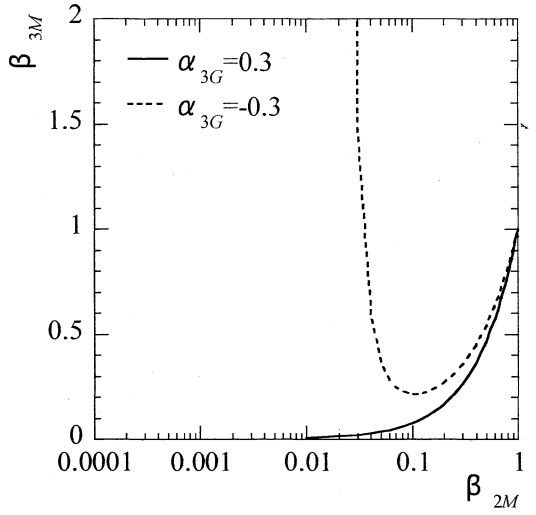

Fig. A β_{3M} with respect to β_{2M} in the case of $\beta_{2M}\to 0^+$.

The opposite result can be obtained when $\beta_{2M}\to 0^-$.

REFERENCES

[1] Zhao, Y.G. *et al.* A simple third-moment method for structural reliability. *Journal of Asian Architecture and Building Engineering*, 2006, 5 (1): 129-136.

[2] Huang B.Q. *et al.* Uncertainty analysis by dimension reduction integration and saddlepoint approximations. *Journal of Mechanical Design*, 2006, 128(1): 26-33.

[3] Huang B.Q. *et al.* Probabilistic uncertainty analysis by mean value first order saddlepoint approximation. *Reliability Engineering and System Safety*, 2008, 93(2): 325-336.

[4] Andrzej S. Nowak *et al. Reliability of Structures*, 2012.

[5] Zhao, Y.G. *et al.* System reliability assessment by method of moments. *J. of Struct. Engrg*, 2003, 129(10): 1341-1349.

CHAPTER 4

Load and resistance factors

4.1 Introduction

Load and resistance factor design (LRFD) is widely used in building codes for reliability design. The 3M method has been proposed to overcome the shortcomings (e.g. inevitable iterative computation, requirement of PDFs of random variables) of other existing methods. In existing 3M method, the iterative is simplified to one time, and the PDFs of random variables are not required. In this chapter, the proposed 3M-3 in Chapter 3 is used in the determination of load and resistance factors. The computation of the existing 3M method is further simplified to no iteration. And the accuracy of the proposed method is proved to be higher than the existing 3M methods. Additionally, with the proposed method, the limitations of applicable range in existing 3M methods are avoided. With the load combination and example in ASCE 7-10 and AIJ, the comparison of the existing 3M method, the ASCE method, the Mori method and the proposed method is given. The results show that the proposed method is accurate, simple, safe, and saving material.

4.2 Proposition of the new method

4.2.1 Computation process for LRFD

As introduced in Chapter 2, the LRFD format is expressed as

$$\varphi R_n \geq \sum_i \Sigma \gamma_i S_{ni} \tag{4-1}$$

The computation process is shown in Fig. 4-1. Before calculating the load and resistance factors, the target reliability index β_T and the distributions of loads should be decided. Then the target mean resistance should be calculated. With the target mean resistance and other variables, the load and resistance could be finally calculated.

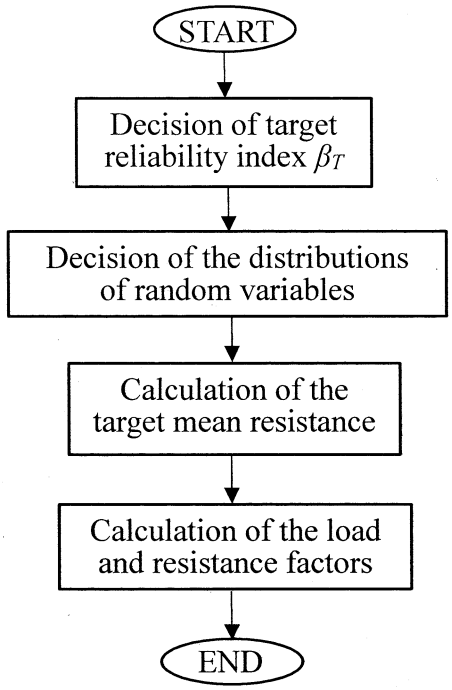

Fig. 4-1 Computation process of load and resistance factors

4.2.2 Simplification of the existing 3M method for LRFD

As introduced in Chapter 2, in the existing 3M method for LRFD, one time iteration for the calculation of the target mean resistance is necessary. In order to simplify the calculation process, the iteration is eliminated in the proposed method.

In the existing 3M method for LRFD, the second-moment target reliability is calculated by [1]

$$\beta_{2T} = \frac{3}{\alpha_{3G}}\left\{1-\exp\left[\frac{\alpha_{3G}}{3}\left(-\beta_T - \frac{\alpha_{3G}}{6}\right)\right]\right\} \tag{4-2}$$

which is the inverse function of the existing 3M reliability index, 3M-2 (introduced in Chapter 3).

In the proposed 3M method for LRFD, the second-moment target reliability is calculated by the inverse function of the proposed 3M reliability index, expressed as

$$\beta_{2T} = \frac{3.8}{\alpha_{3G}}\left[1-e^{\frac{-\alpha_{3G}\beta_T}{3.8}}\right] \tag{4-3}$$

For the inverse function of the proposed 3M reliability index is not exist, Eq. (4-3) is proposed as an approximate inverse function.

The steps for determining the load and resistance factors using the new method are as follows:

1. Calculate μ_{RT} using Eq. (4-4).

$$\mu_{RT} = \sum \mu_{S_i} + \sqrt{a\beta_T^x \sum \sigma_{S_i}^2} \tag{4-4}$$

where a and x are determined by linear fitting (more information below).

2. Calculate σ_G, α_{3G} and β_{2T} using Eq. (4-5), Eq. (4-6) and Eq. (4-3), respectively. Then calculate α_R and α_{Si} with Eq. (4-7).

$$\mu_G = \mu_R - \sum \mu_{S_i}, \quad \sigma_G = \sqrt{\sigma_R^2 + \sum \sigma_{S_i}^2} \tag{4-5}$$

$$\alpha_{3G} = \frac{1}{\sigma_G^3}\left(\alpha_{3R}\sigma_R^3 - \sum \alpha_{3S_i}\sigma_{S_i}^3\right) \tag{4-6}$$

$$\alpha_R = \frac{\sigma_R}{\sigma_G}, \quad \alpha_{S_i} = \frac{\sigma_{S_i}}{\sigma_G} \tag{4-7}$$

3. Determine the load and resistance factors with Eq. (4-8).

$$\phi = (1 - \alpha_R V_R \beta_T)\frac{\mu_R}{R_n} \tag{4-8a}$$

$$\gamma_i = (1 + \alpha_{Q_i} V_{Q_i} \beta_T)\frac{\mu_{Q_i}}{Q_{ni}} \tag{4-8b}$$

In the proposed method, there is no iteration calculation in step 1 and step 2, which is necessary in the existing 3M method for load and resistance factors.

4.2.3 Determination of *a* and *x*

In order to determine a and x in Eq. (4-4), a large amount of examples are used to obtain the target reliability. Then according to the target reliability, a and x can be achieved. One of the examples is introduced here. The performance function is

$$G(\mathbf{X}) = R - (G + Q) \tag{4-9}$$

where

R — the resistance, with unknown PDF, the coefficient of variation v_R = 0.2, the skewness α_R = 0.608.

G — the dead load, with unknown PDF, μ_G = 10, the coefficient of variation v_G = 0.1, the skewness α_G = 0.

Q — the living load, with unknown PDF, μ_Q = 5, the coefficient of variation v_G = 0.4, the skewness α_G = 1.264.

With the calculation process in Section 4.2.2, the load and resistance factors can be calculated. With the calculated load and resistance, finally the reliability can be obtained by MC simulation. When a = 1 and x = 2.7, the calculated reliability of the proposed method is in great agreement with the target reliability, as shown in Fig. 4-2, while the result of the existing method is far from the accurate value (the dotted line).

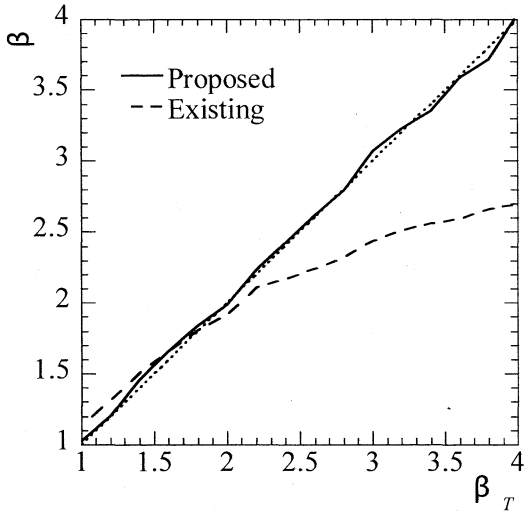

Fig. 4-2 Computed reliability with respect to the target reliability

Considering the influence of the number and variation of loads, the number of loads n and k are introduced, where

$$k = \frac{\sum_{i=1,j} \mu_{S_i} / j}{min(\mu_{S_i})} \tag{4-10}$$

The details of resistance and loads in 10 cases are listed in Table 4-1 to 4-10, in which the random variables in Table 2 is same with that in Eq. (4-9).

Table 4-1 Basic random variables in the case of n = 1

	Mean value	Coefficient of variation	Skewness
R	—	0.15	0.454
S_1	10	0.35	0.772

Table 4-2 Basic random variables in the case of n = 2

	Mean value	Coefficient of variation	Skewness
R	—	0.2	0.608
S_1	10	0.1	0
S_2	5	0.4	1.264

Table 4-3 Basic random variables in the case of $n = 3$

	Mean value	Coefficient of variation	Skewness
R	—	0.15	0
S_1	10	0.35	0.772
S_2	10	0.4	0.8
S_3	10	0.1	0.2

Table 4-4 Basic random variables in the case of $n = 4$

	Mean value	Coefficient of variation	Skewness
R	—	0.1	0.301
S_1	3	0.1	0
S_2	6	0.2	0.4
S_3	9	0.1	1.14
S_4	10	0.3	1.14

Table 4-5 Basic random variables in the case of $n = 5$

	Mean value	Coefficient of variation	Skewness
R	—	0.2	0
S_1	10	0.2	0.608
S_2	5	0.4	1.264
S_3	6	0.4	1.14
S_4	7	0.2	1.14
S_5	8	0.1	0

Table 4-6 Basic random variables in the case of $n = 6$

	Mean value	Coefficient of variation	Skewness
R	—	0.15	0
S_1	10	0.35	0.7
S_2	15	0.4	0.277
S_3	20	0.1	-0.175
S_4	25	0.2	0.4
S_5	30	0.2	1.14
S_6	10	0.1	0.301

Table 4-7 Basic random variables in the case of $n = 7$

	Mean value	Coefficient of variation	Skewness
R	—	0.2	0.608
S_1	5	0.4	0.277
S_2	10	0.5	1.14
S_3	15	0.25	0
S_4	20	0.35	0
S_5	15	0.1	0.2
S_6	10	0.1	0.2
S_7	5	0.2	0.4

Table 4-8 Basic random variables in the case of $n = 8$

	Mean value	Coefficient of variation	Skewness
R	—	0.2	0.608
S_1	5	0.2	-0.352
S_2	5	0.4	0.277
S_3	5	0.1	-0.715
S_4	5	0.4	0.277
S_5	10	0.2	0.608
S_6	30	0.1	0.2
S_7	30	0.4	1.14
S_8	30	0.1	0.301

Table 4-9 Basic random variables in the case of $n = 9$

	Mean value	Coefficient of variation	Skewness
R	—	0.15	0
S_1	7	0.35	1.14
S_2	13	0.26	1.14
S_3	24	0.5	0.566
S_4	19	0.3	-0.026
S_5	31	0.05	0
S_6	20	0.42	1.14
S_7	12	0.17	1.14
S_8	10	0.1	-0.715
S_9	11	0.02	0

Table 4-10 Basic random variables in the case of $n = 10$

	Mean value	Coefficient of variation	Skewness
R	—	0.1	0.301
S_1	20	0.2	0.608
S_2	10	0.3	-0.026
S_3	17	0.4	1.14
S_4	21	0.03	0
S_5	10	0.3	-0.026
S_6	19	0.12	0
S_7	25	0.2	0.4
S_8	29	0.4	0.8
S_9	30	0.01	0
S_{10}	15	0.2	-0.352

In order to obtain a reliability close to the target reliability, the values of a and x are calculated by trial computation. The relationship of x and n, and the relationship of x and k are given in Fig. 4-3 and Fig. 4-4, respectively. From Fig. 4-3, there is no distinct rule in the number of load n and x. As shown in Fig. 4-4 ($a = 1$), the fitting result is in great agreement with the results from 10 examples, where the value of Adj. R-Square is 0.98569. The fitting equation is

$$x = 1.8k \tag{4-11}$$

Therefore, Eq. (4-4) can be expressed as

$$\mu_{RT} = \sum \mu_{S_i} + \sqrt{\beta_T^{1.8k} \sum \sigma_{S_i}^2} \tag{4-12}$$

In the case of $1.8k \geq 5$, the target mean resistance calculated by Eq. (4-12) is too safe. Therefore in the case of $1.8k \geq 5$, Eq. (4-12) is expressed as

$$\mu_{RT} = \sum \mu_{S_i} + \sqrt{\beta_T^5 \sum \sigma_{S_i}^2} \tag{4-13}$$

Considering the mathematical definition of k, $k \geq 1$, accordingly, $x \geq 1.8$.

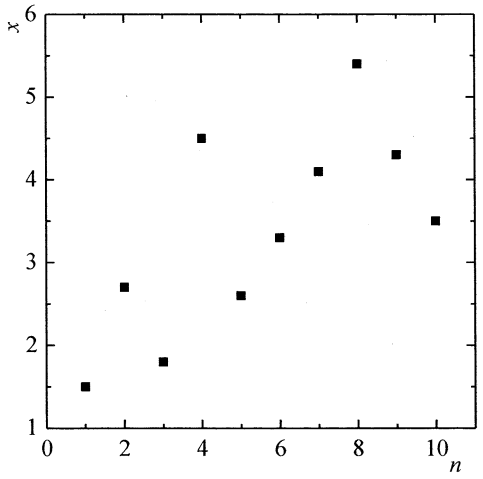

Fig. 4-3 The relationship of x and n

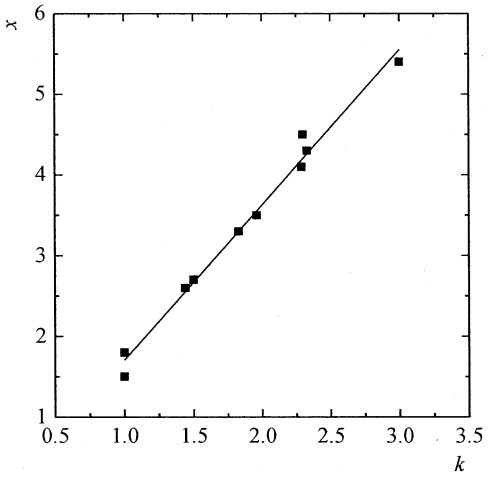

Fig. 4-4 The fitting result of x and k

4.3 Application of the proposed 3M method for load and resistance factors

4.3.1 Influence of numbers of load

With the details of random variables in Table 4-1 ~ 4-10 and the Eq. (4-12), the load and resistance factors can be calculated. Then the design mean resistance can be calculated with

$$\mu_d = \frac{1}{\phi}\sum \gamma_{S_i} \cdot \mu_{S_i} \tag{4-14}$$

As shown in Fig. 4-5(a) ~ (j), the design mean resistance μ_d is calculated with the existing 3M method and the proposed 3M method, respectively. It shows that μ_d calculated by the proposed 3M method is greater than that of the proposed 3M method in most cases. In a few cases, μ_d calculated by the proposed 3M method is almost the same with that of the existing 3M method.

For further analysis of the accuracy of two methods, with the design mean resistance, the reliability is calculated by MC simulation, as shown in Fig. 4-6(a) ~ (j). It shows that in all cases, the reliability calculated by the proposed 3M method is close to the target reliability (the dotted line), while the reliability calculated by the existing 3M method is far from the target reliability in some cases, such as Fig. 4-6(a), (b), (g), (h).

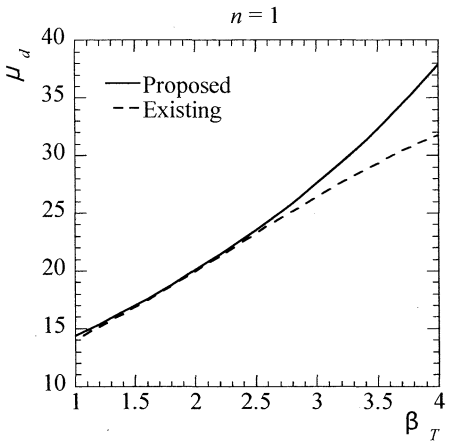
n = 1
μ d
Proposed
Existing
β T

(a)

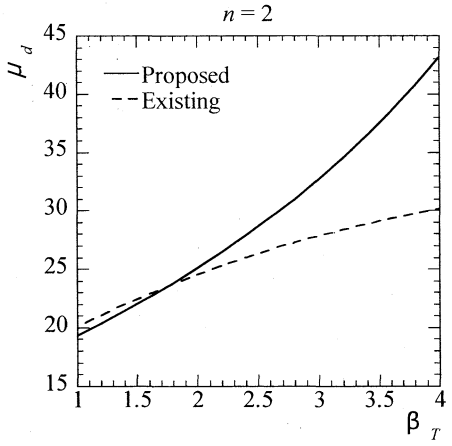
n = 2
μ d
Proposed
Existing
β T

(b)

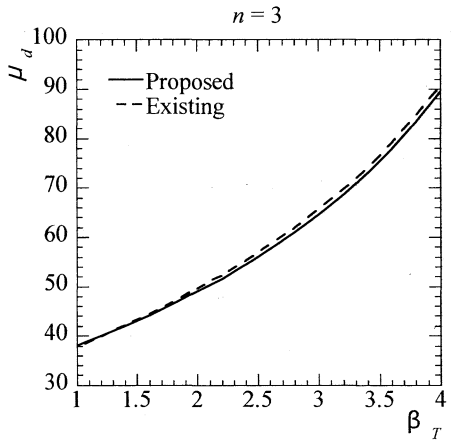
n = 3
μ d
Proposed
Existing
β T

(c)

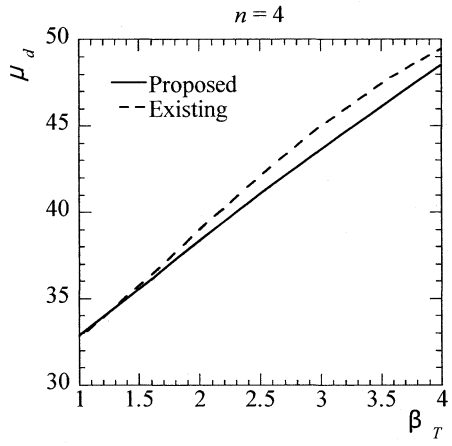
n = 4
μ d
Proposed
Existing
β T

(d)

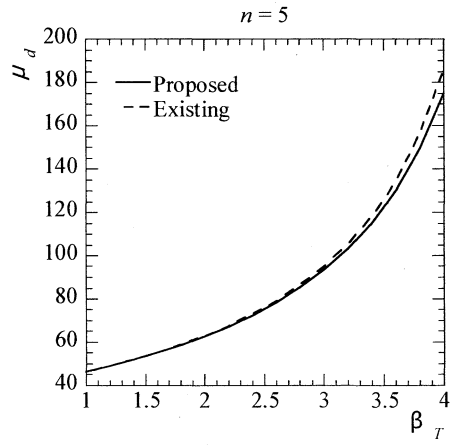
n = 5
μ d
Proposed
Existing
β T

(e)

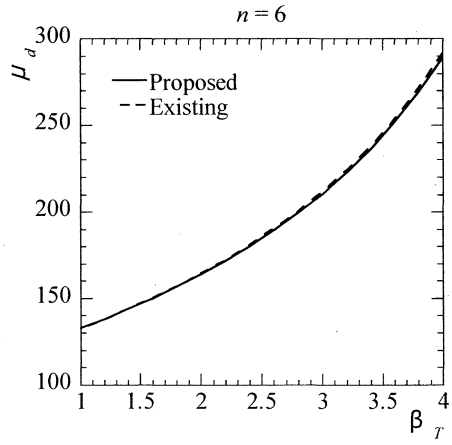
n = 6
μ d
Proposed
Existing
β T

(f)

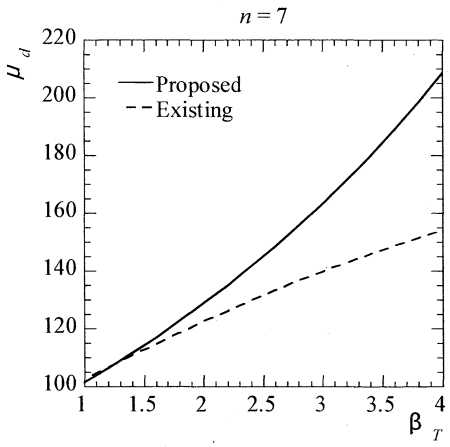

(g)

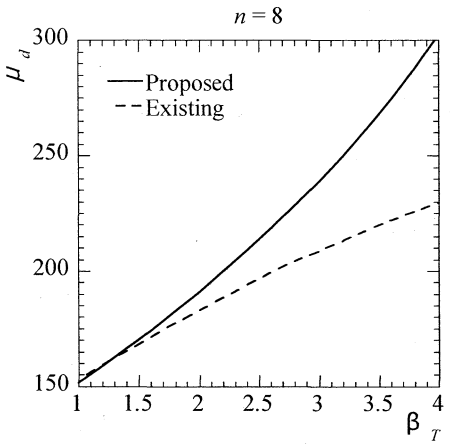

(h)

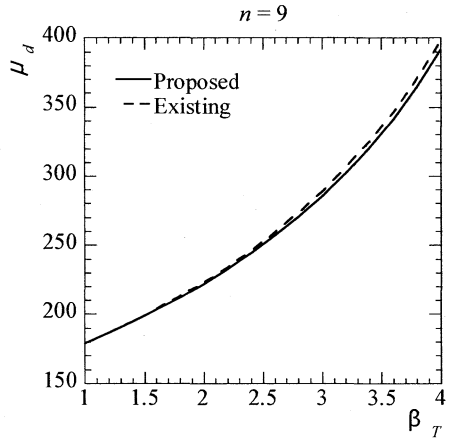

(i)

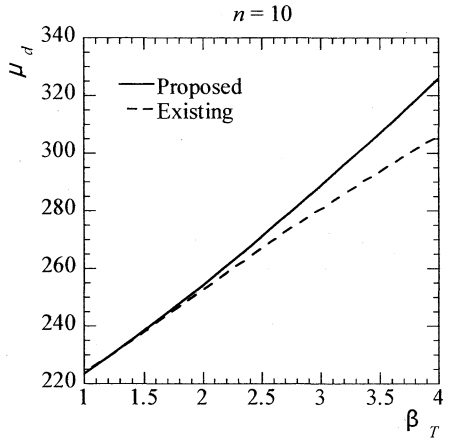

(j)

Fig. 4-5 The design mean resistance with respect to the target reliability

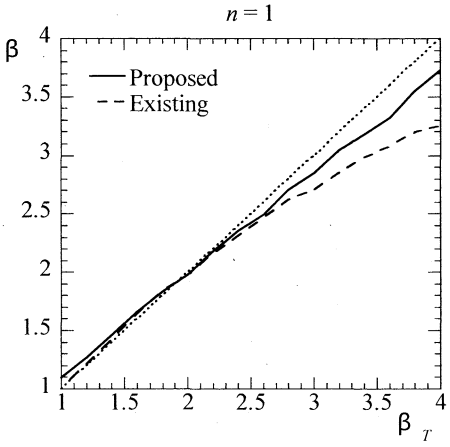

(a)

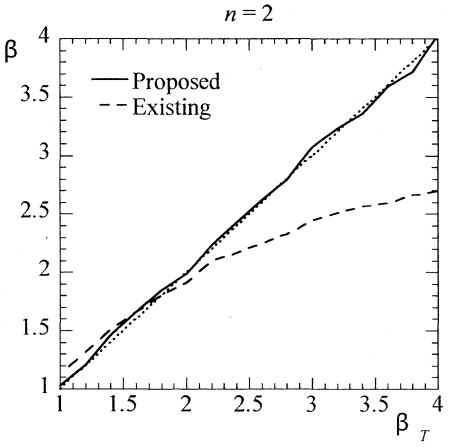

(b)

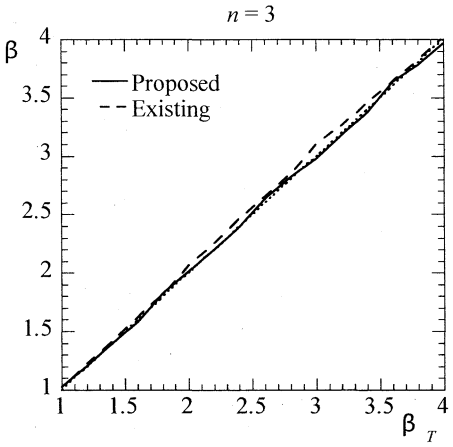
n = 3
Proposed
Existing
β
β T
1
1.5
2
2.5
3
3.5
4

(c)

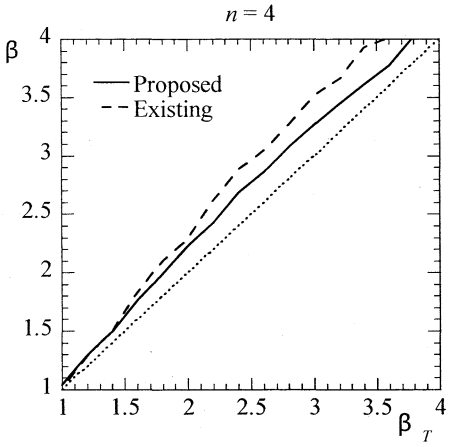
n = 4
Proposed
Existing
β
β T
1
1.5
2
2.5
3
3.5
4

(d)

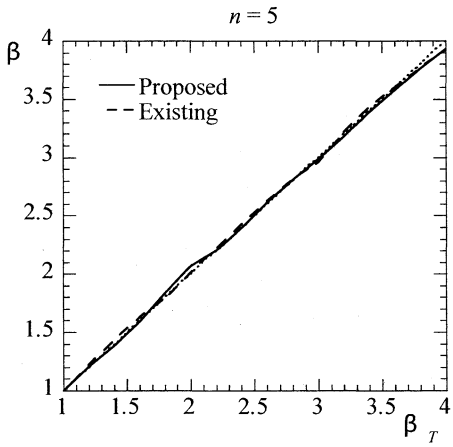
n = 5
Proposed
Existing
β
β T
1
1.5
2
2.5
3
3.5
4

(e)

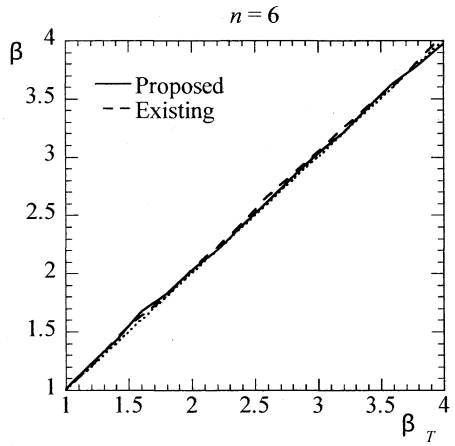
n = 6
Proposed
Existing
β
β T
1
1.5
2
2.5
3
3.5
4

(f)

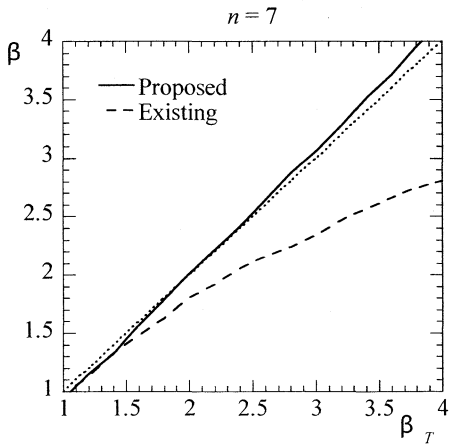
n = 7
Proposed
Existing
β
β T
1
1.5
2
2.5
3
3.5
4

(g)

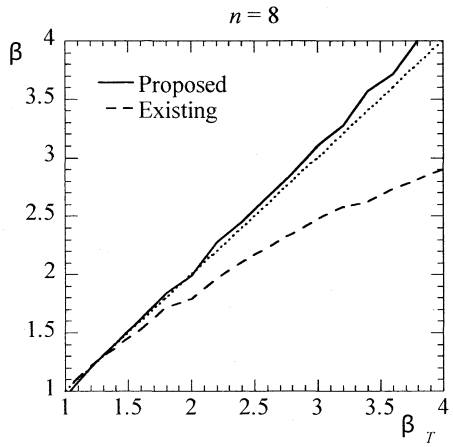
n = 8
Proposed
Existing
β
β T
1
1.5
2
2.5
3
3.5
4

(h)

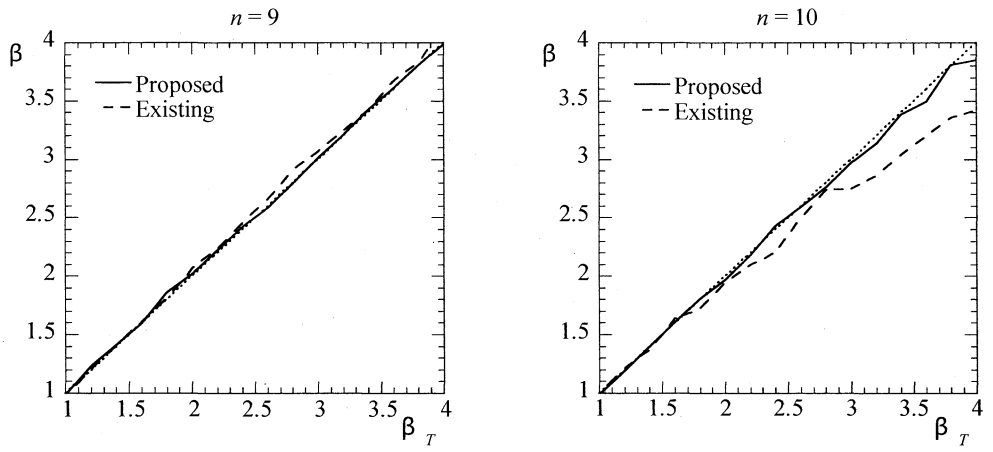

(i) (j)

Fig. 4-6 The calculated reliability with respect to the target reliability

4.3.2 Convergence of the proposed method

In order to compare the convergence of the existing 3M method and the proposed method, the following performance function is considered

$$G(\mathbf{X}) = R - (D + L + S) \tag{4-15}$$

where R, D, L and S are the resistance, dead load, live load and snow load, respectively. The details (the mean value, coefficient of variation and third moment) of the basic variables are same as that in Table 4-3.

As introduced before, there is one time iteration in the existing 3M method, while in the proposed 3M method there is no iteration. In order to compare the convergence property of the two methods, 5 time iterations are considered. As shown in Table 4-11, μ_{d0} is the design mean resistance calculated with no iteration, while μ_{di} is the design mean resistance calculated with i time iterations.

From the results for $\beta_T = 3$, after 3 times iteration, the convergence value of the design mean resistance can be obtained (regard 1% as the critical error) by the proposed 3M method, while 4 times iteration is necessary in the existing 3M method. The convergence speed of the proposed 3M method is slightly faster than the existing 3M method. Because of the convergence value of the design mean resistance is different of two method, further analysis is necessary. Based on the convergence value of the design mean resistance of two methods, the reliability calculated by MC simulation respect to the target reliability (1 ~ 4) is given. As shown in Fig. 4-7, both of the two method are not accurate. Compared with the existing 3M method, the reliability calculated by the convergence value of μ_d of

the proposed 3M method is closer to the accurate value.

Table 4-11 Design mean resistance calculated by iteration

Method	μ_{d0}	μ_{d1}	μ_{d2}	μ_{d3}	μ_{d4}	μ_{d5}
Existing formula	31.25	27.83	27.88	27.91	27.92	27.92
Proposed formula	32.72	29.19	29.44	29.42	29.42	29.42

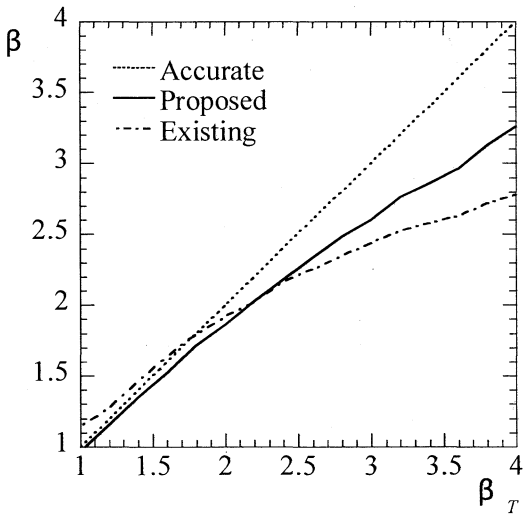

Fig. 4-7 Reliability calculated by convergence value of μ_d respect to the target reliability

4.3.3 Comparison of four methods

In order to compare the application of the proposed method, the following example is considered [2]. The load combination is same as Eq. (4-15). The details (the mean value, coefficient of variation and third moment) of the basic variables are shown in Table 4-12. Although the distribution types of loads and resistance are not necessary in the calculation of load and resistance factors, the distribution types are given for MC simulation.

Table 4-12 Basic random variables for ASCE example

RVs	μ_{Qi}/D_n	V_i	$\sigma_{Qi} = \mu_{Qi}/D_n \cdot V_i$	α_{3i}	μ_R/R_n or μ_{Qi}/Qi_n	Qi_n/D_n	Distribution
R	—	0.09	—	0.27	1.06	—	Lognormal
D	1	0.25	0.25	0	1.0	1	Normal
L	0.175	0.59	0.103	1.18	0.35	0.5	Gamma
S	0.6874	0.21	0.144	1.14	0.982	0.7	Gumbel

4.3.3.1 ASCE method

For target reliability $\beta_T = 3$, with the method in [2], the resistance factor can be calculated as

$$\phi = (\mu_R / R_n)\exp[-\alpha_R \beta V_R] = 0.877 \tag{4-16}$$

where the sensitivity coefficient of resistance $\alpha_R = 0.7$ is an approximate value which introduced in [2].

And the load factors can be calculated as

$$\gamma_D = (\mu_D / D_n)(1 + \alpha_D \beta V_D) = 1.600 \tag{4-17}$$

$$\gamma_L = (\mu_L / L_n)(1 + \alpha_L \beta V_L) = 0.598 \tag{4-18}$$

$$\gamma_S = (\mu_S / S_n)(1 + \alpha_S \beta V_S) = 1.229 \tag{4-19}$$

As introduced in [2], α_Q is a sensitivity coefficient of load that is approximately equal to 0.8 when load Q is a principal action and 0.4 when Q is a companion action.

4.3.3.2 Mori method

Step 1, the distributions of all loads should be transformed into lognormal distribution. According to Eq. (2.4.17), (2.4.18) and (2.4.25) of [3], gumbel distribution of the snow load can be turn to Lognormal distribution by

$$\lambda_S^* = \ln(1 - 0.164 V_S) = -0.035 \tag{4-20}$$

$$\zeta_S = 0.430 \times \ln\left(\frac{1 + 3.14 V_S}{1 - 0.164 V_S}\right) = 0.233 \tag{4-21}$$

$$V_S = \sqrt{\exp(\zeta_S^2) - 1} = 0.236 \tag{4-22}$$

Similarly, the Normal distribution of the dead load and the Gamma distribution of the live load can be transformed into lognormal distribution:

$$\lambda_D^* = 0 \tag{4-23}$$

$$\zeta_D = 0.012 + 0.830 V_D - 0.473 V_D^2 + 0.111 V_D^3 = 0.192 \tag{4-24}$$

$$V_D = \sqrt{\exp(\zeta_D^2) - 1} = 0.194 \tag{4-25}$$

$$\lambda_L^* = 0.002 - 0.022 V_L - 0.267 V_L^2 - 0.079 V_L^3 = -0.120 \tag{4-26}$$

$$\zeta_L = 0.009 + 0.925 V_L - 0.205 V_L^2 + 0.087 V_L^3 = 0.501 \tag{4-27}$$

$$V_L = \sqrt{\exp(\zeta_L^2) - 1} = 0.534 \tag{4-28}$$

Step 2, the sensitivity coefficients of loads and resistance can be obtained by the following calculation.

According to Eq. (4-27), c_S, c_D, c_L can be calculated.

$$c_i = \frac{\exp\left(\lambda_{Q_i}^* + \frac{1}{2}\sigma_{\ln Q_i}^2\right)\frac{Q_{ni}}{D_n}\frac{\mu_{Q_i}}{Q_{ni}}}{\sum_j \exp\left(\lambda_{Q_j}^* + \frac{1}{2}\sigma_{\ln Q_i}^2\right)\frac{Q_{nj}}{D_n}\frac{\mu_{Q_j}}{Q_{nj}}} \tag{4-29}$$

$$c_S = 0.363, \quad c_D = 0.543, \quad c_L = 0.094 \tag{4-30}$$

Then α_R^* and α_S^* are expressed as

$$\alpha_R^* = \frac{\sigma_{\ln R}}{\sqrt{\sigma_{\ln R}^2 + \sum_j \left(c_j \cdot \sigma_{\ln Q_j}\right)}} \tag{4-31}$$

$$\alpha_{Q_i}^* = \frac{c_i \cdot \sigma_{\ln Q_i}}{\sqrt{\sigma_{\ln R}^2 + \sum_j \left(c_j \cdot \sigma_{\ln Q_j}\right)}} \tag{4-32}$$

where

$$\sigma_{\ln R} = \sqrt{\ln\left(1 + V_R^2\right)} = 0.090 \tag{4-33}$$

The results of α_R^* and α_S^* are

$$\alpha_R^* = 0.369, \quad \alpha_S^* = 0.347, \quad \alpha_D^* = 0.427, \quad \alpha_L^* = 0.193 \tag{4-34}$$

$$u = \frac{1.05}{1 - \left\{1 - \sqrt{\left(\alpha_R^*\right)^2 + \left(\max\alpha_{Q_i}^*\right)^2}\right\} \cdot \Phi\left(\frac{\max V_{Q_i} - 0.6}{0.4}\right)} = 1.335 \tag{4-35}$$

The sensitivity coefficients of loads and resistance can be calculated as

$$\alpha_R = \alpha_R^* \cdot u = 0.493 \tag{4-36}$$

$$\alpha_S = \alpha_S^* \cdot u = 0.463 \tag{4-37}$$

$$\alpha_D = \alpha_D^* \cdot u = 0.570 \tag{4-38}$$

$$\alpha_L = \alpha_L^* \cdot u = 0.258 \tag{4-39}$$

Step 3, the load and resistance factors can be determined.

$$\phi = \frac{1}{\sqrt{1 + V_R^2}} \exp\left(-\alpha_R \beta_T \sigma_{\ln R}\right) \frac{\mu_R}{R_n} = 0.924 \tag{4-40}$$

$$\gamma_S = \frac{1}{\sqrt{1 + V_S^2}} \exp\left(\alpha_S \beta_T \sigma_{\ln S}\right) \frac{\mu_S}{S_n} = 1.328 \tag{4-41}$$

Similarly,

$$\gamma_D = 1.352 \tag{4-42}$$

$$\gamma_L = 0.444 \tag{4-43}$$

4.3.3.3 The Existing 3M method

With 5 steps of the existing 3M method, the load and resistance factors can be calculated.

Step 1, the original target mean resistance can be obtained

$$\mu_{R_0} = \sum \mu_{Q_i} + \sqrt{\beta_T^{3.5} \sum \sigma_{Q_i}^2} = 3.959 \tag{4-44}$$

Step 2, σ_G, α_{3G} and β_{2T} can be obtained

$$\sigma_G = \sqrt{\sigma_R^2 + \sum \sigma_{Q_i}^2} = 0.470 \tag{4-45}$$

where $\sigma_R = \mu_{R_0} \cdot V_R = 0.356$

$$\alpha_{3G} = \frac{1}{\sigma_G^3}\left(\alpha_{3R}\sigma_R^3 - \sum \alpha_{3Q_i}\sigma_{Q_i}^3\right) = 0.072 \tag{4-46}$$

$$\beta_{2T} = \frac{3}{\alpha_{3G}}\left\{1 - \exp\left[\frac{\alpha_{3G}}{3}\left(-\beta_T - \frac{\alpha_{3G}}{6}\right)\right]\right\} = 2.906 \tag{4-47}$$

Step 3, the target mean resistance μ_{RT} can be obtained

$$\mu_{RT} = \sum \mu_{Q_i} + \beta_{2T}\sigma_G = 3.228 \tag{4-48}$$

Step 4, repeat step 2 with μ_{RT}, σ_G, α_{3G} and β_{2T} are obtained as

$$\sigma_G = \sqrt{\sigma_R^2 + \sum \sigma_{Q_i}^2} = 0.422 \tag{4-49}$$

where $\sigma_R = \mu_{RT} \cdot V_R = 0.291$

$$\alpha_{3G} = \frac{1}{\sigma_G^3}\left(\alpha_{3R}\sigma_R^3 - \sum \alpha_{3Q_i}\sigma_{Q_i}^3\right) = 0.025 \tag{4-50}$$

$$\beta_{2T} = \frac{3}{\alpha_{3G}}\left\{1 - \exp\left[\frac{\alpha_{3G}}{3}\left(-\beta_T - \frac{\alpha_{3G}}{6}\right)\right]\right\} = 2.967 \tag{4-51}$$

Then the corresponding sensitivity coefficients of loads and resistance are

$$\alpha_R = \frac{\sigma_R}{\sigma_G} = 0.688 \tag{4-52}$$

$$\alpha_D = \frac{\sigma_D}{\sigma_G} = 0.592 \tag{4-53}$$

$$\alpha_L = \frac{\sigma_L}{\sigma_G} = 0.244 \tag{4-54}$$

$$\alpha_S = \frac{\sigma_S}{\sigma_G} = 0.342 \tag{4-55}$$

Step 5, the load and resistance factors can be finally determined

$$\phi = (1 - \alpha_R V_R \beta_{2T}) \frac{\mu_R}{R_n} = 0.865 \tag{4-56}$$

$$\gamma_D = (1 + \alpha_D V_D \beta_{2T}) \frac{\mu_D}{D_n} = 1.439 \tag{4-57}$$

$$\gamma_L = (1 + \alpha_L V_L \beta_{2T}) \frac{\mu_L}{L_n} = 0.500 \tag{4-58}$$

$$\gamma_S = (1 + \alpha_S V_S \beta_{2T}) \frac{\mu_S}{S_n} = 1.191 \tag{4-59}$$

4.3.3.4 The proposed 3M method

With 3 steps of the proposed method, the load and resistance factors can be calculated.

Step 1, in this example, $k = 3.55$, $1.8k \geq 5$, therefore the target mean resistance can be obtained with Eq. (4-13)

$$\mu_{RT\text{-new}} = \sum \mu_{Q_i} + \sqrt{\beta_T^5 \sum \sigma_{Q_i}^2} = 6.638 \tag{4-60}$$

Step 2, σ_G, α_{3G} and β_{2T} can be obtained, respectively

$$\sigma_G = \sqrt{\sigma_R^2 + \sum \sigma_{Q_i}^2} = 0.671 \tag{4-61}$$

where $\sigma_R = \mu_{RT} \cdot V_R = 0.597$

$$\alpha_{3G} = \frac{1}{\sigma_G^3} \left(\alpha_{3R} \sigma_R^3 - \sum \alpha_{3Q_i} \sigma_{Q_i}^3 \right) = 0.175 \tag{4-62}$$

$$\beta_{2T} = \frac{3.8}{\alpha_{3G}} \left[1 - e^{\frac{-\alpha_{3G} \beta_T}{3.8}} \right] = 2.802 \tag{4-63}$$

Then the corresponding sensitivity coefficients of loads and resistance are

$$\alpha_R = \frac{\sigma_R}{\sigma_G} = 0.890 \tag{4-64}$$

$$\alpha_D = \frac{\sigma_D}{\sigma_G} = 0.372 \tag{4-65}$$

$$\alpha_L = \frac{\sigma_L}{\sigma_G} = 0.153 \tag{4-66}$$

$$\alpha_S = \frac{\sigma_S}{\sigma_G} = 0.214 \tag{4-67}$$

Step 3, the load and resistance factors can be finally calculated

$$\phi = (1 - \alpha_R V_R \beta_{2T}) \frac{\mu_R}{R_n} = 0.822 \tag{4-68}$$

$$\gamma_D = (1 + \alpha_D V_D \beta_{2T}) \frac{\mu_D}{D_n} = 1.261 \tag{4-69}$$

$$\gamma_L = (1 + \alpha_L V_L \beta_{2T}) \frac{\mu_L}{L_n} = 0.439 \tag{4-70}$$

$$\gamma_S = (1 + \alpha_S V_S \beta_{2T}) \frac{\mu_S}{S_n} = 1.106 \tag{4-71}$$

4.3.3.5 Results comparison

The results of load and resistance factors in different methods are listed in Table 4-13. The results show that the resistance factors ϕ calculated by three methods are in great agreement. The results of the dead load factor γ_D are also close, while γ_L and γ_S calculated by Mori method is different from that of other methods.

In order to compare the accuracy of four methods, with the load and resistance factors in Table 4-13, the design mean resistance is also calculated with

$$\frac{\mu_R}{D_n} = \frac{\mu_R}{R_n} \cdot \frac{R_n}{D_n} = \frac{\mu_R}{R_n} \cdot \frac{1}{\phi} \left(\gamma_D \cdot \frac{D_n}{D_n} + \gamma_L \cdot \frac{L_n}{D_n} + \gamma_S \cdot \frac{S_n}{D_n} \right) \tag{4-72}$$

As shown in Table 4-14, the design mean resistance calculated by ASCE method is the largest, while result of Mori method is the smallest. The results of the proposed 3M method is slightly larger than the existing 3M method.

Table 4-13 Results of load and resistance factors

	ϕ	γ_D	γ_L	γ_S
ASCE method	0.877	1.600	0.598	1.229
Mori method	0.924	1.328	1.352	0.444
Existing 3M method	0.865	1.439	0.500	1.191
Proposed method	0.822	1.261	0.439	1.106

Table 4-14 Results of design mean resistance

Method	ASCE method	Mori method	Existing 3M method	Proposed 3M method
μ_R/D_n	3.335	2.656	3.091	2.907

With the design mean resistance and the values of μ_D/D_n, μ_L/D_n and μ_S/D_n, the reliability calculated by MC simulation (100,000 samples) are shown in Table 4-15, reliability 3.02 of the proposed 3M method is closest to the target reliability 3.0. Therefore, the proposed 3M method is considered accurate and safe. The existing 3M method is also accurate and safe, but in this method, there are a lot of limitations and one time iteration is inevitable. The ASCE method is much simple, but the reliability by this method is much greater than the target reliability, which is safe but waste of structural materials. Conversely, the reliability calculated by Mori method is much smaller than the target reliability, which means the design is not safe.

Table 4-15 Reliability of MC simulation with different methods

	ASCE method	Mori method	Existing 3M method	Proposed method
β	3.53	2.46	3.08	3.02

The advantages and disadvantages of different methods are listed in Table 4-16. ASCE method is simple and applicable for most structures. But it is too safe for reliability design, which means it is a waste of material. Mori method in this example is difficult and not safe. In the case of the distributions of resistance and loads are very different from lognormal distribution, the calculation error may be large in Mori method [4]. The existing 3M method is safe and material-saving, but the calculation is difficult for designers for one time iteration is necessary. And there are limitations of applicable range. The proposed 3M method is accurate, safe, material-saving, without any mathematical limitations and no necessary for iteration calculation. Therefore the proposed 3M method is considered to be the most applicable for practical structural reliability design.

Table 4-16 Comparison of different methods

	ASCE method	Mori method	Existing 3M method	Proposed method
Applicable range	Large	Large	Narrow	large
Safety degree	Safe	Dangerous	Safe	Safe
Material saving degree	Waste	Saving	Medium	Saving
Difficulty degree	Simple	Difficult	Difficult	Medium

4.3.4 Design for wind load

4.3.4.1 The calculation of wind load and other variables

Based on the method in [3], the horizontal wind load can be expressed as

$$W_D = q_H C_D G_D A \tag{4-73}$$

$$q_H = \frac{1}{2}\rho U_H^2 \tag{4-74}$$

$$U_H = U_0 k_{Rw} K_D K_S E_H \tag{4-75}$$

where

W_D — wind load (N) at hight Z (m) (from ground);

q_H — velocity pressure (N/m^2);

C_D — coefficient of wind pressure;

G_D — influence coefficient of gust in the wind direction;

A — area of building in the vertical direction of wind load (m^2);

ρ — density of atmosphere, 1.22 kg/m^3;

U_H — design wind speed (m/s);

U_0 — basic wind speed (m/s);

k_{Rw} — conversion coefficient of the reproduction period;

K_D — wind directionality factor;

K_S — seasonal factor;

E_H — vertical factor of the wind speed according to the surface condition of the building site.

In the case of reproduction period 100 years, without considering the influence of K_D and K_S, Eq. (4-73) can be expressed as

$$W_D = \frac{1}{2}\rho(U_0 E_H)^2 C_D G_D A \tag{4-76}$$

Considering the uncertainty of ρ, E_H, C_D, G_D, the details are given in Table 4-17 based on assumption.

Table 4-17 Details of random variables

	Distribution	Coefficient of variation	Lognormal mean value	Lognormal standard deviation	Skewness
ρ	Lognormal	0.1	-0.0050	0.0998	0.301
E_H	Lognormal	0.1	-0.0050	0.0998	0.301
C_D	Lognormal	0.15	-0.0111	0.149	0.453
G_D	Lognormal	0.15	-0.0111	0.149	0.453

Based on the basic wind speed U_0 in Tokyo and the wind speed in reproduction period 500 years, U_{500}, the wind load in reproduction period 50 years can be expressed as

$$\mu_W / W_n = \left[1 - 0.0688 \times \left(\frac{40}{36} - 1\right)\right]^2 = 0.985 \tag{4-77}$$

Where

μ_W — the mean value of the maximum wind load in 50 years;

W_n — the nominal value of the maximum wind load in 50 years.

The coefficient of variation, third moment, and fourth moment of μ_W, can be calculated, too.

$$V_U = \frac{1.28 \times \left(\frac{40}{36} - 1\right)}{1.72 - 0.111 \times \frac{40}{36}} = 0.0891,\ \alpha_{3U} = 1.14,\ \alpha_{4U} = 5.4 \tag{4-78}$$

The details of resistance, dead load and live load are given in Table 4-18. The value of W_n/D_n varies from 0.25 to 4.0 [3]. In this example, it is assumed $W_n/D_n = 2$.

Table 4-18 The details of resistance, dead load and live load

	Distribution	Coefficient of variation	μ_R/R_n or μ_{Qi}/Qi_n	Qi_n/D_n	Skewness
Resistance R	Lognormal	0.2	1.14	—	0.608
Dead load D	Normal	0.1	1.0	1.0	0
Live load L	Gamma	0.59	0.8	0.8	1.18

Different from the snow load analysis in Section 4.3.3, the distribution type of the wind load in Section 4.3.4 is unknown. Therefore the MC simulation cannot be used as a comparing method. In the following analysis, the load and resistance factors are calculated by Mori method, the Existing 3M method and the proposed 3M method.

4.3.4.2 Mori method

Firstly, the gumbel distribution of the maximum wind speed in 50 years should be transformed to lognormal distribution.

$$\lambda_U^* = \ln(1 - 0.164 \times 0.089) = -0.0147 \tag{4-79}$$

$$\zeta_U = 0.430 \times \ln\left(\frac{1 + 3.14 \times 0.0891}{1 - 0.164 \times 0.0891}\right) = 0.112 \tag{4-80}$$

$$V_U = \sqrt{\exp(\zeta_U^2) - 1} = 0.113 \tag{4-81}$$

Other variables are also transformed into lognormal distribution with Eq. (4-82), as shown in Table 4-18.

$$\lambda_X^* = \ln\left(\frac{1}{\sqrt{1+V_X^2}}\right) \tag{4-82}$$

Therefore, the wind load can be transformed into lognormal distribution as

$$\lambda_W^* = 2\cdot\lambda_U^* + 2\cdot\lambda_{E_H}^* + \lambda_\rho^* + \lambda_{C_D}^* + \lambda_{G_D}^* = -0.0666 \tag{4-83}$$

$$\zeta_W = \sqrt{(2\cdot\zeta_U)^2 + (2\cdot\zeta_{E_H})^2 + \zeta_\rho^2 + \zeta_{C_D}^2 + \zeta_{G_D}^2} = 0.380 \tag{4-84}$$

$$V_W = \sqrt{\exp(\zeta_W^2) - 1} = 0.394 \tag{4-85}$$

The same as the calculation of snow load, other parameters can be calculated.

$$\exp\left(-0.0666 + \frac{1}{2}\times 0.380^2\right)\times 2\times 0.985 = 1.98 \tag{4-86}$$

$$c_W = \frac{1.98}{1.98+1+0.176} = 0.546,\ c_D = 0.276,\ c_L = 0.178 \tag{4-87}$$

$$\alpha_R^* = 0.0.487,\ \alpha_W^* = 0.511,\ \alpha_D^* = 0.062,\ \alpha_L^* = 0.220 \tag{4-88}$$

$$u = \frac{1.05}{1-\left(1-\sqrt{0.633^2+0.762^2}\right)\cdot\Phi\left(\frac{0.534-0.6}{0.4}\right)} = 1.204 \tag{4-89}$$

The sensitivity coefficients of loads and resistance are

$$\alpha_R = 0.587,\ \alpha_W = 0.615,\ \alpha_D = 0.0742,\ \alpha_L = 0.264 \tag{4-90}$$

The load and resistance factors can be calculated.

$$\phi = 0.869,\ \gamma_W = 1.361,\ \gamma_D = 1.005,\ \gamma_L = 0.811 \tag{4-91}$$

The design mean resistance can be finally calculated as

$$\frac{R}{D_n} = \frac{1}{\phi}\left(\gamma_W\cdot\frac{W_n}{D_n} + \gamma_D\cdot\frac{D_n}{D_n} + \gamma_Q\cdot\frac{L_n}{D_n}\right) = \frac{1}{0.869}\times(1.361\times 2 + 1.005\times 1 + 0.811\times 0.8) = 5.04 \tag{4-92}$$

4.3.4.3 The existing 3M method

Firstly, the wind load can be expressed as the product of independent variables.

$$Y = \prod_{i=1}^{n} X_i \tag{4-93}$$

The standard deviation and the third moment of Y can be calculated by

$$\sigma_Y^2 = \mu_Y^2\left[\prod_{i=1}^{n}\left(1+V_i^2\right)-1\right] \tag{4-94}$$

$$\alpha_{3Y} = \left[\prod_{i=1}^{n}\left(\alpha_{3i}V_i^3+3V_i^2+1\right)-3\prod_{i=1}^{n}\left(1+V_i^2\right)+2\right]\Big/V_Y^3 \tag{4-95}$$

If X obeys lognormal distribution, the coefficient of variation and third moment of $Y = X^a$ are expressed as

$$V_Y^2 = \left(1+V_X^2\right)^{a^2}-1 \tag{4-96}$$

$$\alpha_{3Y} = 3V_Y+V_Y^3 \tag{4-97}$$

If X obeys other distribution, the coefficient of variation and third moment of $Y = X^2$ are expressed as

$$V_Y = \frac{V_X}{1+V_X^2}\sqrt{4+4\alpha_{3X}V_X+\left(\alpha_{4X}-1\right)V_X^2} \tag{4-98}$$

$$\alpha_{3Y} = \left(1-V_X\right)\alpha_{3X}+1.5\left(\alpha_{4X}-1\right)V_X \tag{4-99}$$

Therefore, the coefficient of variation and third moment of the parameters in Eq.(4-93) can be calculated:

(1) The coefficient of variation and third moment of $Y = U^2$ are

$$V_Y = \frac{V_U}{1+V_U^2}\sqrt{4+4\alpha_{3U}V_U+\left(\alpha_{4U}-1\right)V_U^2} = 0.186 \tag{4-100}$$

$$\alpha_{3Y} = \left(1-V_U\right)\alpha_{3U}+1.5\left(\alpha_{4U}-1\right)V_U = 1.626 \tag{4-101}$$

(2) The coefficient of variation and third moment of $X = E_H^2$ are

$$V_X = \sqrt{\left(1+V_{E_H}^2\right)^4}-1 = 0.202 \tag{4-102}$$

$$\alpha_{3X} = 3V_X+V_X^3 = 0.613 \tag{4-103}$$

Then the coefficient of variation and third moment of wind load are expressed as

$$V_W = \sqrt{\prod_{i=1}^{n}\left(1+V_i^2\right)-1} = 0.370 \tag{4-104}$$

$$\alpha_{3W} = \frac{1}{V_W^3}\left[\prod_{i=1}^{n}\left(\alpha_{3i}V_i^3+3V_i^2+1\right)-3\prod_{i=1}^{n}\left(1+V_i^2\right)+2\right] = 1.342 \tag{4-105}$$

The original target mean resistance can be calculated.

$$\mu_{R0} = \sum \mu_{Q_i} + \sqrt{\beta_T^{3.5} \sum \sigma_{Q_i}^2} = 6.39\mu_D \tag{4-106}$$

With μ_{R0}, the following factors can be calculated.

$$\sigma_{G0} = \sqrt{\sigma_{R0}^2 + \sum \sigma_{Q_i}^2} = 1.522\mu_D \tag{4-107}$$

$$\alpha_{3G0} = \frac{\alpha_{3R}\sigma_{R0}^3 - \sum \alpha_{3Q_i}\sigma_{Q_i}^3}{\sigma_{G0}^3} = 0.195 \tag{4-108}$$

$$\beta_{2T0} = \frac{3}{\alpha_{3G0}}\left\{1 - \exp\left[\frac{\alpha_{3G0}}{3}\left(-\beta_T - \frac{\alpha_{3G0}}{6}\right)\right]\right\} = 1.904 \tag{4-109}$$

Repeat Eq. (4-107) ~ (4-109),

$$\sigma_{G0} = 1.542\mu_G,\ \alpha_{3G} = 0.207,\ \beta_{2T} = 1.898 \tag{4-110}$$

The sensitivity coefficients of loads and resistance are

$$\alpha_R = 0.844,\ \alpha_D = 0.065,\ \alpha_L = 0.245,\ \alpha_W = 0.473 \tag{4-111}$$

$$\phi = 0.775,\ \gamma_D = 1.012,\ \gamma_L = 1.019,\ \gamma_W = 1.312 \tag{4-112}$$

The design mean resistance can be finally calculated as

$$\frac{R}{D_n} = \frac{1}{\phi}\left(\gamma_W \cdot \frac{W_n}{D_n} + \gamma_D \cdot \frac{D_n}{D_n} + \gamma_Q \cdot \frac{L_n}{D_n}\right) = \frac{1}{0.775} \times (1.312 \times 2 + 1.012 \times 1 + 1.019 \times 0.8) = 5.74 \tag{4-113}$$

4.3.4.4 The proposed 3M method

The coefficient of variation and third moment of the wind load are same as the results of the existing 3M method. The target mean resistance is calculated as

$$\mu_{RT\text{-new}} = \sum \mu_{Q_i} + \sqrt{\beta_T^{3.38} \sum \sigma_{Q_i}^2} = 6.278\mu_D \tag{4-114}$$

where $x = 1.8k = 3.38$.

$$\sigma_G = \sqrt{\sigma_R^2 + \sum \sigma_{Q_i}^2} = 1.504\mu_D \tag{4-115}$$

where $\sigma_R = \mu_{RT} \cdot V_R = 1.256\mu_D$

$$\alpha_{3G} = \frac{1}{\sigma_G^3}\left(\alpha_{3R}\sigma_R^3 - \sum \alpha_{3Q_i}\sigma_{Q_i}^3\right) = 0.183 \tag{4-116}$$

$$\beta_{2T} = \frac{3.8}{\alpha_{3G}}\left[1 - e^{\frac{-\alpha_{3G}\beta_T}{3.8}}\right] = 1.907 \tag{4-117}$$

Then the corresponding sensitivity coefficients of loads and resistance are

$$\alpha_R = 0.835,\ \alpha_D = 0.067,\ \alpha_L = 0.251,\ \alpha_W = 0.485 \tag{4-118}$$

Finally, the load and resistance factors can be finally calculated

$$\phi = 0.777,\ \gamma_D = 1.013,\ \gamma_L = 1.026,\ \gamma_W = 1.322 \tag{4-119}$$

The design mean resistance can be finally calculated as

$$\frac{R}{D_n} = \frac{1}{\phi}\left(\gamma_W \cdot \frac{W_n}{D_n} + \gamma_D \cdot \frac{D_n}{D_n} + \gamma_Q \cdot \frac{L_n}{D_n}\right) = \frac{1}{0.777} \times (1.322 \times 2 + 1.013 \times 1 + 1.026 \times 0.8) = 5.76 \tag{4-120}$$

According to the design mean resistance, the results of the proposed 3M method is in agreement with the existing 3M method, while the result of Mori method is much smaller than other methods.

4.4 Conclusions

In this chapter a simplified third-moment method for determining the load and resistance factors is proposed. Compared with the ASCE method, Mori method and the existing 3M method, the following advantages of the proposed method are considered significant.

1. The proposed 3M method is simpler than the existing 3M method. The one time iteration in the computation of the target mean resistance in the existing 3M method is simplified to no iteration in the proposed method.
2. The convergence of the proposed method in the computation is better than the existing 3M method. Simultaneously, the accuracy of the proposed method is good enough.
3. There is no mathematical limitation in the computation of the target reliability in the proposed method, while in the existing 3M method, the mathematical limitation is inevitable.
4. Compared with ASCE method and Mori method, the proposed method is considered safe and material-saving.

REFERENCES

[1] Zhao Y.G. *et al.* Estimation of load and resistance factors using the third-moment method based on the 3P-lognormal distribution, *Frontiers of Architecture and Civil Engineering in China*, 2011, 5(3): 315-322.

[2] ASCE. Minimum design loads for buildings and other structures. *ASCE Standard 7-10, ASCE*, Reston, Va. 2010.

[3] Architectural Institute of Japan. *Recommendations for limit state design of buildings*. 2015.

[4] Mori, Y.. Practical method for load and resistance factors for use in limit state design (in Japanese), *J. of Struct. Constr. Eng., AIJ*, 2002, 559: 39-46.

CHAPTER 5

Probabilistic durability analysis

5.1 Introduction

In section 5.2, the improved analytical model of corrosion initiation was given, where the concept of crack rate η_w was proposed. Then the corresponding stochastic model was built to analyze the corrosion probability. And the accuracy of the proposed 3M method was compared with MC simulation (sample size 10000). The influence of the mean value, the coefficient of variation and the distribution of factors was analyzed respectively in durability assessment.

In section 5.3, the analytical model of cover cracking was built. The stress intensity factor arrive fracture toughness was regard as the limit state of cover cracking. And the initial micro-cracking was considered as an influence factor of cover cracking. The same as the stochastic analysis of corrosion initiation, the influence of the mean value, the coefficient of variation and the distribution of factors was also analyzed in the evaluation of the failure of cover cracking. Some conclusions that are different from the analysis of corrosion initiation were proposed.

In section 5.4, from the analytical model and stochastic analysis of corrosion initiation and cover cracking, there were several conclusions, which can give structure designers some opinions to prevent chloride corrosion of RC structures.

5.2 Corrosion initiation

5.2.1 Analytical model

Numerous studies [1-5] have indicated that chloride penetration through concrete can be empirically described by Fick's second law:

$$C(x,t_1)=C_s\left[1-erf\left(\frac{x}{2\sqrt{D\cdot t_1}}\right)\right] \tag{5-1}$$

where t_1 is the spent time from start of exposure to corrosion initiation (s), $C(x,t_1)$ is the corresponding chloride concentration at depth x (m) (%/m^3), and *erf* is the Gaussian error function:

$$erf(z)=\frac{2}{\sqrt{\pi}}\int_0^z \exp(-t_1^2)dt_1 \tag{5-2}$$

As an inherent and inevitable phenomenon in the formation of concrete mixture, early-age micro-cracking will obviously influence the chloride penetration into concrete and consequently the time to corrosion initiation. Some previous studies [2, 5] have already found that the patterns of chloride penetration in cracked concrete are obviously different with that in sound condition. Therefore, early-age micro cracking will be included in the diffusion coefficient D (m^2/s) in Eq. (5-1) to assess its effect on corrosion initiation. The diffusion coefficient D here can be divided into two parts (namely, D_{cr} and D_0, Fig. 5-1) and is expressed as:

$$D=\frac{D_{cr}A_{cr}+D_0A}{A_{cr}+A}=\frac{D_{cr}\eta_w+D_0}{1+\eta_w} \tag{5-3}$$

where

D_{cr} — the value of chloride diffusion coefficient inside the early-age micro-cracking;

D_0 — the corresponding value for sound area;

A_{cr} — the area of micro cracking (m^2);

A — the exposed surface area of the concrete element (m^2).

In order to quantify the influence of the early-age micro cracking, in this study η_w is referred as the crack rate, which equals to A_{cr}/A.

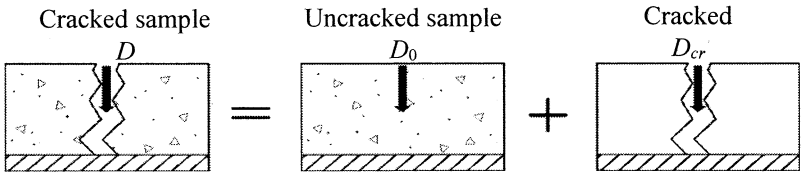

Fig. 5-1 Partition hypothesis of chloride diffusion through cracked concrete

It has been indicated [6-7] that the value of chloride diffusion coefficient inside a crack of concrete cover (namely D_{cr}, m^2/s) is independent of material effects, even if tortuosity and roughness are different. Djerbi et al. [8] suggested the following relationship between the crack width w_0 in concrete cover and its diffusion coefficient D_{cr} inside the crack:

$$\begin{cases} D_{cr} = 2\times10^{-11}w_0 - 4\times10^{-10}, 30\mu m \le w_0 \le 80\mu m \\ D_{cr} \approx 14\times10^{-10}, w_0 \ge 80\mu m \end{cases} \tag{5-4}$$

Besides penetration in the micro cracked area of concrete cover, the chloride will also diffuse in its sound area. The environmental parameters such as relative humidity and temperature, along with the exposure time of RC structures affect the diffusion in sound concrete greatly [1-5, 6-9]. In order to discuss the coupling effects of these influencing factors on the corrosion initiation, here the parameters are accounted for via corrections to the diffusion coefficient D_0, as follows:

$$D_0 = \lambda_h \lambda_T \lambda_t D_{28} \tag{5-5}$$

where

λ_h — the correction coefficient for environmental relative humidity h (%);

λ_T — the corresponding coefficient for temperature T (K);

λ_t — the coefficient for exposure time t_1 (day);

D_{28} — the chloride diffusion coefficient for a specimen under standard curing (28 days) [9]:

$$D_{28} = 10^{(-12.06+2.4w/c)} \tag{5-6}$$

where w/c is the water-to-cement ratio. Also the parameters λ_h, λ_t, and λ_T can be respectively expressed as:

$$\lambda_h = \left[1 + \frac{(1-h)^4}{(1-h_c)^4}\right]^{-1} \tag{5-7}$$

$$\lambda_t = \left(\frac{t_{28}}{t_1}\right)^m \tag{5-8}$$

$$\lambda_T = \exp\left[\frac{U}{R}\left(\frac{1}{T_{28}} - \frac{1}{T}\right)\right] \tag{5-9}$$

where

h_c — the threshold relative humidity (h_c=75%);

t_{28} — the time of standard curing (28 days);

m — the age factor related to w/c by m=3(0.55 — w/c);

U — the activation energy equal to 35000 J/mol;

R — the gas constant;

T_{28} — the temperature for standard curing on day 28 (293 K).

Corrosion initiation occurs when chloride concentration on the surface of the steel bar $C(x = c, t_1)$ (where c is the thickness of the concrete cover) exceeds the critical threshold chloride concentration C_{cr}. Therefore, the following equation can be regarded as the criterion for the corrosion initiation of the steel bar.

$$C(c,t_1) \geq C_{cr} \tag{5-10}$$

5.2.2 Stochastic model

Base on the analytical solution for corrosion initiation (Eq. (5-1) ~ Eq. (5-10)), it can be found that the chloride concentration on the surface of the steel bar $C(c, t_1)$ is a function of a number of basic random variables (i.e. C_s, c, D, η_w, w/c, h, T and t_1). The critical threshold chloride concentration C_{cr} and $C(c, t_1)$ in Eq. (5-10) are identified with interior resistance R and effect of exterior deterioration S, respectively. The performance function governing the initiation of corrosion can be written as

$$G_1(X) = C_{cr} - C(c,t_1) \tag{5-11}$$

The corresponding failure probability of corrosion initiation, $P_1(t_1)$, can be estimated as

$$P_1(t_1) = P_1[G_1(X) \leq 0] = P_1[C(c,t_1) \geq C_{cr}] \tag{5-12}$$

5.2.3 Durability assessment

5.2.3.1 Efficiency and accuracy of the present method

In order to verify the efficiency and accuracy of the present method in analyzing the probability of corrosion-induced failure, the following example of corrosion initiation is given in this paper to compare the proposed 3M reliability index with the previous used MC simulation. The statistical parameters of corrosion-induced failure adopted for the corresponding verification and following assessment are summarized in Table 5-1.

Table 5-1 Values of basic variables in the stochastic analysis of corrosion initiation

Basic variables	Mean	Coefficient of variation	Distribution	Sources
C_{cr}	0.9 (0.6 to 1.2) kg/m^3	0.19	Lognormal	[10]
C_s	1 kg/m^3	0.5	Weibull	[10]
η_w	0.2 %	0.4	Lognormal	[10]
w/c	0.5	0.1	Normal	—
h	75%	0.05	Normal	[10]
T	20 °C	0.2	Lognormal	—
c	70 mm	0.14	Normal	[11]

For corrosion initiation, the prediction of the failure probability derived from the proposed 3M methods is compared with the result from MC simulation (sample size N 10000). One can see from Fig. 5-2 that the results of all 3M methods are in good agreement with that of MC simulation. 3M-1 is the most accurate method. However, in the case of t_1 is great (t_1 = 50 year), the lifetime of structure may be underestimated. Considering the advantages of 3M-3 method mentioned in Chapter 3, the proposed 3M method is chose in the following analysis.

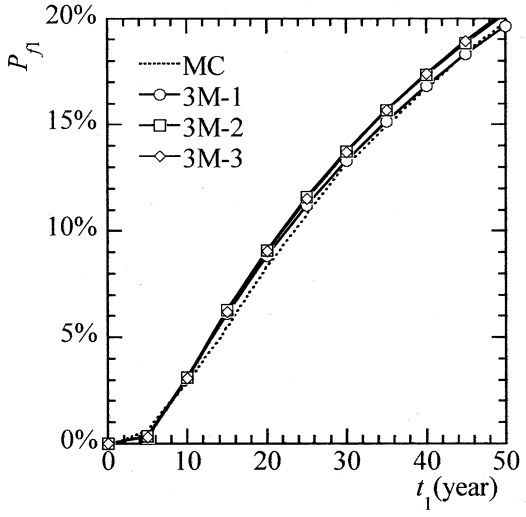

Fig. 5-2 Probability of corrosion initiation

5.2.3.2 Influence of the mean value of variables

One of the advantages of stochastic analysis is the possibility to examine the sensitivity of different variables affecting the probability of corrosion initiation. A parametric study was conducted on the basic variables deemed to be significant in corrosion initiation, as provided in Table 5-1. The time-dependent probability of corrosion initiation influenced by the mean values of these factors is presented in Figs. 5-3 to 5-10.

Among these variables illustrated in Figs. 5-3 to 5-10, the water-to-cement ratio *w/c* has the great effect on the probability of corrosion initiation. For example, the structure lifetime when its corrosion probability reaches 10% (Fig. 5-3) is shown to increase from approximately 4 years to 50 years as *w/c* changes from 0.6 mm to 0.4 mm. *w/c* is directly related to the pores of the concrete structure, thus implying that improving concrete quality is also an efficient method for increasing service life.

The humidity h is the second important influence factor. As shown in Fig. 5-4, the decrease of humidity from 90% to 60% can prolong the structure lifetime from 12 years to 40 years (critical failure probability 10%).

As shown in Fig. 5-5, the structure lifetime increases from 2 years to 22 years as c increases from 30 cm to 70 cm (critical failure probability 10%). This demonstrates that increasing c is an efficient method for prolonging the service life of corroded RC structures.

The surface chloride concentration C_s and the critical chloride concentration C_{cr} are also important in evaluation of structure lifetime. As shown in Fig. 5-6, 0.1 %/m^3 increase of C_s can shorten the structure lifetime 5 ~ 10 years. Conversely, 0.1 kg/m^3 increase of C_{cr} can prolong structure lifetime for about 5 years (critical failure probability 10%), as illustrated in Fig. 5-7.

The influence of the crack rate η_w and the temperature T is quite obvious and should not be ignored, as shown in Fig. 5-8 and 5-9. However, η_w in Fig. 5-8 changes from 0.1% to 0.3%. In the case of high crack rate, the corrosion probability may reach to the critical probability rapidly. In Fig. 5-9, the temperature changes from 10 to 30 ℃, sometimes in summer the surface temperature of structure is up to 60 ℃. In the case of high temperature, the structure may be corroded quickly.

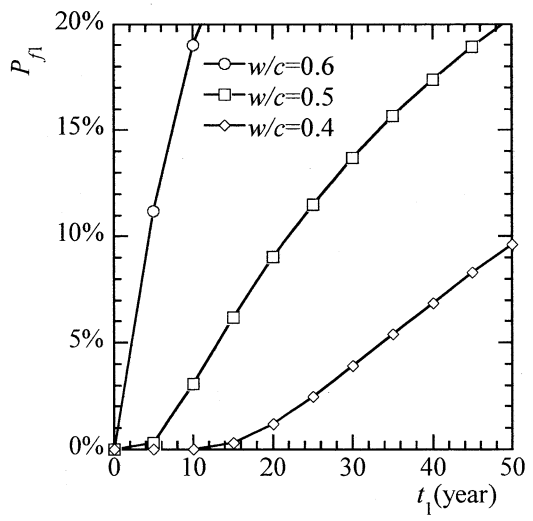

Fig. 5-3 Influence of w/c on P_{fl}

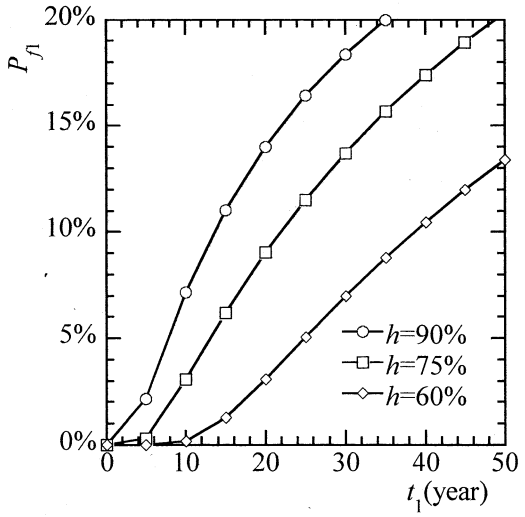

Fig. 5-4 Influence of h on P_{fl}

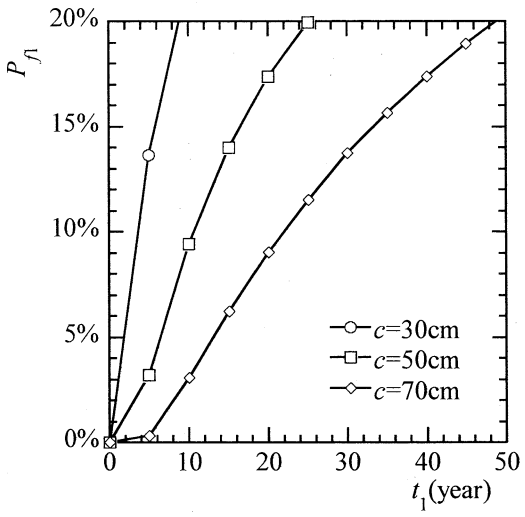

Fig. 5-5 Influence of c on P_{f1}

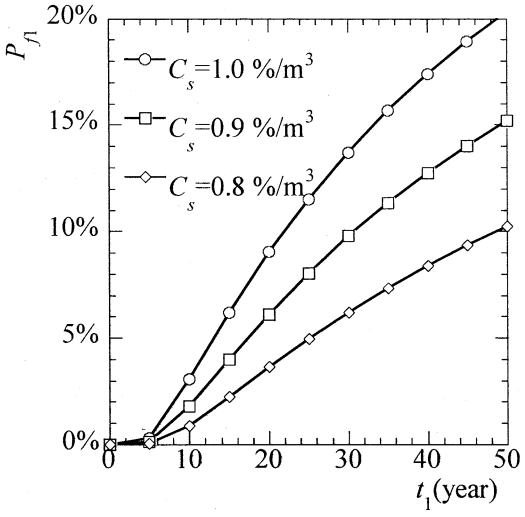

Fig. 5-6 Influence of C_s on P_{f1}

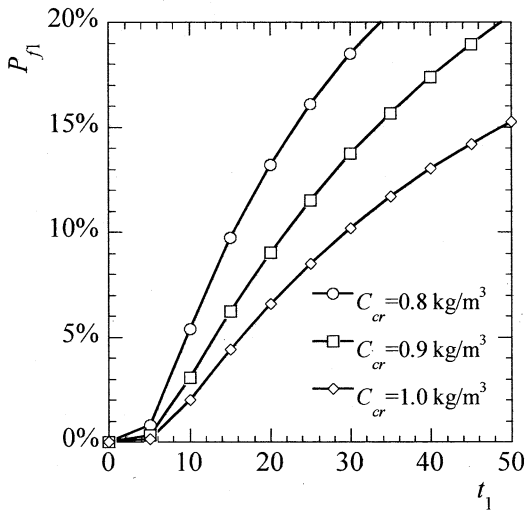

Fig. 5-7 Influence of C_{cr} on P_{f1}

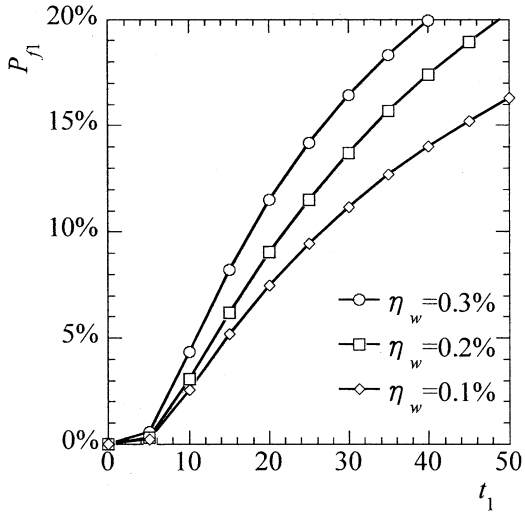

Fig. 5-8 Influence of η_w on P_{f1}

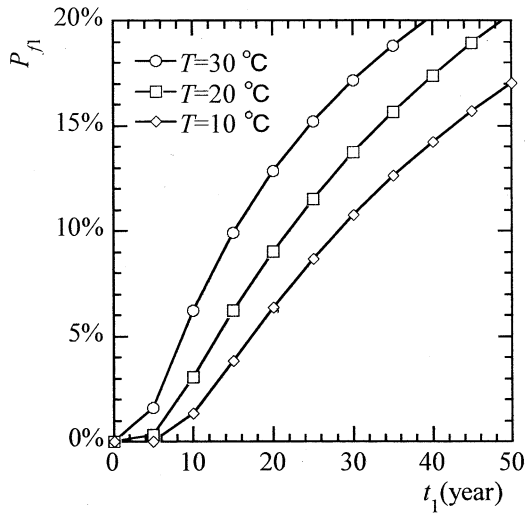

Fig. 5-9 Influence of T on P_{f1}

5.2.3.3 Influence of the distribution of variables

The complexity of natural corrosion of a real engineering structure under aggressive chloride environments makes it difficult to accurately understand the statistical parameters of the variables. Thus different types of the distribution are generally assumed in many previous researches [12-20] to predict the probability of corrosion-induced failure. The corrosion probability gaining from different distributions of variables is investigated here to analyze the effects of the type of distribution (such as the 4 variables in Figs. 5-10 ~ 5-13). It is found that the specific choice of distribution has almost no influence on corrosion probability. This result shows that the probability of corrosion initiation is not sensitive to the choice of distribution of variables. The same results can be found in the analysis of other variables.

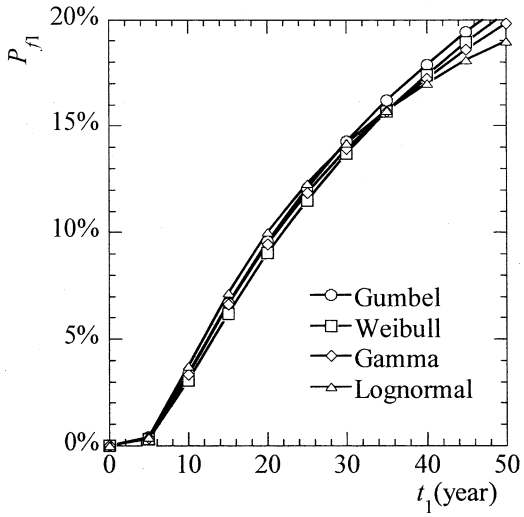

Fig. 5-10 Influence of C_s on P_{f1}

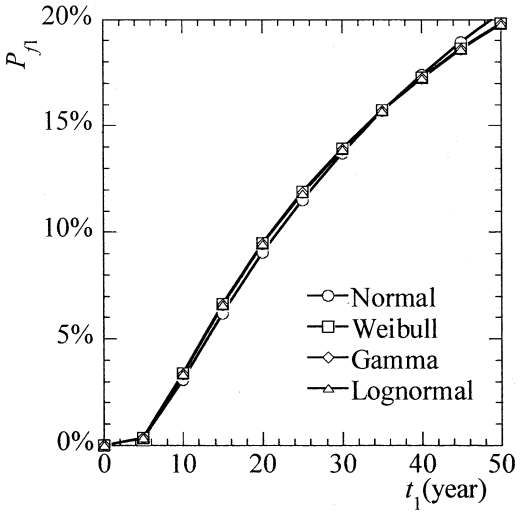

Fig. 5-11 Influence of c on P_{f1}

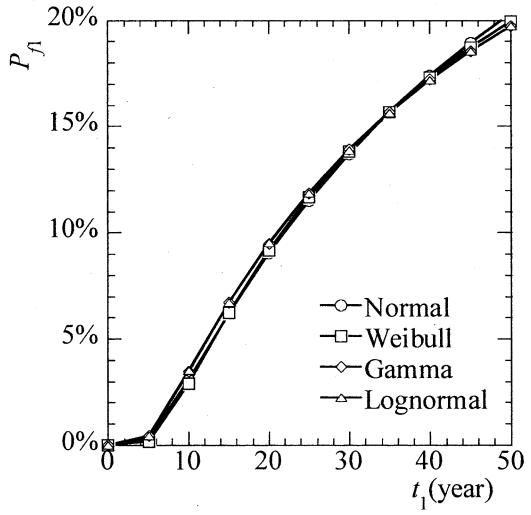

Fig. 5-12 Influence of w/c on P_{f1}

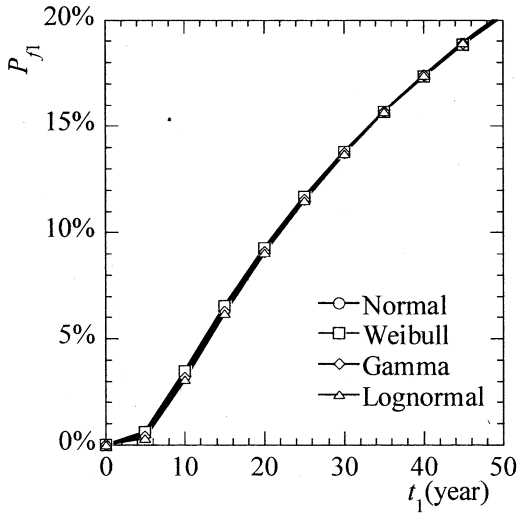

Fig. 5-13 Influence of C_{cr} on P_{f1}

5.2.3.4 Influence of the coefficient of variation of variables

The mean of a variable is generally used to study its effect on the probability of corrosion-induced failure. However, the values of variables are generally uncertain and change frequently in natural corrosion of exposure environments. Thus, different coefficients of variation v are also tested here to study the effect of the variation of variables on the probability of corrosion initiation (Figs. 5-14 to 5-20).

As shown in Fig. 5-14 and 5-15, corrosion probability is sensitive to variations in C_s and C_{cr} which is same as the influence of the mean value of C_s and C_{cr}.

The influence of coefficient of variation of variables is relative to exposure time, such as Fig. 5-16 and 5-17. In early times, a larger coefficient of variation of c and w/c may lead to a higher corrosion probability. Then the influence may get less obvious.

The influence of coefficient of variation of η_w and T is negligible, as shown in Fig. 5-18 and Fig. 5-19.

In Figs. 5-14 to 5-19, the greater the coefficient of variation, the faster the corrosion failure increases. From Fig. 5-20, a contrary tendency can be found. The corrosion failure is higher in the case of the coefficient of variation is small.

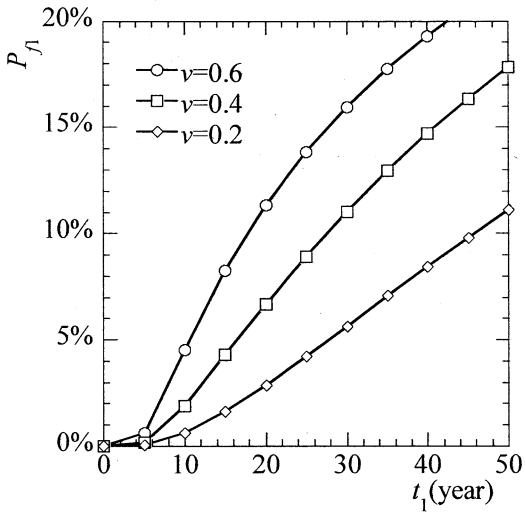

Fig. 5-14 Influence of C_s on P_{f1}

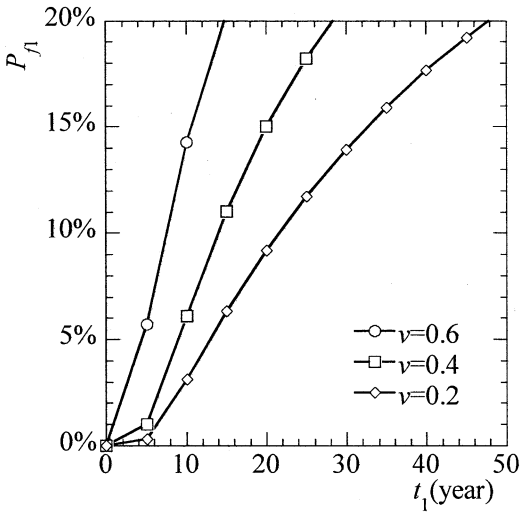

Fig. 5-15 Influence of C_{cr} on P_{f1}

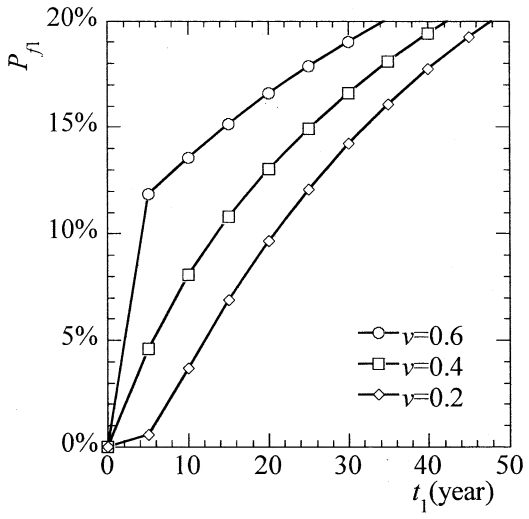

Fig. 5-16 Influence of c on P_{f1}

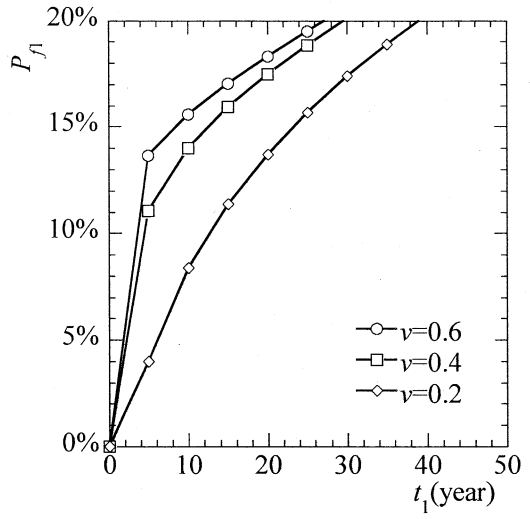

Fig. 5-17 Influence of w/c on P_{f1}

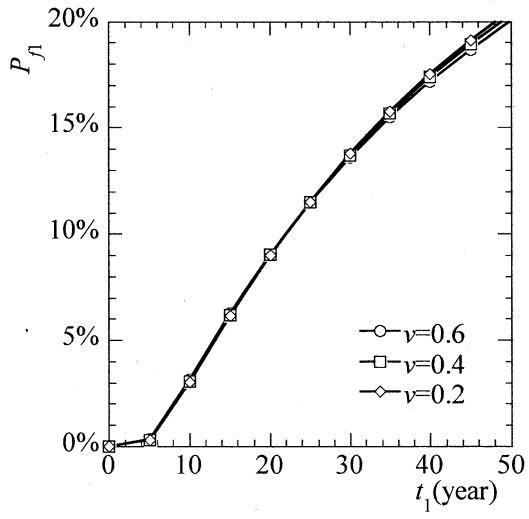

Fig. 5-18 Influence of η_w on P_{f1}

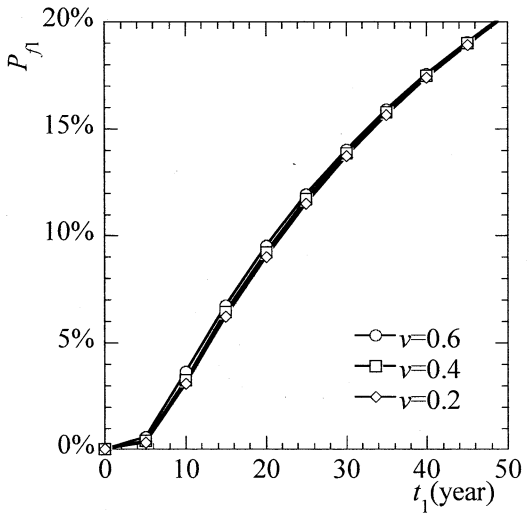

Fig. 5-19 Influence of T on P_{f1}

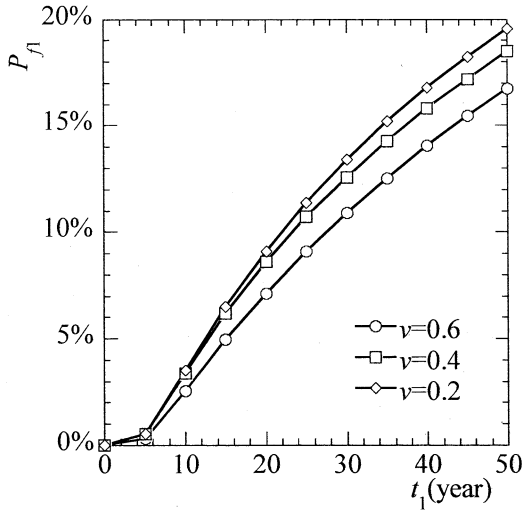

Fig. 5-20 Influence of h on P_{f1}

5.3 Surface cracking

Several engineers deem the point of corrosion initiation of reinforcing steel as too conservative to be a criterion for the failure of service life of corroded RC structures, and instead regard the point of surface cracking of concrete cover as more appropriate. Therefore, the surface cracking of concrete cover is generally considered as another useful indicator in evaluating the corresponding service life.

5.3.1 Analytical model

For corrosion-induced cracking, concrete with embedded reinforcing steel bar can be modeled [21-33] as a thick-walled cylinder with a bar in the center of the cylinder (Fig. 5-21). The initial defect such as micropore structure and random fine crack occurring in the formation of concrete mixture has a certain effect on the corrosion-induced stress field in concrete cover and thus maybe affect the time to cover cracking [33], especially on the scale of the cover thickness (<100mm). Hence, the effect of initial defect on surface cracking will be taken into account in this thesis. The initial defect is assumed to be a fine crack starting on the surface of the bar. Firstly the pore band and fine crack will be filled with rust products (Fig. 5-21 (a)). Then further increase of the amount of products will inevitably result in internal pressure on the surface of the bar (Fig. 5-21 (b)). When the stress intensity factor K_I of the concrete cover exceeds its corresponding fracture

toughness K_{IC}, the crack can grow and propagate rapidly to the concrete surface, as shown in Fig. 5-21 (c).

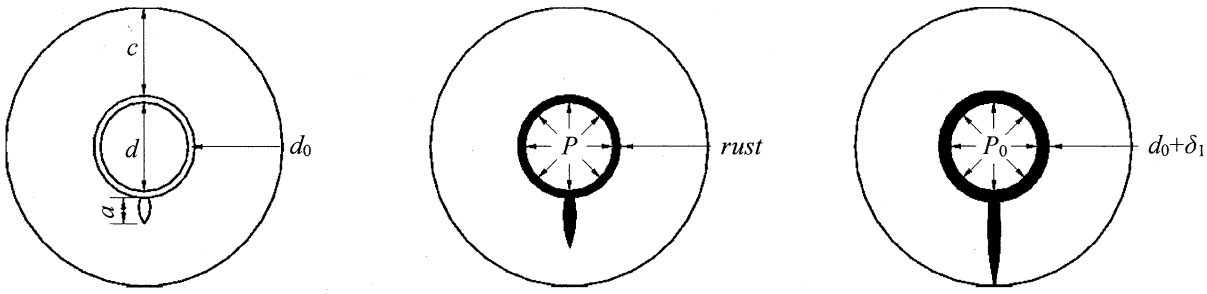

(a) Depassivation and filling full in pore (b) Cracking development (c) Surface cracking

Fig. 5-21 Cover cracking process initiation from the interface defect

At the moment of cover cracking, K_I can be determined [34] by following equation after including the effective crack propagation of the initial defect:

$$K_I = F_1 P_0 \sqrt{\pi(a+\Delta a)} \tag{5-13}$$

where a is the length of the initial defect, Δa is the length of effective crack propagation, P_0 is the critical corrosion-induced pressure, and F_1 is given by

$$F_1 = \frac{A_1/(\ln b)^{0.3} + A_2/(\ln b)^{0.8}}{\sqrt{1-(1/b)^{0.25}}} \tag{5-14}$$

in which

$$\begin{cases} A_1 = 0.854 - 1.812(a/c)^{0.5} - 0.212(a/c)^2 \\ A_2 = -0.114 + 1.193(a/c)^{0.5} - 0.656(a/c)^2 \end{cases} \tag{5-15}$$

$$b = (d/2+c)/(d/2) \tag{5-16}$$

If the parabola model of concrete materials is used to determine the softening characteristic of concrete cover and to consider the size and boundary effect of K_{IC}, Δa can be given as

$$\Delta a = \frac{1}{2\pi}\left(\frac{K_{IC}}{f_t}\right)^2 \tag{5-17}$$

where f_t is the tensile strength of concrete.

When the surrounding concrete is subjected to a corrosion-induced pressure P_0, the corresponding mass of steel per unit length of the reinforcement being consumed by corrosion W as well as time to cover cracking t_2 can be obtained from the radial

displacement of the concrete u_1 [26, 28] on the surface of the reinforcing bars, i.e.,

$$u_1 = \frac{P_0(r_1 + d_0)}{E}\left[\frac{(r_1 + d_0)^2 + r_2^2}{r_2^2 - (r_1 + d_0)^2} + \mu\right] \tag{5-18}$$

where r_1 is the radius of the reinforcement bar, $r_2 = r_1 + d_0 + c$, d_0 is the thickness of the annular layer of the concrete pores at the interface between the reinforcing bar and the concrete, μ is the Poisson's ratio of concrete, and E is the effective modulus of elasticity of concrete cover, which is given by

$$E = \frac{E_c}{1.0 + \theta} \tag{5-19}$$

where E_c and θ are the initial tangent modulus and creep coefficient of concrete cover, respectively.

After determining the radial displacement of the concrete u_1 by Eq. (5-18), W can be given by

$$W = \frac{\pi\rho_s\left[(r_1 + d_0 + u_1)^2 - r_1^2\right]}{n - 1.0} \tag{5-20}$$

where ρ_s is the mass density of reinforcing steel, and n is the ratio of the volume of expansive corrosion products to the volume of iron consumed during corrosion [26, 28].

Also the formula of cracking time of concrete cover t_2 (in years) is

$$t_2 = W^2 / 2k_s \tag{5-21}$$

where k_s is a function of the rate of metal loss, i.e.,

$$k_s = 0.196\alpha\pi r_1 i \tag{5-22}$$

where α is the ratio of the molecular weight of iron to the molecular weight of the corrosion products (α=0.57), and i is the corrosion rate ($\mu A/cm^2$).

5.3.2 Stochastic model

Corrosion-induced cracking of concrete cover occurs when its stress intensity factor K_I exceeds the corresponding fracture toughness K_{IC}. If t_{cr} represents the critical time when crack propagation arrives the cover surface (gained by the value of K_{IC} of concrete cover), the following criterion can be used to define the occurrence of concrete surface cracking:

$$t_2 \geq t_{cr} \tag{5-23}$$

Just like the assessment of corrosion in concrete structure, whether the surface cracking happen or not can be determined by the following performance criterion

$$G_2(\mathbf{X}) = t_{cr} - t_2 \tag{5-24}$$

in which $G_2(\mathbf{X})$ is the performance function. The failure probability P_f of corrosion

initiation or surface cracking can be calculated as

$$P_2(t_2) = P_2[G_2(\mathrm{X}) \le 0] = P_2[t_2 \ge t_{cr}] \tag{5-25}$$

As introduced in Section 5.2.3.1, the proposed 3M-3 method is also applicable (The details is not given).

5.3.3 Durability assessment

Note that the corrosion and cover cracking are two stages, the failure time of cover cracking t_2 in this Section 5.3.3 doesn't contain the time to corrosion initiation t_1.

5.3.3.1 Influence of the mean value of variables

With the values of the basic variables that are deemed to be important for surface cracking in Table 5-2, the corresponding failure probability of cover cracking influenced by the mean values of these factors are listed in Figs. 5-22 to 5-29. From Figs. 5-22 to 5-29, it is obvious that the probability of cover cracking increases rapidly after corrosion initiation. As shown in Fig. 5-22 and 5-23, the probability of cover cracking in 0.1 year is given. The ratio of the volume of expansive corrosion products n is the most important factor, which depends on the environment of the RC structure is exposed to. The different corrosion products will have different volume expansions as presented in Table 5-3. It is shown that an increase of n from 2 to 4 can greatly shorten the structural lifetime. The similar rule of corrosion rate can be found in Fig. 5-23. At the time of 0.1 year, 0.5 μA/cm^2 increase of i can result in 3% ~ 5% increase of the failure probability.

Table 5-2 Values of the basic variables in the stochastic analysis of surface cracking

Basic variables	Mean	Coefficient of variation	Distribution type	Sources
n	2	0.2	Lognormal	[35]
i	1.5 (1 to 2) μA/cm^2	0.33	Normal	[10]
f_t	5.725 MPa	0.2	Normal	[16]
E	18820 MPa	0.12	Normal	[16]
d	25 mm	0.2	Normal	[16]
K	1.118 MPa·m$^{1/2}$	0.177	Normal	[34]
c	70 mm	0.14	Normal	[36]

Table 5-3 n for various corrosion products

Name of corrosion products	FeO	Fe_3O_4	Fe_2O_3	$Fe(OH)_2$	$Fe(OH)_3$	$Fe(OH)_3 \cdot 3H_2O$
n	1.80	2.00	2.20	3.75	4.20	6.40

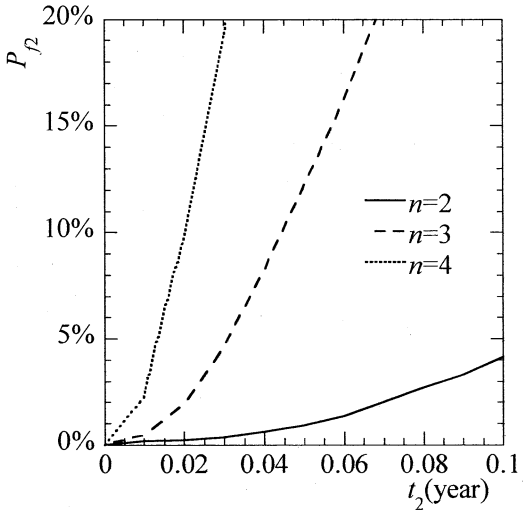

Fig. 5-22 Influence of n on P_{f2}

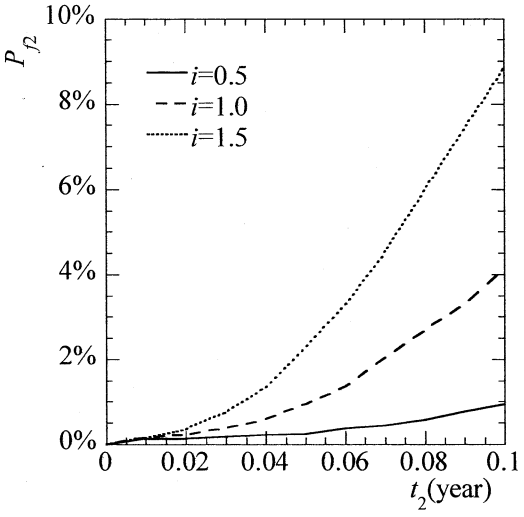

Fig. 5-23 Influence of i on P_{f2}

The influence of c, d and E on the probability of cover cracking is also obvious, as shown in Figs. 5-24 to 5-26. Within 0.5 year the variation of the mean value of c, d and E has a significant impact on the failure of cover cracking. The increase of cover thickness can delay the failure of cover cracking, as shown in Fig. 5-24. It worth noting that the failure probability in the case of the diameter of reinforcing bar 25mm is lower than that of d = 15mm and d = 35mm (Fig. 5-25), which means making d too great or too small will increase the probability of cover cracking. As shown in Fig. 5-26, P_{f2} increases with the increase of the elasticity modulus E.

Contrary to the elasticity modulus of concrete, P_{f2} decreases with the increase of the fracture toughness K, as shown in Fig. 5-27. The similar rule can be found in Fig. 5-28, the tensile strength of concrete f_t is also slightly influence the probability of cover cracking. The slightest influence factor is the length of the initial defect a, as shown in Fig. 5-29.

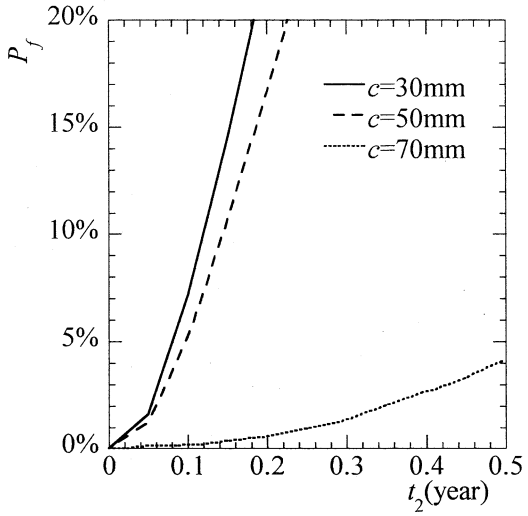

Fig. 5-24 Influence of c on P_{f2}

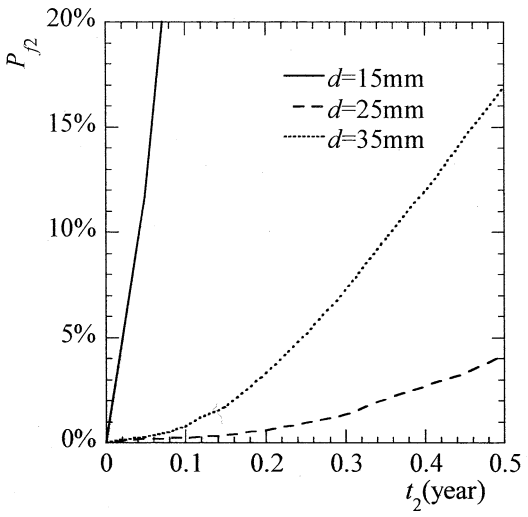

Fig. 5-25 Influence of d on P_{f2}

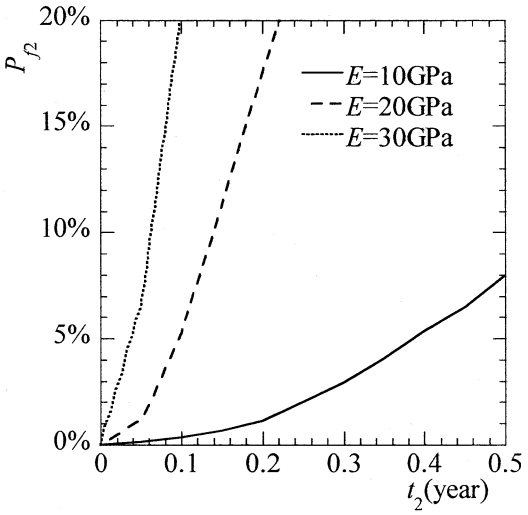

Fig. 5-26 Influence of E on P_{f2}

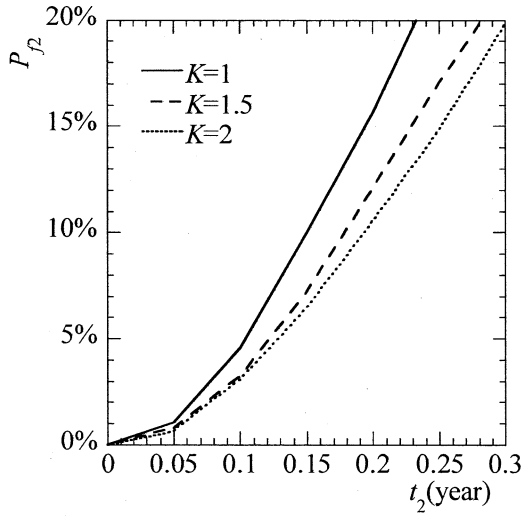

Fig. 5-27 Influence of K on P_{f2}

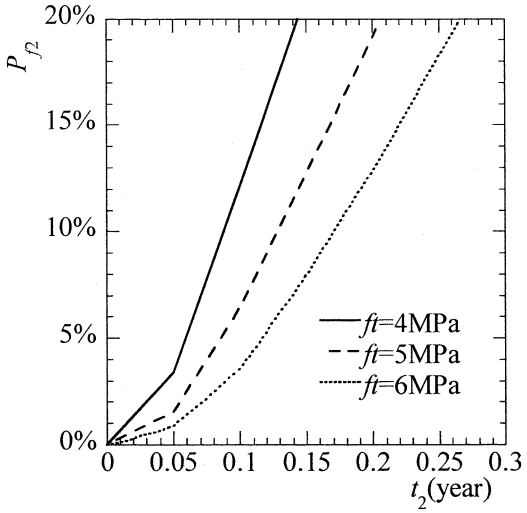

Fig. 5-28 Influence of f_t on P_{f2}

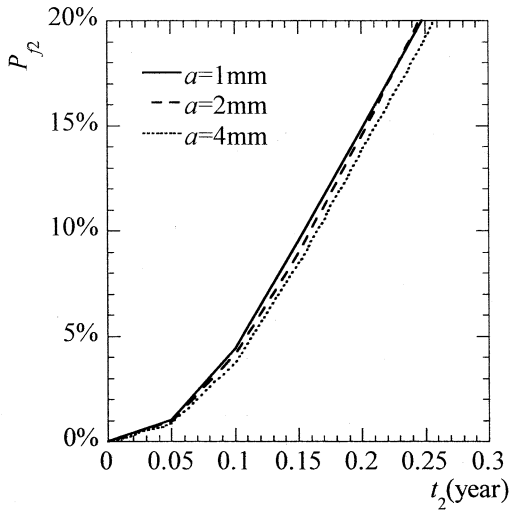

Fig. 5-29 Influence of a on P_{f2}

5.3.3.2 Influence of the coefficient of variation of variables

The influence of the coefficient of variation on P_{f2} is very different from the mean value of factors, which is shown in Figs. 5-30 to 5-37. For all influence factors, the increase of the coefficient of variation v will accelerate the failure of cover cracking.

As shown in Figs. 5-30 and 5-31, the influence of v_n and v_i is the most significant, which is the same with the influence of their mean value. In Fig. 5-31, there is a turning-point in the case of $v_i = 0.6$, which means in the case of v_i is very large, P_{f2} will increase rapidly after corrosion initiation, then the increase rate will become slow.

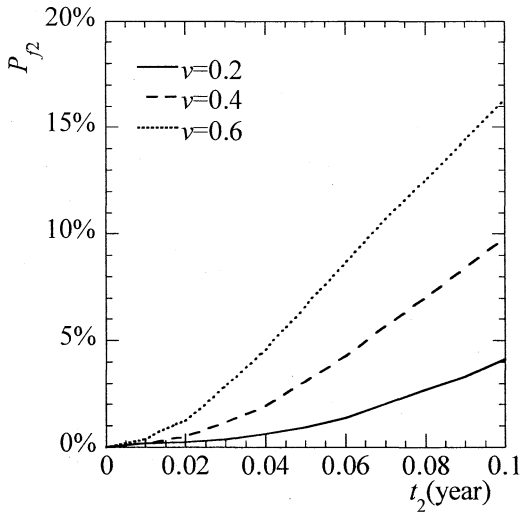

Fig. 5-30 Influence of v_n on P_{f2}

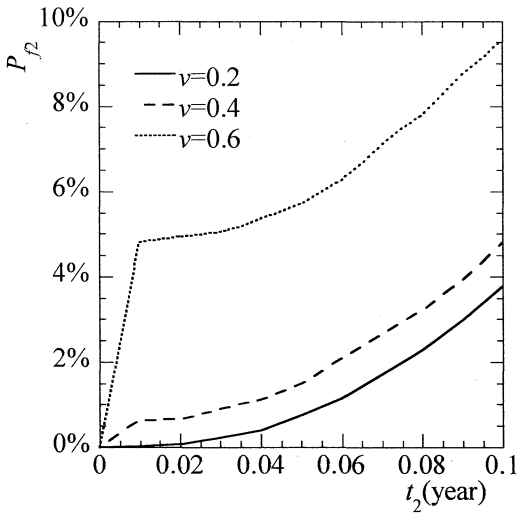

Fig. 5-31 Influence of v_i on P_{f2}

The coefficient of variation of d also has obvious influence on P_{f2}, as shown in Fig. 5-32. Thus controlling v_d under 0.2 is significant in reducing the risk of cover cracking.

From Figs. 5-33 to 5-35 we can see, the coefficients of variation of E, K and f_t are slightly influence the probability failure of cover cracking.

Different from the mean value of c, the influence of the coefficient of variation of c on P_{f2} is negligible, as shown in Fig. 5-36. And both of the mean value and the coefficient of variation of a have the slightest influence on the failure probability of cover cracking.

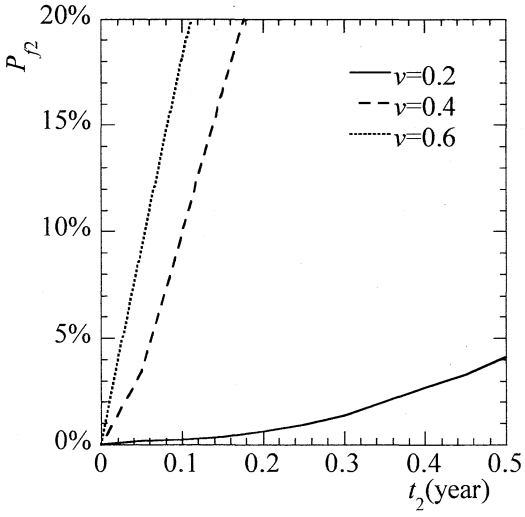

Fig. 5-32 Influence of v_d on P_{f2}

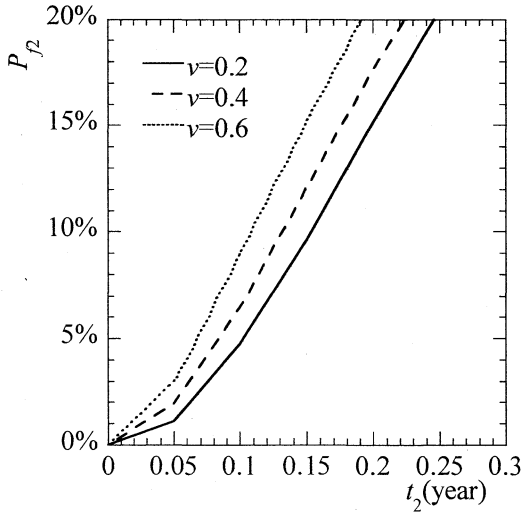

Fig. 5-33 Influence of v_E on P_{f2}

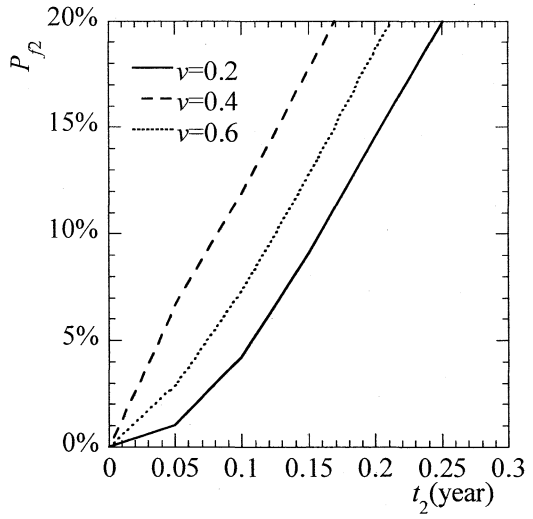

Fig. 5-34 Influence of v_K on P_{f2}

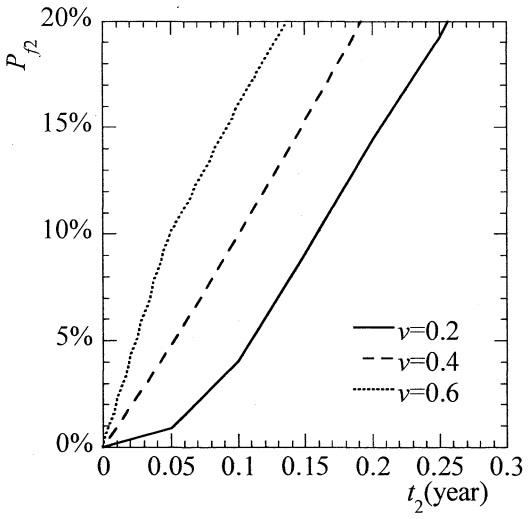

Fig. 5-35 Influence of v_{ft} on P_{f2}

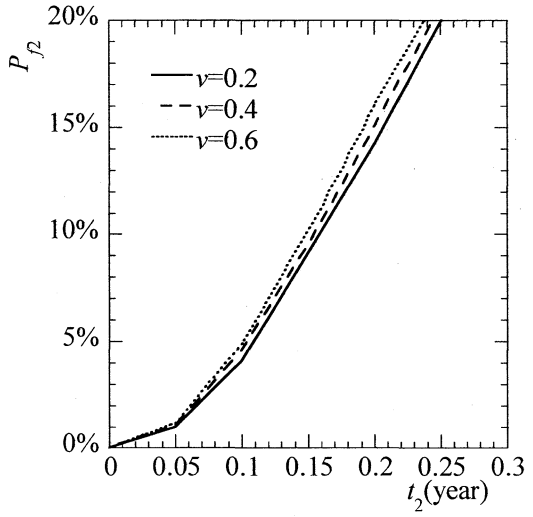

Fig. 5-36 Influence of v_c on P_{f2}

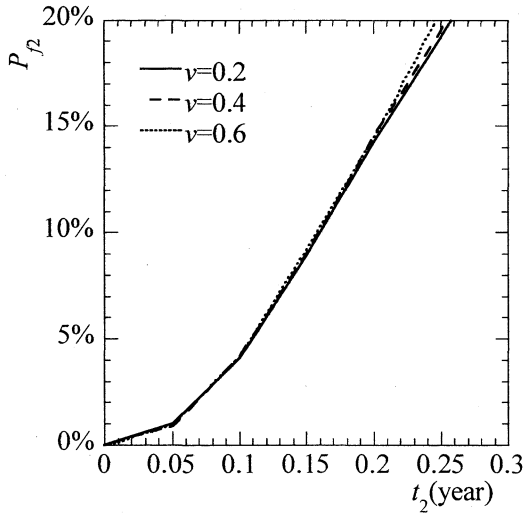

Fig. 5-37 Influence of v_a on P_{f2}

5.3.3.3 Influence of the distribution type of variables

The influence of the distribution type on P_{f2} is different from the analysis on P_{f1}, as shown in Figs. 5-38 to 5-45. For most influence factors, the result of P_{f2} when influence factors obey gumbel distribution is very different from other cases, as shown in Figs. 5-38 to 5-43. In Fig. 5-38 and 5-39, the gumbel distribution of n or E will decrease the failure probability of cover cracking. On the contrary, the gumbel distribution of d, K and f_t will

increase the failure probability of cover cracking, as shown in Fig. 5-40 to 5-42.

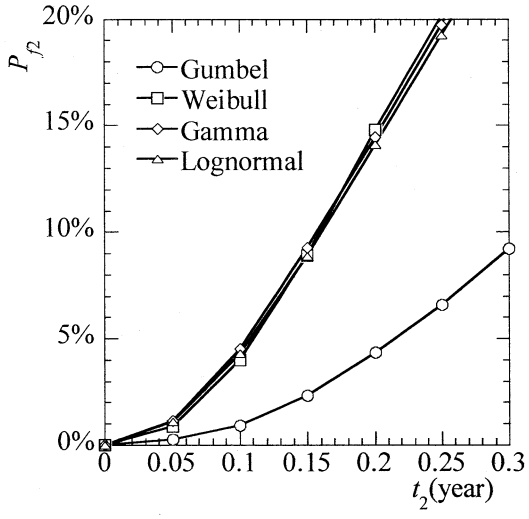

Fig. 5-38 Influence of the distribution of n on P_{f2}

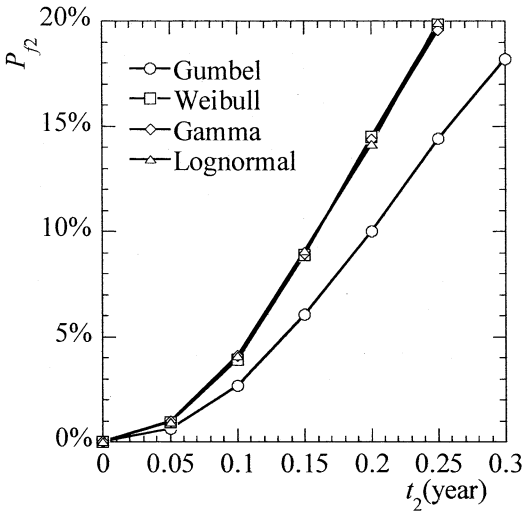

Fig. 5-39 Influence of the distribution of E on P_{f2}

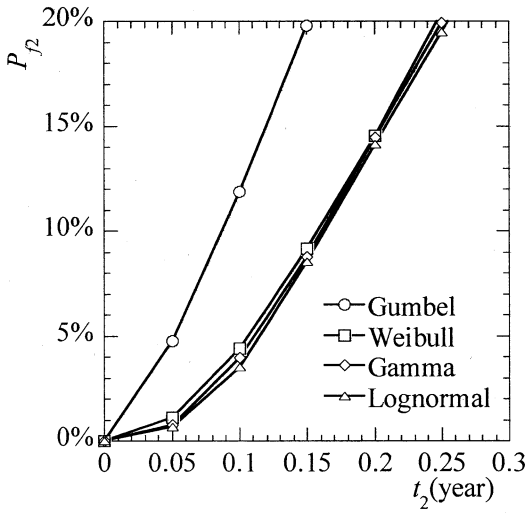

Fig. 5-40 Influence of the distribution of d on P_{f2}

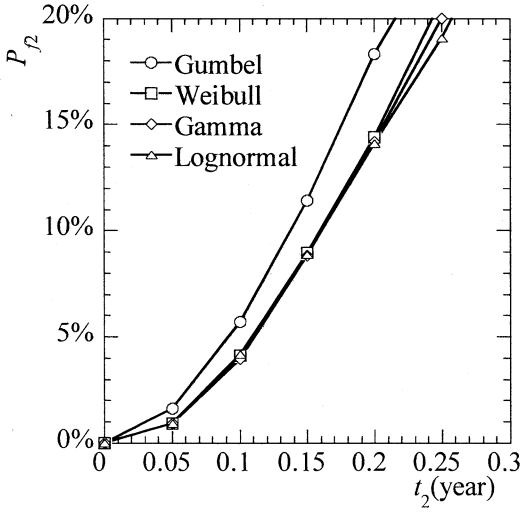

Fig. 5-41 Influence of the distribution of K on P_{f2}

In Fig. 5-43, at the beginning of curve, the gumbel distribution of i will cause a great P_{f2}, after the turning-point, the gumbel distribution of i will decrease the P_{f2}.

The influence of the distribution type of n is not obvious (Fig. 5-44), which is opposite to the influence of the mean value of n, while the influence of the distribution type of a

on P_{f2} is negligible, consistent with the influence of its mean value.

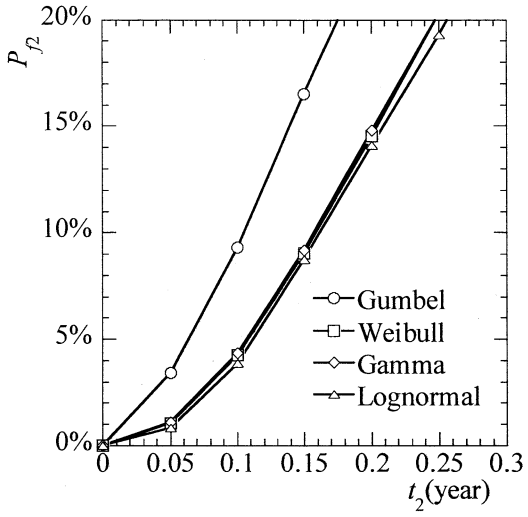

Fig. 5-42 Influence of the distribution of f_t on P_{f2}

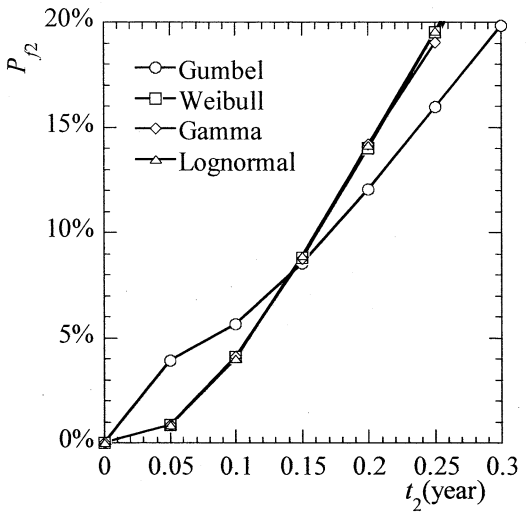

Fig. 5-43 Influence of the distribution of i on P_{f2}

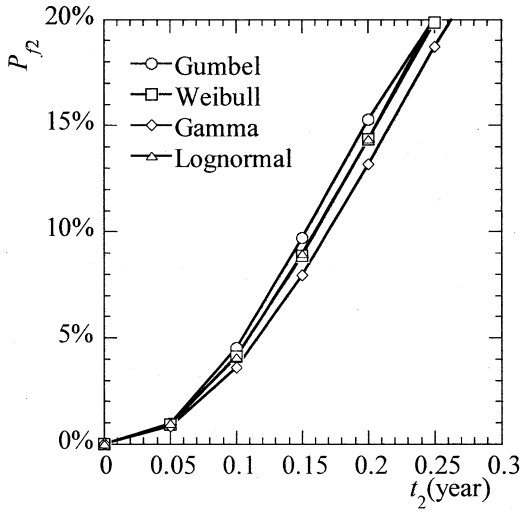

Fig. 5-44 Influence of the distribution of n on P_{f2}

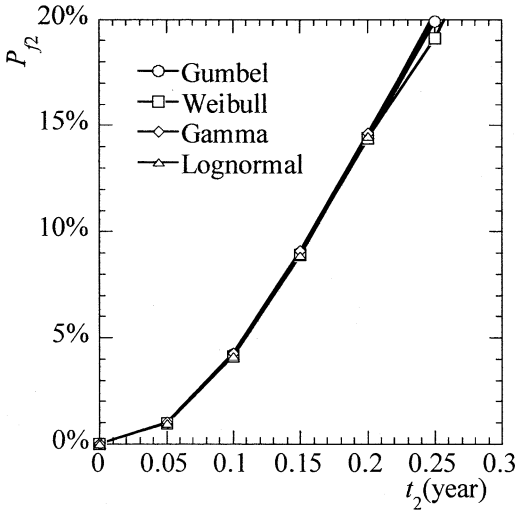

Fig. 5-45 Influence of the distribution of a on P_{f2}

5.4 Conclusion

After improving the analytical solutions of corrosion initiation and surface cracking of

corroded RC structures, the stochastic models of corrosion-induced failure are developed by using the proposed 3M method. With such models, the time when the structure approaches an unacceptably probability of corrosion- or cracking-induced failure can be obtained, and thus the required time of repair can be carried out with confidence. Based on such models, the different effects of many influencing factors on the time-dependent probability of corrosion initiation and surface cracking are also discussed. From the investigation of the present study, the following conclusions can be obtained.

(1) The proposed 3M method was proved to be much simpler and more efficient than traditional methods like MC simulation in the stochastic analysis of corrosion initiation and surface cracking.

(2) The increase of corrosion probability is slow, while the increase of cover cracking probability is quite rapid. Thus taking measures to prevent the diffusion of chloride ions is significant.

(3) The results clearly demonstrate that the distributions of influencing factors have almost no effect on the failure probability of corrosion, whereas the mean of basic variables or its coefficient of variation affects it to various extents.

(4) The gumbel distribution has a remarkable influence on the cover cracking probability, while in the analysis of corrosion probability, the influence of gumbel distribution is negligible.

REFERENCES

[1] Song H.W. *et al.* Factors influencing chloride transport in concrete structures exposed to marine environments. *Cem. Concr. Compos.*, 2008, 30(2): 113-121.

[2] Erdoğdu Ş. *et al.* Determination of chloride diffusion coefficient of concrete using open-circuit potential measurements. *Cem. Concr. Res.*, 2004, 34(4): 603-609.

[3] Bitaraf M. *et al.* Analysis of chloride diffusion in concrete structures for prediction of initiation time of corrosion using a new meshless approach. *Constr. Build Mater.*, 2008, 22: 546-556.

[4] Matsumura T. *et al.* Verification method for durability of reinforced concrete structures subjected to salt attack under high temperature conditions. *Nucl. Eng. Des.*, 2008, 238(5): 1181-1188.

[5] Pour-Ghaz M. *et al.* The effect of temperature on the corrosion of steel in concrete. part 1: simulated polarization resistance tests and model development. *Corros. Sci.* 2009, 51: 415-425.

[6] Rodriguez O.G. *et al.* Influence of cracks on chloride ingress into concrete. *ACI*

Mater. J., 2003, 100(2): 120-126.

[7] Boulfiza M. *et al.* Prediction of chloride ions ingress in uncracked and cracked concrete. *ACI Mater. J.*, 2003, 100(1): 38-49.

[8] Djerbi A. *et al.* Influence of traversing crack on chloride diffusion into concrete. *Cem. Concr. Res.*, 2008, 38(6): 877-883.

[9] Tang L.P. *et al.* On the mathematics of time-dependent apparent chloride diffusion coefficient in concrete. *Cem. Concr. Res.*, 2007, 37(4): 589-595.

[10] Lu Z.H. *et al.* Probabilistic evaluation of initiation time in RC bridge beams with load-induced cracks exposed to de-icing salts. *Cem. Concr. Res.*, 2011, 41: 365-372.

[11] Weyers R.E. *et al.* Bridge deck cover depth specifications. *Concr. Int.*, 2003, 25(2): 61-64.

[12] Kim A.T.V. *et al.* Predicting the likelihood and extent of reinforced concrete corrosion-induced cracking. *J. Struct. Eng.-ASCE*, 2005, 131: 1681-1689.

[13] Dimitri V.V. *et al.* Probabilistic evaluation of initiation time of chloride-induced corrosion. *Reliab. Eng. Syst. Safe.*, 2008, 93:364-372.

[14] Li C.Q.. Life cycle modeling of corrosion affected concrete structures Propagation. *J. Struct. Eng.*-ASCE, 2003, 129(6): 753-761.

[15] Li C.Q. *et al.* Prediction of concrete crack width under combined reinforcement corrosion and applied load. *J. Eng. Mech.-ASCE*, 2011, 137(11): 722-731.

[16] Li C.Q. *et al.* Time-dependent reliability analysis of corrosion-induced concrete cracking. *ACI Struct. J.*, 2005, 102(4): 543-549.

[17] Kwon S.J. *et al.* Service life prediction of concrete wharves with early-aged crack: probabilistic approach for chloride diffusion. *Struct. Saf.*, 2009, 31(1): 75-83.

[18] Marita L.A.. Probability of corrosion induced cracking in reinforced concrete. *Cem. Concr. Res.*, 1995, 25(6): 1179-1190.

[19] Bastidas-Arteaga E. *et al.* A comprehensive probabilistic model of chloride ingress in unsaturated concrete. *Eng. Struct.*, 2011, 33: 720-730.

[20] Bentz E.C.. Probabilistic modeling of service life for structures subjected to chlorides. *ACI Mater. J.*, 2003, 100(5): 391-97.

[21] Torres-Acosta A.A. *et al.* Residual life of corroding reinforced concrete structures in marine environment. *J. Mater. Civil Eng.*, 2003, 15(4): 344-353.

[22] Guzmán S. *et al.* Cover cracking of reinforced concrete due to rebar corrosion induced by chloride penetration. *Cem. Concr. Res.*, 2011, 41(8): 893-902.

[23] Yüzer N. *et al.* Prediction of time to crack initiation in reinforced concrete exposed to chloride. *Constr. Build Mater.*, 2008, 22: 1100-1107.

[24] Jang B.S. *et al.* Effects of non-uniform corrosion on the cracking and service life of

reinforced concrete structures. *Cem. Concr. Res.*, 2010, 40(9): 1441-1450.

[25] AI-Harthy A.S. *et al.* Concrete cover cracking caused by steel reinforcement corrosion. *Mag. Concrete Res.*, 2011, 63(9): 655-667.

[26] Liu Y.P. *et al.* Modeling the time-to-corrosion cracking in chloride contaminated reinforced concrete structures. *ACI Mater. J.*, 1998, 95(6): 675-681.

[27] Pantazopoulou S.J. *et al.* Modelling cover-cracking due to reinforcement corrosion in RC structures. *J. Eng. Mech.-ASCE*, 2001, 127(4): 342-51.

[28] Tamer E.M. *et al.* A model for prediction of time from corrosion initiation to corrosion cracking. *Cem. Concr. Compos.*, 2007, 29: 168-75.

[29] Zhong J.Q. *et al.* Stiffness degradation and time to cracking of cover concrete in reinforced concrete structures subject to corrosion. *J. Eng. Mech.-ASCE*, 2010, 136(2): 209-219.

[30] Lu C.H. *et al.* Reinforcement corrosion-induced cover cracking and its time prediction for reinforced concrete structures. *Corros. Sci.*, 2011, 53: 1337-1347.

[31] Malumbela G. et al. Model for cover cracking of RC beams due to partial surface steel corrosion. *Constr. Build Mater.* 2011, 25: 987-991.

[32] Zhang X.G. *et al.* Dynamic corrosion-induced cracking process of RC considering effect of initial defects. *J. Asian Archit. Build. Eng.*, 2010, 9(2): 439-446.

[33] Xu S.L. *et al.* Determination of fracture parameters for crack propagation in concrete using an energy approach. *Eng. Fract. Mech.*, 2008, 75(15): 4292-4308.

[34] Zhao Y.X. *et al.* Comparison of uniform and non-uniform corrosion induced damage in reinforced concrete based on Gaussian description of the corrosion layer. *Corros. Sci.*, 2011, 53(9): 2803-2814.

CHAPTER 6

Conclusions

Civil infrastructure facilities must be designed to satisfy the service requirement and withstand environmental events such as earthquake and wind. In engineering design, an important consideration is how to handle the unavoidable uncertainties of the environmental events and ensure structural safety.

The traditional FORM and SORM are proved to be complicated and not accurate enough. In this study, a simple and accurate 3M method, with wider applicable range and less mathematical limitation was proposed. In the existing 3M methods, there is either square root or antilogarithm in the equation of reliability calculation. In the proposed 3M method, the exponential function was used to replace the function with square root and antilogarithm. Then the proposed 3M method was applied to the calculation of simple structures and systems, respectively. Its application was verified by several examples.

In current codes and guidelines, the load and resistance factors (LRF) are used for reliability design. And the target reliability is used to ensure structural safety. Compared with the first and second order reliability methods, the third-moment (3M) method offers advantages in both simplicity and accuracy. However, it leaves much to be improved, such as the one time iteration and applicable range limitation. With the proposed 3M method, the computation process of load and resistance factors was simplified to no iteration. Simultaneously, the accuracy of the proposed 3M method was ensured.

The number and the diversity of loads were also considered when the new formula of target mean resistance was given. Analysis results show that the influence of the number of load on the calculation of the target mean resistance is negligible, while the diversity of loads has remarkable influence on the calculation of the target mean resistance. With several examples, in which the influence of different number, mean value, coefficient of variation, and distribution of loads was considered, the application of the new method was verified. Finally, several load combinations, in which the snow load and wind load were considered, were proposed to investigate the application of the proposed method. The results show that comparing with other methods, the proposed method has either the same or higher accuracy.

Based on the proposed 3M method, a full set of methods for evaluation of structural durability were given. The analysis includes two parts: the corrosion initiation and the cover cracking of RC structures, which are two main points to judge structural failure. Firstly, the analytical models of corrosion initiation and cover cracking were improved, respectively. In the analytical model of chloride-induced corrosion, the initial micro-cracking, for its influence on the whole diffusion process of chloride ions, was considered. And the concept of the crack rate was proposed to qualify the influence level. Then in the analytical model of cover cracking, the stress intensity factor arriving to the fracture toughness was considered as the limit state of failure, which is more reasonable to compare with judging failure with tensile strength. And the initial defect in concrete was considered as an influence factor in the analysis of cover cracking. This is more reasonable because many initial defects such as micro pore structures and random fine cracks occur during the formation of the concrete mixture.

The failure probabilities of corrosion initiation and cover cracking calculated by the proposed 3M method are compared with MC simulation. The results show that the proposed 3M method has enough accuracy in the assessment of durability. Compared the corrosion time and cover cracking time, after corrosion initiation the failure of cover cracking increases rapidly. Therefore, preventing the diffusion of chloride ions is a good way to prolong structural lifetime. The mean value, coefficient of variation, and the distribution of influence factors are analyzed, respectively. The results show that the coefficient of variation and the mean value of influence factors have very different influence on the analysis of failure probability. There is not inevitable connection with the mean value and the coefficient of variation of the influence factors. Moreover, the distribution type of influence factors has almost no influence on the analysis of corrosion initiation, while in the analysis of cover cracking analysis, the Gumbel distribution of some influence factors affects the failure probability a lot.

ACKNOWLEDGEMENT

First of all, I want to express my special thanks to Prof. Zhao Yan-gang, my supervisor, for his helpful suggestions in topic selection of the thesis. Without his patience assistance and friendly encouragement, it would not be possible for me to complete this thesis in such a short period of time without reducing its scholarly quality. I benefited much from his critical thinking, copious knowledge, scholarly expertise, and kind encouragement long before I entered Kanagawa University.

Second, I want to express my thanks to Prof. Saito Takasuke, who gives me a lot of help in every respects. He always smiles to everyone and help us solve every small problems patiently. He speaks Japanese slowly for us to understand, never tired of repeating explanation.

Moreover, I want to thank my friends for their very patient and time-consuming assistance in analyses and language translation. Needless to say, all their assistance has greatly facilitated my study and hence also enhanced the quality of this research.

Grateful acknowledgement is given to the Ministry of Education, Science, and Culture, Government of Japan for granting me the scholarship which made this study possible.

Finally, I want to thank my families. Without their understanding and support, I cannot finish this thesis on time.